NEW CONTROL METHODS FOR MULTI-TIME-SCALE LINEAR SYSTEMS WITH SMART GRID APPLICATIONS

BY KLITI KODRA

A dissertation submitted to the

Graduate School—New Brunswick

Rutgers, The State University of New Jersey

in partial fulfillment of the requirements

for the degree of

Doctor of Philosophy

Graduate Program in Electrical Engineering

Written under the direction of

Professor Zoran Gajić

and approved by

_____

_____

_____

_____

_____

New Brunswick, New Jersey

May, 2017

ABSTRACT OF THE DISSERTATION

New Control Methods for Multi-Time-Scale Linear Systems with Smart Grid Applications

by Kliti Kodra

Dissertation Director: Professor Zoran Gajić

Power systems within smart grid architectures are generally large scale and have a tendency to exhibit multiple time-scales when modeled in their entirety due to the presence of physical components of different nature and parasitic parameters associated with them. Research in current literature primarily focuses on studying power system architectures based on a two time-scale decomposition. In this dissertation, we use singular perturbation theory to investigate time-scale decomposition and related anomalies and propose new control methods by considering the presence of multiple time-scales.

We start with an open-loop study of a simplified model of an islanded microgrid in singularly perturbed form with highly oscillatory and highly damped modes. Simulation results and analytical analysis conclude that the model does not contain any slow time-scales even though the eigenvalue distribution of the model tells otherwise. While the singular perturbation parameter is very small, the classical two time-scale decomposition in this case is not effective. On the other hand, the modes corresponding to the fastest time-scales provide a very accurate approximation of the original model. The results obtained via singular perturbation methods are also corroborated by using the balancing realization technique. Namely, only the states corresponding to the fastest

modes are dominant.

Motivated by the structure of the state-space input matrix of the previous problem, we consider a new class of singularly perturbed systems where individual inputs control slow and fast modes independently. We study the linear quadratic regulator optimal control problem for three cases that are common in real physical systems, namely when the inputs are completely decoupled or independent, when weak coupling is present between the inputs, and when the fast subsystem is weakly controlled. We obtain the zero-order approximation solution of the continuous algebraic Riccati equations for each case in terms of simplified sub-problems which avoid possible ill-conditioning. As a follow-up, parallel recursive algorithms based on fixed-point methods are proposed to improve the error of the approximations leading to the accurate solution of Riccati equations and the cost functional in a few iterations of the algorithm. These results are further extended to the stochastic case. The linear-quadratic Gaussian control problem is investigated and its solution is also obtained very accurately in an iterative fashion.

Lastly, implicit singularly perturbed systems with multiple time-scales are considered. The Schur decomposition is utilized to transform the control matrix into an upper quasi-triangular form where the time-scales are explicitly ordered and a singularly perturbed model is obtained after perturbation parameters are evaluated and extracted. The standard multi-time-scale system is then decoupled into individual time-scales by sequentially applying an invariant transformation. Multi-time-scale control of the Schur-decomposed system is then considered. Control based on the eigenvalue placement method is initially proposed, where the individual decoupled states are fed back sequentially instead of the whole state vector. Furthermore, we design a combined optimal control-eigenvalue placement scheme, where linear-quadratic control is applied to the fastest subsystem and eigenvalue assignment is used for the rest of the states.

Acknowledgements

First and foremost, I would like to express my gratitude to my advisor, Professor Zoran Gajić for never hesitating to help and for always having an optimistic attitude toward my research. His vast knowledge on the subject matter has helped me grow immensely as a researcher and I am indebted to him for all my achievements during my graduate studies.

Special thanks go also to Professor Hana Godrich, Professor Dario Pompili, and Professor Jingang Yi for taking time from their busy schedules to serve as members of my defense committee and provide valuable comments on this dissertation. In addition, I would like to thank Professor Ningfan Zhong for his suggestions and for agreeing to be an outside committee member in my defense given the inconvenient logistics. It has been a pleasure collaborating with him on several research projects during the past two years. I can not forget to express my gratitude to Professor Yicheng Lu who has always considered me a colleague rather than a student. I would like to thank him for the academic advice, witty jokes, and interesting discussions on politics as they made the time during my graduate studies a lot more enjoyable.

This work would not have been possible without the financial support provided by the Electrical and Computer Engineering Department at Rutgers University and the School of Engineering. I am grateful to everyone who was involved in the process and made it happen.

While graduate school is usually stressful, the presence of great friends and fellow students makes it always fun. I would like to thank the numerous people that helped alleviate the stress over the years without mentioning any names as I know I would forget someone. Special thanks go to my high school friends for always finding time to do spontaneous things on weekends, go on unforgettable trips, work out, and even

review my papers (thanks Bobi!). I would also like to thank all my fellow graduate students at Rutgers whom I had the pleasure to share the joy and pain of research and celebrate many occasions over the past few years.

Lastly, I would like to thank my parents and my little sister. Their moral support has always motivated me to keep going even when I thought I could not do it. Words can not express how much they have done for me! The completion of this dissertation is a major relief for them too.

Dedication

To the memory of my grandfather, N. Kodra.

Table of Contents

List of Tables

List of Figures

Abbreviations

AMI	Advanced metering infrastructure (p. 3)
CARE	Continuous algebraic Riccati equation (p. 11)
DER	Distributed energy resources (p. 4)
DG	Distributed generation (p. 19)
DOE	Department of Energy (p. 1)
DT	Direct truncation (p. 13)
HSV	Hankel singular values (p. 32)
IM	Islanded microgrid (p. 8)
LQ	Linear quadratic (p. 47)
LQG	Linear-quadratic Gaussian (p. 10)
LQR	Linear-quadratic regulator (p. 10)
LTI	Linear time-invariant (p. 14)
MIMO	Multiple-input multiple-output (p. 93)
MOR	Model order reduction (p. 4)
PCC	Point of common coupling (p. 2)
PEMFC	Proton exchange membrane fuel cell (p. 97)
SISO	Single-input single-output (p. 92)
VSC	Voltage-sourced converter (p. 19)

Chapter 1

Introduction

1.1 Motivation

HIGH demands in energy worldwide and outdated power grid infrastructures have lead to a new paradigm shift that is commonly referred as the *smart grid*. While the traditional grid is unidirectional in nature, the smart grid is characterized by a two-way flow of electricity and information between the utility and the customer. In addition to being more efficient than the current infrastructure, the smart grid offers a lower environmental impact by incentivizing consumers to better manage and efficiently use energy [1]. While there are major technical challenges to be overcome prior to a full-scale implementation, current research has been promising and experimental modern grids set up worldwide have shown superior benefits over the existing grid [2]-[4]. Table 1.1 shows a side by side comparison of the traditional grid versus the new and improved smart grid [1].

A formal definition of the concept of smart grid is provided by the U.S. Department of Energy (DOE) [5]:

"An automated, widely distributed energy delivery network, the Smart Grid will be characterized by a two-way flow of electricity and information and will be capable of monitoring everything from power plants to customer preferences to individual appliances. It incorporates into the grid the benefits of distributed computing and communications to deliver real-time information and enable the near-instantaneous balance of supply and demand at the device level."

Several advantages have been identified in the implementation of smart grids. The benefits among others include [6]:

- Improved reliability;

- Increased physical, operational, and cyber-security against attack or natural disasters;

- Ease of repair;

- Increased information available to users;

- Increased energy efficiency;

- Integration of renewable sources;

- Reduction in peak demand.

Table 1.1: Traditional vs. smart grid

Traditional Grid	Smart Grid
Centralized generation	Generation everywhere
One way power flow	Power flows from everywhere
Utility controlled	Anyone may participate
Predictable behavior	Chaotic behavior

An advantage of the smart grid is that it treats the overall grid as network of smart *microgrids*. A microgrid is simply defined as an electrical energy distribution network that includes a cluster of loads, distributed sources (including renewable sources), transmission systems and storage systems [6]. Because a microgrid contains both loads and sources (typically renewable sources such as wind turbines, solar panels, fuel cells etc.), electric power can be generated within the microgrid. The latter can be coupled with utility power grid via a single connection known as point of common coupling (PCC). The electrical energy can flow in either direction based on customer needs or unexpected emergencies. For example, if a microgrid is "islanded" (disconnected from the main grid), the sources within the microgrid continue to power the users without requiring power from the utility grid. Other advantages include self-healing capabilities and power usage from the utility if any disturbances are present in the microgrid [5]. Besides a relatively high initial investment, there are additional hurdles associated with

smart grids as well as microgrids. Majority of the issues that need to be addressed fall into the following categories [7]

- Communications;

- Demand response applications;

- Security;

- Integration of energy sources in the microgrid.

As it was stated earlier, for a power grid to be "smart" a two-way interaction between the grid and the user is necessary hence communication technologies are paramount for reliable operation and management. Various of these existing communication and networking technologies be it wired or wireless can be utilized in the smart grid [8]. The challenge is to design communication protocols that would be necessary to provide reliable information for areas such as advanced metering infrastructure (AMI), wide-area situational awareness, and distribution grid management. Ongoing research in wireless communications is addressing these questions [9]-[11].

When it comes to demand response applications, the goal is to allow the utility company to manage the users' electric loads. Using incentives such as lowering the price or offering coupons, the utility company can temporarily modify the use of electricity during peak times. This in turn increases the efficiency and reduces the odds of frequent blackouts. While the user-utility interaction seems simplistic, it is quite a complicated process. Tools such as control techniques, optimization, game theory, and microeconomics have been used to study this two-way interaction [12]-[13]. Recent research encompasses development of new machine learning algorithms to aid the demand response application process and make scheduling easier for the user [14]-[15]. Among the bullet points listed above, one of the most important and challenging areas of the overall smart grid infrastructure is cybersecurity. The latter is convoluted in nature due to the diversity of the architecture but nonetheless it is a top priority and is indispensable to avoid cyber attacks which might go undetected and compromise the whole system [16]. Intrusions in the grid such as malware attacks can have devastating

consequences leading to major blackouts. Due its importance, cybersecurity in smart grids has had special attention by researchers lately [16]-[17]. Most recently, control theoretic methods to devise security measures for protection from cyber attacks have been developed [18]-[19]. While recent results are promising for the time being, adversarial attacks will always be a concern hence new strategies will have to be developed continuously to guarantee uninterrupted operation.

Lastly, integration of renewable energy sources such as fuel cells, solar panels, and wind turbines in microgrids is essential in maintaining a steady power flow as well as important to achieve independence from non-renewable sources. One of the most prevalent fields to address issues arising in this area has been control theory. The latter has been used extensively in modeling, optimization, controller and filter design, and estimation to ensure effective integration of renewable sources into the grid [7], [20]-[24]. One area that has been overlooked in the distributed energy resources (DERs) that are connected to microgrids as well as the microgrids themselves are the different time-scales that arise when they are modeled and the impact of time-scales in model order reduction (MOR). While techniques for time-scale separation and order reduction have been used in different formulations for DERs, microgrids, and storage devices [25]-[26] anomalies or proper time-scale decomposition considerations and how they can be effectively used in MOR have not been investigated.

Motivated by these shortcomings, we attempt to address the aforementioned issues in this dissertation by making use of singular perturbation theory. Specifically, the dissertation focuses on three different areas of need: (i) correctly identifying time-scales present in microgrid or DER models, (ii) investigation of the optimal control problem for said models by introducing two input control and developing corresponding algorithms to efficiently obtain the solutions, (iii) develop schemes to obtain explicit multi-time-scale models from implicit ones and design controllers based on individual time-scales. The methods developed in this dissertation improve on computational savings, simplify design, avoid possible ill-conditioning, and help to clearly identify available time-scales in the system.

1.2 Background

Time-scale decomposition and MOR of power systems have been studied extensively in literature, see [27]-[30] and references therein. In this section we review existing literature on order reduction methods and time-scale decomposition as well as their application to DERs and other elements within the microgrid.

1.2.1 Model Order Reduction

Model reduction is an indispensable tool used in analysis, controller design, and simulations of large-scale systems primarily due to very high orders that these models can reach [31]-[36]. The premise of model reduction algorithms is to obtain new reduced-order models that have the same characteristics as the original one, hence simplifying the design process and alleviating computational costs. Because of the various parameters associated with each plant, there is no universal model reduction algorithm [31]. In this section, we review a few common MOR methods and their applications to power grid elements such as DERs and microgrids.

Model reduction is very helpful and generally necessary for transient/small signal analysis in power grid elements models such as machine interconnections, DERs, and microgrids due to the fact that their physical models contain a large number of variables. To rectify this drawback, numerous order reduction algorithms have been developed over the years to decrease the system order without affecting the performance. Some of the most effective methods used in power systems are balancing transformation [31]-[36], Krylov subspace methods [37], Kron reduction [26], gramian-based methods [38], and singular perturbation techniques [26]-[29]. Depending on the type of the model under investigation, each method has its own advantages. For example, in [37], Krylov subspace techniques has been used to simplify complicated models of power systems that can be used in a microgrid environment. This family of order reduction algorithms is based on moment matching methods where the leading coefficients of the power series expansion of the reduced transfer around a nominal point has to match the leading coefficients of the original transfer function to ensure accuracy [37]. One of the main

advantages of Krylov subspace algorithms lies in the computational efficiency. In [38], gramian-based reduction methods are used to investigate large sparse power system descriptor models. These techniques avoid computation of spectral projections onto deflating subspaces of finite eigenvalues which are typically needed when dealing with descriptor systems [38]. Again, this method is beneficial for computational efficiency especially when used in large scale systems (more than one thousand states). Kron reduction is another popular method used in power systems and lately has found to be effective in the study of microgrids [26], [39]. The concept of Kron reduction is fairly simple; it eliminates the nodes in an electrical network where the voltage or current is zero. In addition to computational savings, the reduction simplifies transient and small signal analysis.

Lastly, singular perturbation methods have been very effective when parasitic parameters are identified in the system. For power system this could mean parasitic resistance, capacitance, or inductance during interconnections of DERs between themselves or the grid [29], [40]-[41]. The small parameter, which in this dissertation will be denoted by ε, causes a *slow* and *fast* time-scale separation and if the fast time-scale is much faster, the slow subsystem with a boundary layer correction from the fast subsystem provides a good approximation of the original model [42]-[43]. Singular perturbation methods have also been used in conjunction with other methods such as Kron [26] and balancing [30] (see [44]-[45] for additional information on balancing-singular perturbation combination) to attain even better results. One interesting observation that has not been investigated earlier with the use of singular perturbations in power systems is that existing modes may be misclassified. For example, seemingly slow modes might in fact be fast modes. This dissertation addresses this observation.

As discussed earlier, each method has its own advantages and can be superior over others depending on the application. The system and the problem formulation are the prime factors that influence the selection of the most effective technique to carry out order degeneration.

1.2.2 Time-Scale Separation

Time-scale separation in this dissertation is exclusively based on singular perturbation theory hence the discussion in this section is limited to time-scale separation using singular perturbation methods. As mentioned in the previous sub-section, one of the main reasons for separation of time-scales lies in the degeneration of the original model to a low-order one. Fast transients generally attenuate very rapidly therefore the slow subsystem can be used to approximate the original plant [46]. In addition, separating the modes is also beneficial for modeling purposes. An example where the fast subsystem is used to detect the fast transients occurring in a power system is mentioned in the next paragraph. Since singular perturbation theory is the basis theoretical framework for the contributions in this dissertation, a more detailed overview of it is presented in the next chapter.

A brief survey of singular perturbation theory applied to power systems modeling and stability analysis is discussed in [27]. Topics in [27] include synchronous machine modeling, decomposition of large power networks, order reduction of dynamic models, and transient stability analysis using direct methods. The discussion in [27] is restricted to two time-scale systems with slow and fast dynamics. Time-scale separation in power systems has focused in numerous areas over the years. For example, in [29], the problem is focused on generators used in the grid. Here, singular perturbation techniques have been utilized to obtain the slow and fast modes associated with the generators. These fast subsystem is then used to model the generators and other related components such as static exciters and power system stabilizers. Similarly in [40], time-scale decomposition is used for order-reduction and modeling in interconnected multi-machine power systems. Singular perturbation theory is used in this case to produce improved models without adding the network transient equations. Both slow and fast subsystems are used for analysis and modeling in [40], unlike in [29] where only fast modes are of interest. In [47], time-scale decomposition is used for modeling for dynamic voltage analysis. The *quasi-steady state* equation is used for order reduction implying that the slow modes serve as a good approximation of the overall model. In addition, integral

manifold theory is used to compare the results of the reduced-order model and the original. In [41], a different approach is considered compared to the aforementioned literature. The authors still consider a two time-scale singularly perturbed problem but they explore the case when high oscillations and low damping occurs in power systems such as machine interconnection. The oscillations are classified as fast modes.

As evident by the literature review, the use of singular perturbation methods in power systems has been primarily used for modeling or order reduction in the two-time-scale sense. In this dissertation, multi-time-scale singularly perturbed systems have been studied and techniques for control design have been proposed. Furthermore, the case when separate inputs control slow and fast time-scales has been investigated. The latter is motivated by models of real physical systems that can be controlled more efficiently by introducing corresponding inputs for each time-scale.

1.3   Dissertation Objective

Earlier it was discussed that singular perturbation techniques have been heavily used in power systems in the context of two time-scales. Depending on the application, slow or fast modes can be used separately or in conjunction for modeling, control, or both. Some examples such as renewable energy sources or events such as the occurrence of islanded microgrids (IMs) [48] or interconnection of DERs within a microgrid were discussed previously. To ensure high accuracy in MOR and proper time-scale decomposition, it is essential to carefully investigate these models prior to designing controllers or filters. For example, while for a two time-scale model with a large separation of its time-scales might seem right to use the slow subsystem to approximate the original model, it is not always true as it will be shown later. This large separation between the slow and fast modes also serves as motivation to design dedicated controllers instead of using the same one for both time-scales. In addition, we are not always dealing with a two time-scale decomposition (e.g. [49]-[50] where three time-scales are evident), hence it is necessary to develop a theoretical framework to address these issues for better results.

The objective of this research is to investigate system having the same properties as the aforementioned examples. Inspired by real physical systems, we propose methods to simplify multi-time-scale modeling as well as develop new control design methods using the simplified models. Furthermore, we consider two time-scale systems controlled by two inputs controlling the slow and the fast subsystems independently and solve the optimal control problem iteratively to avoid ill-conditioning which is prone in singular perturbation systems. While one input is frequently used and it has been shown to work well, two inputs are more effective when the time-scale separation is large. Here, it is important to note that the input matrix is partitioned in a specific structure as it will be discussed later [48].

Previous work on the theoretical methods developed in this research comes from several references. For example, for the multi-time-scale problem, the work is primarily based on [51]. In [51], the Chang transformation [52] is sequentially applied to decouple multi-time-scale systems. In contrast, we initially use an ordered Schur decomposition prior to applying the sequential algorithm. To accomplish the ordered decomposition methods from [53]-[58] have been utilized. For the work in **Chapter 3**, the main references are [59]-[60]. Our work differs from [59]-[60] in the sense that two control inputs are used for control instead. Additional references concerning recursive methods for the solution of deterministic as well as stochastic linear singular perturbation systems are given in [67]-[70].

1.4   Dissertation Outline and Contributions

The dissertation is organized into five chapters. **Chapter 1** serves as the introduction of the dissertation and covers the motivation behind this work, background and literature review, the dissertation objective and outline, and the contributions made. **Chapter 2** is a time-scale analysis of an IM model derived in [48]. In this chapter, we start off with the model description and background on singular perturbation methods. Then, the latter are used to analyze the MOR performance of the IM model open-loop model. Several remarks and findings are presented in this chapter but the major observation is an anomaly in time-scale decomposition using singular perturbation methods.

Chapter 3 covers a new class of singular perturbation systems. Here, optimal control of singularly perturbed systems containing different structure input matrices is considered. The case when two inputs are present instead of one is investigated. The optimal linear-quadratic regulator (LQR) is solved iteratively in terms of reduced-order sub-problems to avoid possible ill-conditioning. In addition, the problem has been extended to stochastic linear filtering where the optimal linear-quadratic Gaussian (LQG) is also solved iteratively. **Chapter 4** focuses on multi-time-scale singularly perturbed systems. Ordered Schur decomposition is used to convert a general implicit multi-time-scale model into explicit form where all the available time-scales are ordered. The new model is later decoupled into individual time scales. Initial control is proposed by utilizing eigenvalue placement and then a hybrid optimal LQR eigenvalue placement controller design follows. Finally, **Chapter 5** contains conclusions and directions for ongoing and future work. A graphical organization of the dissertation is shown in Fig. 1.1.

Note on Notation: In several instances throughout this dissertation, the same symbols have been used for similar quantities. Unless otherwise stated or referenced, the quantities pertain to the specific chapter or section where they are used.

    The major contributions of this dissertation are as follows.

1. In **Chapter 2** a sixth-order linear model of an IM system with highly damped and highly oscillatory behavior is analyzed. Open-loop analysis is initially performed on the said model and based on simulation results we show that the slow subsystem does not generate an accurate representation of the original model as is typical in singular perturbation theory. On the other hand, the fourth-order fast subsystem provides a good approximation of the original sixth-order system. Further analytical analysis of the eigenvalues of the model reveals that instead it contains fast and very fast modes i.e. the *slow* modes are nonexistent and the *very fast* modes contain the system's dynamics. The anomaly in singular perturbation theory unveiled in this chapter was published in [71] and is another manuscript is under preparation for journal publication [72].
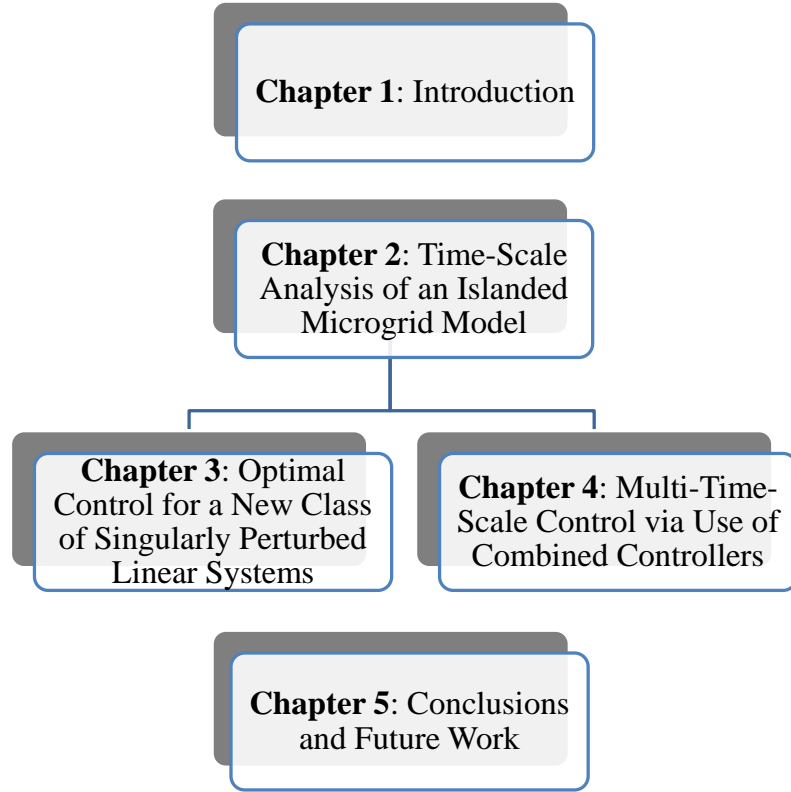
Figure 1.1: Outline of the dissertation

2. In **Chapter 3**, motivated by the system discussed in **Chapter 2** as well as other physical systems [59]-[60], we consider a new class of singularly perturbed systems which has uniquely partitioned input matrix structures and is controlled by two inputs. The LQR problem is initially investigated. We start by obtaining the zero-order solution of the continuous algebraic Riccati equations (CAREs) and show that that instead of solving two separate CAREs to obtain the LQR gain, only one CARE and a matrix algebraic equation are sufficient to obtain the solution. Parallel algorithms based on fixed-point iteration methods are proposed to determine the error of the original CARE equations and their corresponding zero-order approximations. This work is further extended to the LQG problem where the solution has been similarly simplified and parallel algorithms have been proposed to obtain the accurate cost function in a few iterations. The developed methods

improve on computational efficiency as well as avoid possible ill-conditioning arising due to the presence of perturbation parameter ε. The deterministic part of this research was published in [73]. The stochastic part was published in [74] and a more extended version is currently under review for journal publication in [75].

3. In **Chapter 4** we consider systems containing multiple time-scales. An ordered Schur form decomposes the system matrix into a quasi-triangular form where eigenvalues are clustered in 1×1 or 2×2 blocks (for real and complex eigenvalues respectively) in a ordered fashion. The ratio of the magnitude of the fastest eigenvalue of the slowest cluster with the slowest eigenvalue of the rest of clusters determines the perturbation parameters and from there an explicit singularly perturbed system is obtained. Next, Chang transformation [52] is used sequentially to completely decouple the system into independent time-scales. We show that our method simplifies time-scale decoupling due to the quasi-triangular form of the system matrix. Then, controller design is proposed based on individual time-scales. The eigenvalue placement method is investigated where individual states from the decoupled subsystems are fed back sequentially instead of the whole state vector. Lastly, controller design based on a combination of pole placement and optimal control is considered where LQR has been used as a primary tool for the fastest subsystem and eigenvalue assignment is used for the rest of the subsystems. Part of this research was published in [76] and another manuscript is currently in preparation for journal publication.

Chapter 2

Time-scale Analysis of an Islanded Microgrid Model

M ICROGRIDS are considered building blocks of the future smart grid because they are very reliable, integrate renewable energy sources, and can operate independent of the main grid (islanded mode) if needed [7]. In addition, they enable generation of energy at the point of consumption which is cost efficient, helps avoid blackouts, and is to control. As the current electrical grid is slowly upgraded to a state-of-the-art system, extensive research is necessary in all areas encompassing operation, control, and safety to ensure uninterrupted operation [5]-[7].

One of the main issues associated with microgrids and the DERs within them is modeling of the system [6]. It is typical for microgrid, DERs, or other elements such as synchronous machines and their interconnections to reach order of hundreds of variables when modeled in their entirety. In addition to computational burdens, the large system order makes controller design quite difficult to implement due to numerous feedback loops hence, almost always there is a need for MOR. In **Chapter 1**, we reviewed related literature on order reduction methods applied to microgrids and DERs as well as some challenges faced during the process.

In this chapter, we focus on a six-order model of an IM system [48]. This model represents a simplified scenario right after the microgrid has been disconnected from the main grid. Two model-reduction methods have been considered to simplify the dynamics; first the singular perturbation method and then direct truncation (DT) method of the balanced model. Three different singular perturbation techniques have been utilized for analysis:

- Residualized singular perturbation (perturbation parameter ε is 0)

- Generalized singular perturbation (perturbation parameter ε is not 0)

- Order reduction based on the fast subsystem

While the model under consideration is not large-scale, the motivation behind order reduction is to exploit an anomaly in the time-scale decomposition using singular perturbations.

The rest of the chapter is organized as follows. Section 2.1 contains an overview of the main theoretical framework of this dissertation, namely singular perturbation methods. In Section 2.2 a description of the model is provided. The performance evaluation of the order reduction techniques is discussed in Section 2.3. Section 2.4 discusses some remarks and findings. We explicitly show that the microgrid model under investigation containing both highly and lightly damped, highly oscillatory modes contains fast and very fast but no slow modes. Hence, we cannot have an approximation of the original model based on the slow subsystem as is typical in singular perturbation methods. In Section 2.5 we show that the IM model can be also successfully analyzed using model order-reduction methods based on the balancing transformation. In this section a table containing numerical errors of the reduced-order models for different input is also provided. In Section 2.6, the frequency responses of the reduced-order models using the combination of both techniques have been explored and finally, Section 2.7 concludes the chapter.

2.1   Background on Singular Perturbation Methods

Singular perturbation theory has its origins in the 1950s initially appearing in applied mathematics research [77]. The theory was later adopted for use in controls due to its versatility in time-scale separation and order reduction. In this section we give a brief overview of singular perturbation techniques for linear systems. While this background would be adequate for this dissertation, the reader can refer to [43], [46] and references therein for more advanced topics. A standard linear time-invariant (LTI)

singularly perturbed system given in equation (2.1), [46]

$$\dot{x}_1(t) = \mathbf{A}_1 x_1(t) + \mathbf{A}_2 x_2(t) + \mathbf{B}_1 u(t), \quad x_1(t_0) = x_{10}$$

$$\varepsilon \dot{x}_2(t) = \mathbf{A}_3 x_1(t) + \mathbf{A}_4 x_2(t) + \mathbf{B}_2 u(t), \quad x_2(t_0) = x_{20} \tag{2.1}$$

$$y(t) = \mathbf{C}_1 x_1(t) + \mathbf{C}_2 x_2(t) + \mathbf{D} u(t)$$

For the system in (2.1), the following is assumed.

Assumption 2.1: Pairs $(\mathbf{A}, \mathbf{B})$ and $(\mathbf{A}, \mathbf{C})$ are controllable and observable respectively.

We denote

$$\mathbf{A} = \begin{bmatrix} \mathbf{A}_1 & \mathbf{A}_2 \\ \frac{1}{\varepsilon}\mathbf{A}_3 & \frac{1}{\varepsilon}\mathbf{A}_4 \end{bmatrix}, \mathbf{B} = \begin{bmatrix} \mathbf{B}_1 \\ \frac{1}{\varepsilon}\mathbf{B}_2 \end{bmatrix}, \mathbf{C} = \begin{bmatrix} \mathbf{C}_1 & \mathbf{C}_2 \end{bmatrix}, \mathbf{D} = 0 \tag{2.2}$$

where ε is a small positive singular perturbation parameter $(0 < \varepsilon \ll 1)$ that for a real physical system might represent parameters such as small time constants in electrical circuits or small masses in mechanical systems. In this dissertation we assume that the perturbation parameter ε is obtained from the ratio of eigenvalues of adjacent time-scale clusters unless stated otherwise. Specifically, ε is evaluated as the ratio of the fastest eigenvalue of the slow subsystem with the slowest eigenvalue of the fast subsystem.

Matrices $\mathbf{A}_1$ and $\mathbf{A}_4$ are of dimensions $r \times r$ and $(n-r) \times (n-r)$, respectively. While not always the case (see for example [78]), in the rest of the dissertation the following is assumed.

Assumption 2.2: Matrix $\mathbf{A}_4$ is invertible and asymptotically stable.

For sufficiently small ε, the dynamics of singularly perturbed system in (2.1) can be approximated by the dynamics of lower-dimensional slow and fast subsystems [46], [79].

The slow subsystem is given by

$$\dot{\bar{x}}_1(t) = \mathbf{A}_0 \bar{x}_1(t) + \mathbf{B}_0 u(t)$$

$$y(t) = \mathbf{C}_0 \bar{x}_1(t) + \mathbf{D}_0 u(t) \tag{2.3}$$

Equation (2.3) is known as the *residualized* model and is obtained by solving the second equation of the quasi-steady state system of (2.1) obtained by setting $\varepsilon = 0$. The

matrices $\mathbf{A}_0$, $\mathbf{B}_0$, $\mathbf{C}_0$, and $\mathbf{D}_0$ are defined in (2.4).

$$\mathbf{A}_0 := \mathbf{A}_1 - \mathbf{A}_2 \mathbf{A}_4^{-1} \mathbf{A}_3, \quad \mathbf{C}_0 := \mathbf{C}_1 - \mathbf{C}_2 \mathbf{A}_4^{-1} \mathbf{A}_3$$

$$\mathbf{B}_0 := \mathbf{B}_1 - \mathbf{A}_2 \mathbf{A}_4^{-1} \mathbf{B}_2, \quad \mathbf{D}_0 := \mathbf{D} - \mathbf{C}_2 \mathbf{A}_4^{-1} \mathbf{B}_2$$

(2.4)

The fast subsystem is given by

$$\varepsilon \dot{\bar{x}}_2(\tau) = \mathbf{A}_4 \bar{x}_2(\tau) + \mathbf{B}_2 u(\tau)$$

$$y(\tau) = \mathbf{C}_2 \bar{x}_2(\tau) + \mathbf{D} u(\tau)$$

(2.5)

where $\tau = \frac{t}{\varepsilon}$. According to the theory of singular perturbation [46], the approximations satisfy

$$x_1(t) = \bar{x}_1(t) + O(\varepsilon), \quad \forall t \geq t_0$$

$$x_2(t) = \bar{x}_2(t) - \mathbf{A}_4^{-1}(\mathbf{A}_3 \bar{x}_1(t) + \mathbf{B}_2 u(t)) + O(\varepsilon), \quad \forall t \geq t_0 + O(\varepsilon)$$

(2.6)

The eigenvalues of the system in equation (2.3), $\lambda(\mathbf{A}_0)$, differ by an $\mathcal{O}(\varepsilon)$ perturbation from the slow eigenvalues of the original system. Similarly, the eigenvalues of the fast subsystem (2.5) differ by an $\mathcal{O}(\varepsilon)$ perturbation from the fast eigenvalues $\lambda(\mathbf{A}_4/\varepsilon)$ of the full-order model. Hence, the smaller ε, the better the approximation.

A summary of the important features of the singularly perturbed systems are given as follows [43].

1. The residualized system in (2.3), is of reduced order and cannot satisfy all of the given boundary conditions of the original perturbed problem.

2. There exists a boundary layer where the solution changes rapidly. The boundary conditions that are lost during the process of degeneration are buried inside the boundary layer.

3. To recover the lost initial conditions and improve on the approximation, a correction is usually needed and that is accomplished by stretching the boundary layer using a stretching transformation such as $\tau = t/\varepsilon$.

4. The singularly perturbed problem in (2.1) has two separated characteristic roots giving rise to slow and fast modes in its solution hence the reason for a two-time scale property. The simultaneous presence of slow and fast phenomena makes the problem ill-conditioned from a numerical solution point of view.

Comments: In this dissertation, the term "sufficiently small" is used in a few occasions to indicate that the singular perturbation parameter ε is small enough such that theory holds. It is important to note that while ε is generally much smaller than one, it is problem dependent. Its variation has been discussed in [80]-[81] and more recently in [45].

2.1.1 Exact Time-Scale Decomposition

Earlier we pointed out that degenerating the full-order model by setting $\varepsilon = 0$, only an approximation of the original model is obtained and a boundary layer correction is needed to account for setting $\varepsilon = 0$. Fortunately, there is a similarity transformation usually referred as the Chang transformation that decouples the dynamics of a two time-scale system into independent slow and fast subsystems. A linear singularly perturbed system (2.1) can be transformed into pure-slow and pure-fast subsystems via this transformation as follows [52].

$$\begin{bmatrix} z_1(t) \\ z_2(t) \end{bmatrix} = \begin{bmatrix} \mathbf{I} - \varepsilon\mathbf{ML} & -\varepsilon\mathbf{M} \\ \mathbf{L} & \mathbf{I} \end{bmatrix} \begin{bmatrix} x_1(t) \\ x_2(t) \end{bmatrix} = \mathbf{T} \begin{bmatrix} x_1(t) \\ x_2(t) \end{bmatrix} \tag{2.7a}$$

$$\begin{bmatrix} x_1(t) \\ x_2(t) \end{bmatrix} = \begin{bmatrix} \mathbf{I} & \varepsilon\mathbf{M} \\ -\mathbf{L} & \mathbf{I} - \varepsilon\mathbf{LM} \end{bmatrix} \begin{bmatrix} z_1(t) \\ z_2(t) \end{bmatrix} = \mathbf{T}^{-1} \begin{bmatrix} z_1(t) \\ z_2(t) \end{bmatrix} \tag{2.7b}$$

The application of the transformation in equation (2.7) to a singularly perturbed system leads to

$$\begin{aligned} \dot{z}_1(t) &= (\mathbf{A}_1 - \mathbf{A}_2 L)z_1(t) + (\mathbf{B}_1 - \mathbf{MB}_2 - \varepsilon\mathbf{MLB}_1)u(t) \\ &= \mathbf{A}_s z_1(t) + \mathbf{B}_s u(t) \\ \varepsilon\dot{z}_2(t) &= (\mathbf{A}_4 + \varepsilon\mathbf{LA}_2)z_2(t) + (\mathbf{B}_2 + \varepsilon\mathbf{LB}_1)u(t) \\ &= \mathbf{A}_f z_2(t) + \mathbf{B}_f u(t) \\ y(t) &= (\mathbf{C}_1 - \mathbf{C}_2\mathbf{L})z_1(t) + (\mathbf{C}_2 - \varepsilon\mathbf{C}_2\mathbf{LM} + \varepsilon\mathbf{C}_1\mathbf{M})z_2(t) + \mathbf{D}u(t) \\ &= \mathbf{C}_s z_1(t) + \mathbf{C}_f z_2(t) + \mathbf{D}u(t) \end{aligned} \tag{2.8}$$

where

$$\mathbf{A}_s = \mathbf{A}_1 - \mathbf{A}_2\mathbf{L}, \quad \mathbf{B}_s = \mathbf{B}_1 - \mathbf{MB}_2 - \varepsilon\mathbf{MLB}_1$$

$$\mathbf{A}_f = \mathbf{A}_4 + \varepsilon\mathbf{LA}_2, \quad \mathbf{B}_f = \mathbf{B}_2 + \varepsilon\mathbf{LB}_1 \tag{2.9}$$

$$\mathbf{C}_s = \mathbf{C}_1 - \mathbf{C}_2\mathbf{L}, \quad \mathbf{C}_f = \mathbf{C}_2 - \varepsilon\mathbf{C}_2\mathbf{LM} + \varepsilon\mathbf{C}_1\mathbf{M}$$

$\mathbf{L}$ and $\mathbf{M}$ satisfy the following algebraic equations [52]

$$\mathbf{A}_4\mathbf{L} - \mathbf{A}_3 - \varepsilon\mathbf{L}(\mathbf{A}_1 - \mathbf{A}_2\mathbf{L}) = 0$$

$$\mathbf{MA}_4 - \mathbf{A}_2 + \varepsilon(\mathbf{MLA}_2 - \mathbf{A}_1\mathbf{M} + \mathbf{A}_2\mathbf{LM}) = 0 \tag{2.10}$$

A unique solution to (2.10) exists when ε is sufficiently small and under Assumption 2.2. Several algorithms that can be used to solve (2.10), see for example [67], [82]-[83]. The algorithm based on the Newton's method has a quadratic rate of convergence of $O(\varepsilon^{2i})$ and is outlined below [84].

$$\mathbf{D}_1^{(i)}\mathbf{L}^{(i+1)} + \mathbf{L}^{(i+1)}\mathbf{D}_2^{(i)} = \mathbf{Q}^{(i)}$$

$$\mathbf{D}_1^{(i)} = \mathbf{A}_4 + \varepsilon\mathbf{L}^{(i)}\mathbf{A}_2 \quad \mathbf{D}_2^{(i)} = -\varepsilon(\mathbf{A}_1 - \mathbf{A}_2\mathbf{L}^{(i)}) \tag{2.11}$$

$$\mathbf{Q}^{(i)} = \mathbf{A}_3 + \varepsilon\mathbf{L}^{(i)}\mathbf{A}_2\mathbf{L}^{(i)} \quad \mathbf{L}^{(0)} = \mathbf{A}_4^{-1}\mathbf{A}_3$$

Once $\mathbf{L}$ is obtained from (2.11), we can solve the second equation in (2.10) as a linear Sylvester equation to obtain $\mathbf{M}$ directly as

$$\mathbf{M}^{(i+1)}\mathbf{D}_1^{(i+1)} + \mathbf{D}_2^{(i+1)}\mathbf{M}^{(i+1)} = \mathbf{A}_2 \tag{2.12}$$

Because the initial guess of this algorithm satisfies $\|\mathbf{L} - \mathbf{L}^{(0)}\| = \mathcal{O}(\varepsilon)$, it converges in only a few iterations. If the algorithm diverges or the performance is not satisfactory then the eigenvector method of [82] or the fixed-point iteration method of [67] must be used. The latter is often very effective due to its linear convergence; after each iteration the accuracy improves by $\mathcal{O}(\varepsilon)$. Equation (2.13) summarizes the fixed-point method to solve the $\mathbf{L}$-equations.

$$\mathbf{A}_4\mathbf{L}^{(i+1)} = \mathbf{A}_3 + \varepsilon\mathbf{L}^{(i)}(\mathbf{A}_1 - \mathbf{A}_2\mathbf{L}^{(i)})$$

$$\mathbf{L}^{(0)} = \mathbf{A}_4^{-1}\mathbf{A}_3, \ i = 0, 1, 2, \dots \tag{2.13}$$

Matrix $\mathbf{M}$ is obtained after each iteration by solving the Sylvester equation in (2.10).
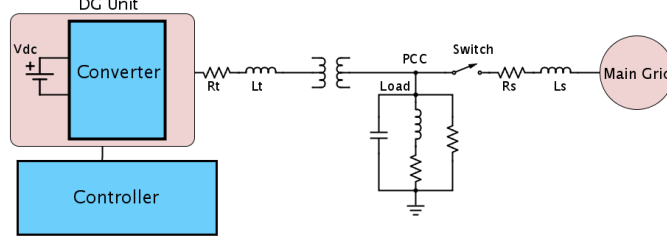
Figure 2.1: Schematic of the islanded system

2.2 Model Description

A simplified diagram of the IM system which is a typical setup used widely in smart grid systems is shown in Fig. 2.1. Kirchhoff's circuit laws have been used to obtain a third-order model. Under balanced conditions the initial model can be transformed into an $\alpha\beta$-reference frame, which is further simplified by applying a dq transformation leading to a six order model [48]. The state variable vector is $x = \begin{bmatrix} V_d & V_q & I_{td} & I_{tq} & I_{Ld} & I_{Lq} \end{bmatrix}' \in \mathbb{R}^6$, the input vector is $u = \begin{bmatrix} V_{td} & V_{tq} \end{bmatrix}' \in \mathbb{R}^2$, and the output vector is $y = \begin{bmatrix} V_d & V_q \end{bmatrix}' \in \mathbb{R}^2$ [48], where V_d and V_q represent the voltages at the point of common coupling (PCC) after the dq transformation, I_{td} and I_{tq} represent the currents originating from the distributed generation (DG) unit, I_{Ld} and I_{Lq} represent load currents, and V_{td} and V_{tq} represent the voltages at the DG unit. Matrices $\mathbf{A}$, $\mathbf{B}$, and $\mathbf{C}$ representing the state, input, and output matrices respectively are given below.

$$\mathbf{A} = \begin{bmatrix} -\frac{1}{RC} & \omega_0 & \frac{1}{C} & 0 & -\frac{1}{C} & 0 \\ -\omega_0 & -\frac{1}{RC} & 0 & \frac{1}{C} & 0 & -\frac{1}{C} \\ -\frac{1}{L_t} & 0 & -\frac{R_t}{L_t} & \omega_0 & 0 & 0 \\ 0 & -\frac{1}{L_t} & -\omega_0 & -\frac{R_t}{L_t} & 0 & 0 \\ \frac{1}{L} & 0 & 0 & 0 & -\frac{\omega_0}{q_l} & \omega_0 \\ 0 & \frac{1}{L} & 0 & 0 & -\omega_0 & -\frac{\omega_0}{q_l} \end{bmatrix}$$

$$\mathbf{B} = \begin{bmatrix} 0 & 0 & \frac{1}{L_t} & 0 & 0 & 0 \\ 0 & 0 & 0 & \frac{1}{L_t} & 0 & 0 \end{bmatrix}^T, \quad \mathbf{C} = \begin{bmatrix} 0 & 1 & 0 & 0 & 0 & 0 \\ 1 & 0 & 0 & 0 & 0 & 0 \end{bmatrix}$$

The numerical values of the parameters in matrices **A** and **B** are given in Table 2.1. They include the resistance and inductance of the voltage-sourced converter (VSC) filter at the DG unit, the load nominal resistance, inductance, and capacitance, the inductor quality factor, and the system nominal frequency. Substituting the quantities,

Table 2.1: Parameters of the IM system

Quantity	Numerical Value
Resistance of VSC filter	$R_t = 1.5\,m\Omega$
Inductance of VSC filter	$L_t = 300\,\mu H$
Load nominal capacitance	$C = 62.86\,\mu F$
Load nominal inductance	$L = 111.9\,mH$
Load nominal resistance	$R = 76\,\Omega$
Inductor quality factor	$q_l = 120$
System nominal frequency	$f_0 = 60\,Hz$

we obtain the following numerical values for the system and control matrices.

$$
\mathbf{A} = \begin{bmatrix}
-209.32 & 376.99 & 15908 & 0 & -15908 & 0 \\
-376.99 & -209.32 & 0 & 15908 & 0 & -15908 \\
-3333.3 & 0 & -5 & 376.99 & 0 & 0 \\
0 & -3333.3 & -376.99 & -5 & 0 & 0 \\
8.9366 & 0 & 0 & 0 & -3.1416 & 376.99 \\
0 & 8.9366 & 0 & 0 & -376.99 & -3.1416
\end{bmatrix}
$$

$$
\mathbf{B} = \begin{bmatrix}
0 & 0 \\
0 & 0 \\
3333.3 & 0 \\
0 & 3333.3 \\
0 & 0 \\
0 & 0
\end{bmatrix}
$$

The model under consideration is stable and exhibits oscillatory behavior as can be observed from the eigenvalues given in Table 2.2. Using the standard theory of singular perturbation, [46], and information about the system eigenvalues, it is obvious that they are clustered into two groups: complex conjugate pairs located close to the

imaginary axis that are considered slow and eigenvalues located far from the imaginary axis which are responsible for the system's fast dynamics. It is customary in singularly perturbed systems to appropriately eliminate the fast modes and approximate the system dynamics by the slow modes only. We will show in the next two sections that such an approximation will produce poor results due to the existence of both lightly and highly damped, highly oscillatory modes. The case of lightly damped highly oscillatory modes has been considered in [41].

Table 2.2: Eigenvalues of the IM model

i	λ_i
1	$-3.15 + 377.0j$
2	$-3.15 - 377.0j$
3	$-107.16 + 7668.06j$
4	$-107.16 - 7668.06j$
5	$-107.16 + 6914.07j$
6	$-107.16 - 6914.07j$

Before investigating model reduction via singular perturbations, it is important to note that the present structure of the model is not in standard singularly perturbed form. To resolve this issue, we introduce a permutation matrix that serves as a similarity transformation.

$$\mathbf{P}_{IM} = \begin{bmatrix} 0 & 0 & 0 & 0 & 0 & 1 \\ 0 & 0 & 0 & 0 & 1 & 0 \\ 0 & 0 & 1 & 0 & 0 & 0 \\ 0 & 0 & 0 & 1 & 0 & 0 \\ 0 & 1 & 0 & 0 & 0 & 0 \\ 1 & 0 & 0 & 0 & 0 & 0 \end{bmatrix}$$

Matrix $\mathbf{P}_{IM}$ swaps the rows of the original matrix such that the new model is in standard singularly perturbed form. That is, the eigenvalues of the residualized system (2.4), $\lambda(\mathbf{A}_0)$ correspond to the two slowest eigenvalues of the system and $\lambda(\mathbf{A}_4/\varepsilon)$ correspond to the remaining four fastest eigenvalues. The new matrices $\bar{\mathbf{A}} = \mathbf{P}_{IM}\mathbf{A}\mathbf{P}_{IM}$, $\bar{\mathbf{A}} = \mathbf{P}_{IM}\mathbf{B}$, and $\bar{\mathbf{C}} = \mathbf{C}\mathbf{P}_{IM}$ of the standard singularly perturbed system are now given as

$$\bar{\mathbf{A}} = \begin{bmatrix} -3.1416 & -376.99 & 0 & 0 & 8.9366 & 0 \\ 376.99 & -3.1416 & 0 & 0 & 0 & 8.9366 \\ 0 & 0 & -5 & 376.99 & 0 & -3333.3 \\ 0 & 0 & -376.99 & -5 & -3333.3 & 0 \\ -15908 & 0 & 0 & 15908 & -209.32 & -376.99 \\ 0 & -15908 & 15908 & 0 & 376.99 & -209.32 \end{bmatrix}$$

$$\bar{\mathbf{B}} = \begin{bmatrix} 0 & 0 & 3333.3 & 0 & 0 & 0 \\ 0 & 0 & 0 & 3333.3 & 0 & 0 \end{bmatrix}^{T}, \quad \bar{\mathbf{C}} = \begin{bmatrix} 0 & 0 & 0 & 0 & 0 & 1 \\ 0 & 0 & 0 & 0 & 1 & 0 \end{bmatrix}$$

2.3 Model Reduction Performance Evaluation

To evaluate the performance of the singular perturbation reduction methods on the IM model, the step and impulse responses are used. We compare the slow and fast subsystems obtained using the classical singular perturbation techniques and exact decoupling via the Chang transformation with the responses of the original full order model shown in Fig. 2.2 and Fig. 2.3. All simulations in this dissertation have been performed using MATLAB$^{\circledR}$.
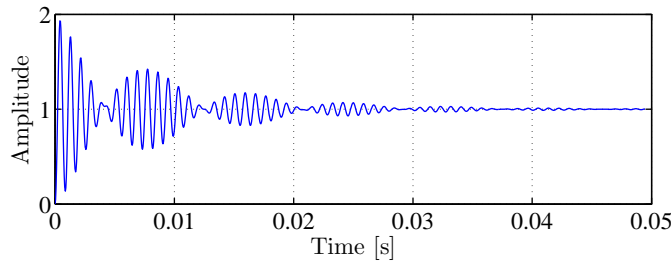
Figure 2.2: Step response of the original model

2.3.1 Order Reduction via Classical Singular Perturbations

Traditionally, the slow subsystem model defined in (2.3) and (2.4) has been successfully used for power systems model reduction [26]-[47]. We attempt the same with our
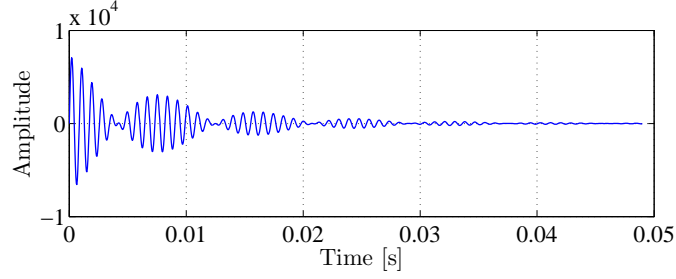
Figure 2.3: Impulse response of the original model
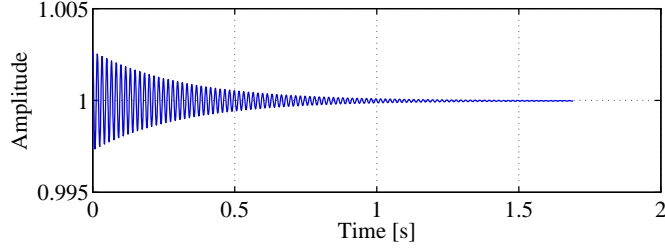
Figure 2.4: Step response of reduced-order slow subsystem (no correction)

IM system by initially residualizing it ($\varepsilon = 0$) to obtain the reduced models. Table 2.3 shows the eigenvalue clusters after the residualization and it is clear that these eigenvalues are very close to the original ones. However, the responses of the residualized system give a very poor approximation of the original perturbed model as presented in Fig. 2.4 and Fig. 2.5 despite the fact that ε is very small (see Fig. 2.2 and Fig. 2.3 and note *different time axis*).

The small parameter ε for our problem is evaluated as the ratio of the real parts of the fastest slow and slowest fast eigenvalues $\varepsilon = \mathrm{Re}\{\lambda_{s_{max}}\}/\mathrm{Re}\{\lambda_{f_{min}}\} \approx 0.03$ [85].

Table 2.3: Slow and fast subsystems eigenvalues of the residualized IM model ($\varepsilon = 0$)

i	λ_i
1	$-3.16 + 378.0j$
2	$-3.16 - 378.0j$
3	$-107.16 + 7658.1j$
4	$-107.16 - 7658.1j$
5	$-107.16 + 6904.3j$
6	$-107.16 - 6904.3j$

It is important to note that the responses in Fig. 2.4 and Fig. 2.5 do not include a
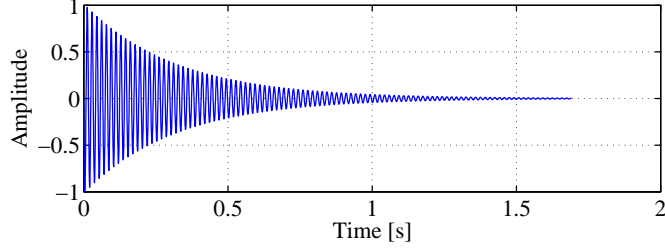
Figure 2.5: Impulse response of reduced-order slow subsystem (no correction)
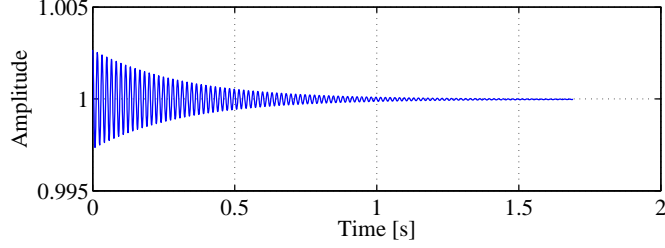
Figure 2.6: Step response of reduced-order slow subsystem (with correction)

boundary layer correction. To improve the approximation, we add the DC gain of the fast subsystem to the residualized model as follows [85].

$$G_{app}(s) \approx \mathbf{C}_0(s\mathbf{I} - \mathbf{A}_0)^{-1}\mathbf{B}_0 + \mathbf{D} - \mathbf{C}_2\mathbf{A}_4^{-1}\mathbf{B}_2 \qquad (2.14)$$

Equation (2.14) has shown to be effective when ε is very small as in our case. The responses due to (2.14) are shown in Fig. 2.6 and Fig. 2.7. Clearly, no improvement is observed over the responses of the residualized model without a boundary layer correction.

Interestingly, looking at the responses of the fast subsystem in Fig. 2.8 and Fig. 2.9 we observe that the behavior of both responses matches that of the original (numerical errors of the original and approximate responses will be evaluated later in this chapter).
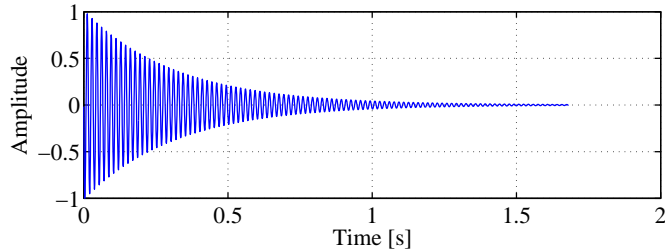
Figure 2.7: Impulse response of reduced-order slow subsystem (with correction)

The impact of the fast subsystem in approximating the perturbed model will be explored later.
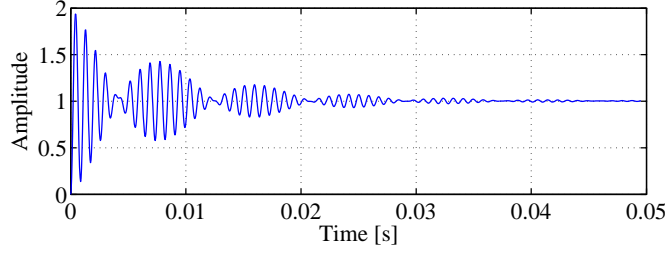
Figure 2.8: Step response of fast subsystem
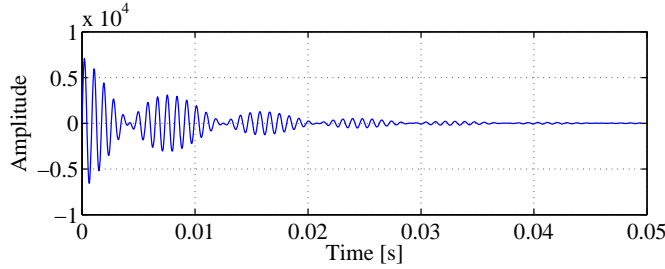
Figure 2.9: Impulse response of fast subsystem

In the next sub-section we make use of the exact decomposition of the time-scales to further investigate the anomaly.

2.3.2   Order Reduction via Exact Time-Scale Decomposition

Since the previous results were not satisfactory, we employ exact time-scale decomposition based on the Chang transformation to re-investigate MOR for the singularly perturbed model. Using the methods of Section 2.1.1, we decouple the model into exactly slow and fast modes. Table 2.4 shows the eigenvalue clusters after the accurate decomposition.

We carry out the same simulations as in the previous section. The step and impulse responses of the slow second order model are initially generated (Fig. 2.10 and Fig. 2.11 respectively).

As in the residualized case (responses are not the same), we see that the approximation is very poor for both responses. While insignificant to our problem, the boundary

Table 2.4: Slow and fast subsystems eigenvalues of the exactly decoupled IM model

i	λ_i
1	$-3.15 + 377j$
2	$-3.15 - 377j$
3	$-107.16 + 7668.1j$
4	$-107.16 - 7658.1j$
5	$-107.16 + 6914.1j$
6	$-107.16 - 6914.1j$
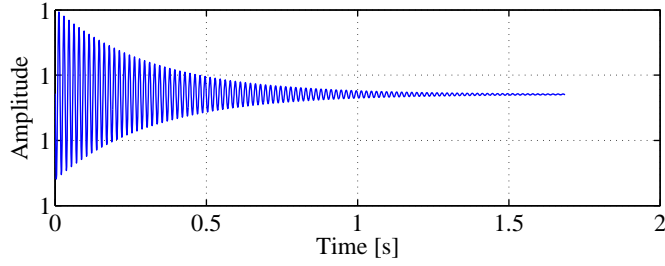
Figure 2.10: Slow subsystem step response via exact decomposition (with correction)

layer correction based on the DC gain of the fast subsystem had a minor effect on the responses of the slow subsystem unlike in the residualized case. The plot belonging to the case without a correction are not shown here due to redundancy.

The responses based on the fast subsystem via Chang are very similar to the ones generated using the fast subsystem method earlier. The step response of the exactly decoupled system in Fig. 2.12 matches that of the original system. Likewise, the impulse response is very accurate (see Fig. 2.13).

Based on both singular perturbation methods that we tested above, we observed that the dynamics of the original system were were more accurately emulated by the fast subsystems. Using this fact as motivation, in the next sub-section we attempt order-reduction just based on the fast subsystem. We assume that $\dot{x}_1(t) = 0$.

2.3.3   Reduced Model Using the Fast Subsystem

In classical singular perturbations when $\varepsilon = 0$, the fast transients cause the fast subsystem to decay rapidly leading to the *quasi-steady-state* model. It was shown earlier using simulations that such a quasi steady-state slow model produces a very
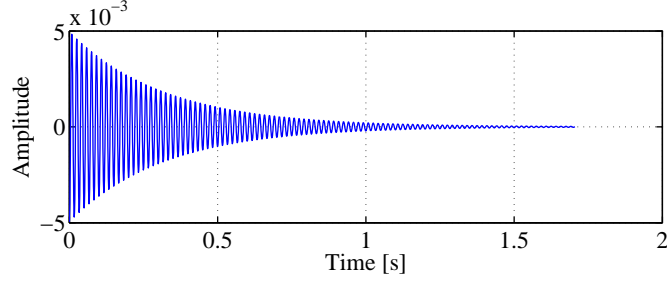
Figure 2.11: Slow subsystem impulse response via exact decomposition (with correction)
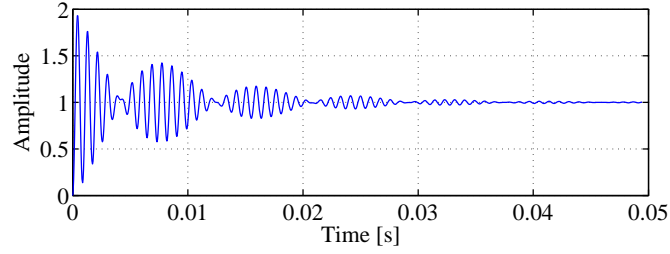
Figure 2.12: Fast subsystem step response via exact decomposition

poor approximation. In this section we investigate the case when the slow subsystem is in steady state and the reduced model is based on the fast subsystem. While this method is not intuitive, we propose it based on our previous observations that the fast subsystem retained the properties of the overall full-order model.

The set of equations for this type of singularly perturbed system is shown in Eq. (2.15).

$$
\begin{aligned}
0 &= \mathbf{A}_1 x_1(t) + \mathbf{A}_2 x_2(t) + \mathbf{B}_1 u(t) \\
\varepsilon \dot{x}_2(t) &= \mathbf{A}_3 x_1(t) + \mathbf{A}_4 x_2(t) + \mathbf{B}_2 u(t) \\
y(t) &= \mathbf{C}_1 x_1(t) + \mathbf{C}_2 x_2(t) + \mathbf{D} u(t)
\end{aligned}
\tag{2.15}
$$

Another assumption pertaining to this section is imposed.

Assumption 2.3: Matrix $\mathbf{A}_1$ is invertible.

An approximation of the model based on the fast subsystem is then given as

$$
\begin{aligned}
\varepsilon \dot{x}_2(t) &= \mathbf{A}_f^f x_2(t) + \mathbf{B}_f^f u(t) \\
y(t) &= \mathbf{C}_f^f x_2(t) + \mathbf{D}_f^f u(t)
\end{aligned}
\tag{2.16}
$$

where

$$
\begin{aligned}
\mathbf{A}_f^f &:= \mathbf{A}_4 - \mathbf{A}_3 \mathbf{A}_1^{-1} \mathbf{A}_2, & \mathbf{C}_f^f &:= \mathbf{C}_2 - \mathbf{C}_1 \mathbf{A}_1^{-1} \mathbf{A}_2 \\
\mathbf{B}_f^f &:= \mathbf{B}_2 - \mathbf{A}_3 \mathbf{A}_1^{-1} \mathbf{B}_1, & \mathbf{D}_f^f &:= \mathbf{D} - \mathbf{C}_1 \mathbf{A}_1^{-1} \mathbf{B}_1
\end{aligned}
\tag{2.17}
$$
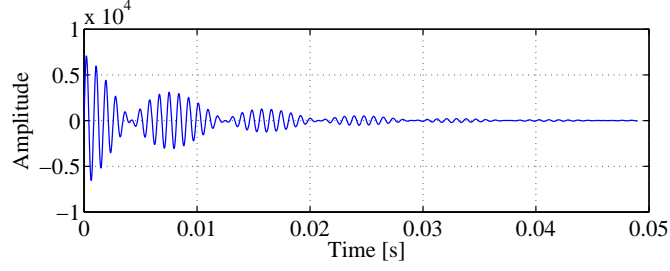
Figure 2.13: Fast subsystem impulse response via exact decomposition
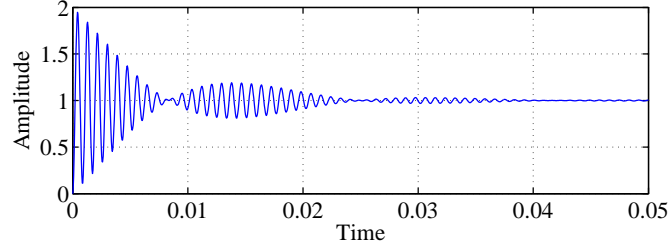
Figure 2.14: Step response based on fast subsystem residualization
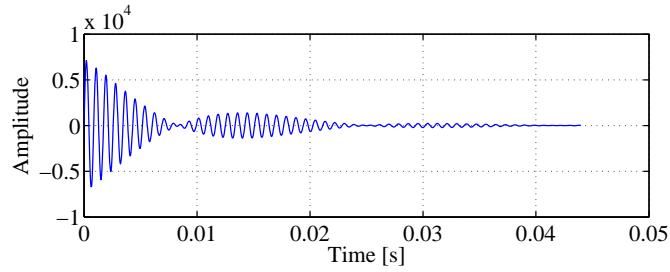
Figure 2.15: Impulse response based on fast subsystem residualization

The eigenvalues of subsystem (2.16)-(2.17) for the IM system are $-106.05 \pm 7472.2j$ and $-111.42 \pm 7095.3j$. Fig.2.14 and Fig. 2.15 shows the step and impulse response respectively of the fast subsystem (2.16)-(2.17). While somewhat similar to the step response of the original model, it is not as accurate as the response of the fast subsystem obtained using the Chang transformation. Nonetheless, the responses are more accurate than the responses of the slow subsystem shown in Fig. 2.6 and Fig. 2.7.

In this section we have explored all the MOR possibilities of slow-fast decomposed system and came to two interesting conclusions:

1. The slow subsystem that is expected to approximate the original model well produced poor results even though parameter ε is very small.

2. The fast subsystem that is not expected to approximate the original model produced better results even though the time-scale separation is large.

In the following section we explain analytically why this anomaly is happening.

2.4 Time-Scales of Highly Damped Highly Oscillatory Systems

It is interesting to note that the model being investigated contains lightly and highly damped and highly oscillatory modes. Relevant analysis and discussions about singularly perturbed systems with sustained high frequency oscillations and slightly damped modes can be found in [41]. The authors use algebraic decomposition and a technique based on (2.7) to decouple the system into slow, fast, and oscillatory subsystems. Then, if the fast modes decay in the fast time scales during a boundary layer interval and the initial conditions of the oscillatory subsystem are much smaller than that of the slow subsystem, an approximation of the original model can be obtained just by using the slow modes. As it will be shown, the IM model under investigation does not contain any slow modes hence the methods presented in [46] and [41] cannot be used to successfully decouple the system.

We start by considering the eigenvalues of the IM model. Using $\varepsilon \approx 0.03$ (see [85]) the model's eigenvalues in Table 2.2 can be rewritten as

Table 2.5: Eigenvalues of the IM model as a function of ε

i	λ_i
1	$-3.15 + \dfrac{11.31}{\varepsilon}j$
2	$-3.15 - \dfrac{11.31}{\varepsilon}j$
3	$\dfrac{-3.2148}{\varepsilon} + \dfrac{6.9013}{\varepsilon^2}j$
4	$\dfrac{-3.2148}{\varepsilon} - \dfrac{6.9013}{\varepsilon^2}j$
5	$\dfrac{-3.2148}{\varepsilon} + \dfrac{6.2227}{\varepsilon^2}j$
6	$\dfrac{-3.2148}{\varepsilon} - \dfrac{6.2227}{\varepsilon^2}j$

To facilitate the problem, we propose to investigate the system transformed into the modal canonical form. A similarity transformation $\mathbf{T}$ can be found such that the system matrix is transformed into the modal form [86]. The same conclusion can be drawn by transforming the system matrix $\mathbf{A}$ into the Schur form via the QR algorithm. The QR algorithm is considered the most efficient method for finding the system eigenvalues [53].

Note that the modal form is known to be numerically ill-conditioned when the eigenvalues are close to each other. Hence, in our case it is only used for theoretical considerations. The Schur form on the other hand is numerically well-conditioned even when the eigenvalues are repeated or close to each-other. The modal form for our model is given by

$$\bar{\mathbf{A}} = \begin{bmatrix} \alpha_1 & \dfrac{\beta_1}{\varepsilon} & \vdots & 0 & 0 & \vdots & 0 & 0 \\[2mm] -\dfrac{\beta_1}{\varepsilon} & \alpha_1 & \vdots & 0 & 0 & \vdots & 0 & 0 \\[2mm] \cdots & \cdots & \vdots & \cdots & \cdots & \vdots & \cdots & \cdots \\[2mm] 0 & 0 & \vdots & \dfrac{\alpha_2}{\varepsilon} & \dfrac{\beta_2}{\varepsilon^2} & \vdots & 0 & 0 \\[2mm] 0 & 0 & \vdots & -\dfrac{\beta_2}{\varepsilon^2} & \dfrac{\alpha_2}{\varepsilon} & \vdots & 0 & 0 \\[2mm] \cdots & \cdots & \vdots & \cdots & \cdots & \vdots & \cdots & \cdots \\[2mm] 0 & 0 & \vdots & 0 & 0 & \vdots & \dfrac{\alpha_3}{\varepsilon} & \dfrac{\beta_3}{\varepsilon^2} \\[2mm] 0 & 0 & \vdots & 0 & 0 & \vdots & -\dfrac{\beta_3}{\varepsilon^2} & \dfrac{\alpha_3}{\varepsilon} \end{bmatrix} \tag{2.18}$$

The state-space form corresponding to the system matrix (2.18) is given as

$$\frac{dz(t)}{dt} \equiv \dot{z}(t) = \bar{\mathbf{A}} z(t) \tag{2.19}$$

Since the term $\frac{1}{\varepsilon}$ is present in all the elements of matrix $\bar{\mathbf{A}}$, (2.19) is multiplied by ε on both sides to obtain

$$\varepsilon \frac{dz(t)}{dt} = \varepsilon \bar{\mathbf{A}} z(t) \tag{2.20}$$

It is clear from (2.18) and (2.20) that all six state variables are fast. In addition, the last four state variables are much faster than the first two since the last four contain elements that are multiplied by $\frac{1}{\varepsilon}$. With a change of time scales, namely $\frac{dt}{\varepsilon} = d\tau$, (2.20)

can be written as

$$\frac{dz(\tau)}{d\tau} = \bar{\mathbf{A}}_\varepsilon z(\tau) = \begin{bmatrix} \varepsilon\alpha_1 & \beta_1 & \vdots & 0 & 0 & \vdots & 0 & 0 \\ -\beta_1 & \varepsilon\alpha_1 & \vdots & 0 & 0 & \vdots & 0 & 0 \\ \cdots & \cdots & \vdots & \cdots & \cdots & \vdots & \cdots & \cdots \\ 0 & 0 & \vdots & \alpha_2 & \dfrac{\beta_2}{\varepsilon} & \vdots & 0 & 0 \\ 0 & 0 & \vdots & -\dfrac{\beta_2}{\varepsilon} & \alpha_2 & \vdots & 0 & 0 \\ \cdots & \cdots & \vdots & \cdots & \cdots & \vdots & \cdots & \cdots \\ 0 & 0 & \vdots & 0 & 0 & \vdots & \alpha_3 & \dfrac{\beta_3}{\varepsilon} \\ 0 & 0 & \vdots & 0 & 0 & \vdots & -\dfrac{\beta_3}{\varepsilon} & \alpha_3 \end{bmatrix} \qquad (2.21)$$

Finally, the system in (2.21) is put in standard singularly perturbed form as follows

$$\dot{z}_1(\tau) = \begin{bmatrix} \varepsilon\alpha_1 & \beta_1 \\ -\beta_1 & \varepsilon\alpha_1 \end{bmatrix} z_1(\tau)$$

$$\varepsilon\dot{z}_2(\tau) = \begin{bmatrix} \varepsilon\alpha_2 & \beta_2 \\ -\beta_2 & \varepsilon\alpha_2 \end{bmatrix} z_2(\tau) \qquad (2.22)$$

$$\varepsilon\dot{z}_3(\tau) = \begin{bmatrix} \varepsilon\alpha_3 & \beta_3 \\ -\beta_3 & \varepsilon\alpha_3 \end{bmatrix} z_3(\tau)$$

It can be observed that in this original system there are no slow dynamics. The *fast* dynamics are represented by state variable $z_1(\tau)$ and the *very fast* dynamics are represented by $z_2(\tau)$ and $z_3(\tau)$. This real physical model shows that its response cannot be approximated by the slower dynamics as it is typical in power systems since here only fast and very fast modes are present. The advantage of the method above is that it explicitly shows that the system under investigation does not contain any slow dynamics, hence we should not expect the slow subsystem obtained via singular perturbation techniques to approximate the overall model. It is interesting to point out that using only the fast modes (belonging to $z_1(\tau)$) does not produce a good approximation. However, the fourth-order approximation based on the very fast modes represented by $z_2(\tau)$ and $z_3(\tau)$ produces an excellent approximation in the original coordinates.

Another interesting observation is that irrespective of the time-scales, the original IM model lacks a feedthrough matrix, i.e. $\mathbf{D} = 0$ but for the residualized system (2.4)

$\mathbf{D}_0 \neq 0$. This occurrence is introducing an input term to the output even though there is no input in the original output equation. Similarly we can look at this event in the frequency domain. The transfer function of the original model is given by

$$\mathbf{G}_{orig}(s) = \mathbf{C}(s\mathbf{I} - \mathbf{A})^{-1}\mathbf{B} \tag{2.23}$$

On the other hand, the transfer function of the residualized model (2.4) due to the added input becomes

$$\mathbf{G}_{residue}(s) = \mathbf{C}_0(s\mathbf{I} - \mathbf{A}_0)^{-1}\mathbf{B}_0 + \mathbf{D}_0 \tag{2.24}$$

This is reflected in the earlier simulation results (more so in the step response). By considering Fig. 2.4 and Fig 2.5 or Fig. 2.6 and Fig. 2.7 where a correction has been introduced, we see that the input dominates the response. For example, while we observe a small jitter in the beginning of the step response, it is practically one, just like the input.

2.5   Model Reduction Based on Balancing

For a linear system in balanced coordinates the Hankel singular values (HSV) serve as a measure for the dynamic importance of state components [31]-[32]. If a HSV is relatively small, the influence of the corresponding state component on the output and input energy is low therefore this state component can be discarded to obtain a reduced-order system [31]. These states also correspond to weakly controllable and weakly observable parts of the system. Let us consider a LTI system represented by

$$\begin{aligned}
\dot{x}(t) &= \mathbf{A}x(t) + \mathbf{B}u(t) \\
y(t) &= \mathbf{C}x(t) + \mathbf{D}u(t)
\end{aligned} \tag{2.25}$$

where $x(t) \in \mathbb{R}^n$ is the system state vector, $u(t) \in \mathbb{R}^m$ is the system input vector and $y(t) \in \mathbb{R}^p$ is the system output vector. The open-loop transfer function is given by

$$G(s) = \mathbf{C}(s\mathbf{I} - \mathbf{A})^{-1}\mathbf{B} + \mathbf{D} \tag{2.26}$$

It is assumed that the system is asymptotically stable and that the pairs $(\mathbf{A}, \mathbf{B})$ and $(\mathbf{A}, \mathbf{C})$ are both controllable and observable [35]. Using the balancing transformation

$x_b(t) = Tx(t)$, $\det(T) \neq 0$, the new system in balanced coordinates becomes

$$\begin{aligned}
\dot{x}_b(t) &= \mathbf{A}_b x(t) + \mathbf{B}_b u(t) \\
y_b(t) &= \mathbf{C}_b x(t) + \mathbf{D}_b u(t)
\end{aligned}$$

(2.27)

The matrices in (2.27) are given by

$$\mathbf{A}_b = \mathbf{T}\mathbf{A}\mathbf{T}^{-1}, \quad \mathbf{B}_b = \mathbf{T}\mathbf{B}, \quad \mathbf{C}_b = \mathbf{C}\mathbf{T}^{-1}, \quad \mathbf{D}_b = \mathbf{D}$$

(2.28)

The system in (2.27) is partitioned as follows

$$\mathbf{A}_b = \begin{bmatrix} \mathbf{A}_1 & \mathbf{A}_2 \\ \mathbf{A}_3 & \mathbf{A}_4 \end{bmatrix}, \mathbf{B}_b = \begin{bmatrix} \mathbf{B}_1 \\ \mathbf{B}_2 \end{bmatrix}, \mathbf{C}_b = \begin{bmatrix} \mathbf{C}_1 & \mathbf{C}_2 \end{bmatrix}, \mathbf{D}_b = \mathbf{D}$$

$$\Sigma = \begin{bmatrix} \mathbf{\Sigma_1} & \mathbf{0} \\ \mathbf{0} & \mathbf{\Sigma_2} \end{bmatrix}$$

$$\mathbf{\Sigma_1} = \mathrm{diag}(\sigma_1, \sigma_2, ...\sigma_r), \quad \mathbf{\Sigma_2} = \mathrm{diag}(\sigma_{r+1}, \sigma_{r+2}, ...\sigma_n)$$

where Σ represents the HSV of the balanced system. Then the reduced-order model obtained via DT is given by

$$\begin{aligned}
\dot{x}_1(t) &= \mathbf{A}_1 x_1(t) + \mathbf{B}_1 u(t) \\
y(t) &= \mathbf{C}_1 x_1(t) + \mathbf{D} u(t) \\
G_1(s) &= \mathbf{C}_1 (s\mathbf{I} - \mathbf{A}_1)^{-1}\mathbf{B}_1 + \mathbf{D}
\end{aligned}$$

(2.29)

(2.29) is also balanced, asymptotically stable, and minimal and it has been shown that its H_∞ norm satisfies [32]

$$\|G(s) - G_1(s)\|_\infty \leq 2(\sigma_{r+1} + \sigma_{r+2} + ... + \sigma_n)$$

(2.30)

It is known that the DT method does not preserve the DC gain. Another order reduction method for balanced linear singularly perturbed systems which preserves the system DC gain is considered in [33] and [85].

2.5.1 Reduced Model via Balancing Transformation

The HSV of the system are key to determining the lowest order the balanced system can be truncated without sacrificing performance. Fig. 2.16 shows the Hankel singular
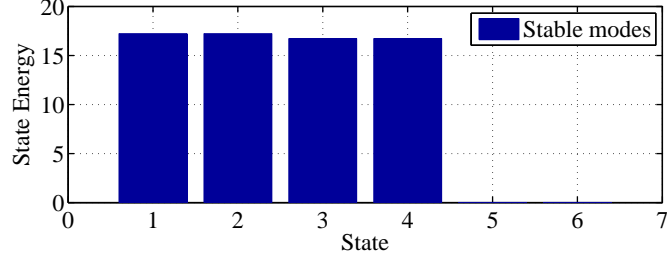
Figure 2.16: Hankel singular values of the original model

values map. Based on the HSV, the last two states can be neglected and we expect an accurate representation of the original model's response using the reduced model.

Fig. 2.17 shows the step response of the balanced model reduced to order four. The response is almost identical to that of the original model (Fig. 2.2). Note that (2.30) can be used as an estimate of the approximation error. In our case the approximation error is $\|G(s) - G_1(s)\|_\infty = 7.87 \times 10^{-4}$.
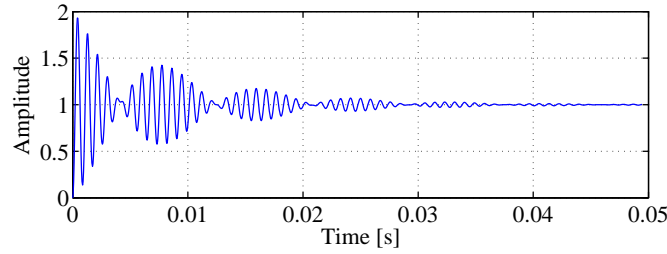
Figure 2.17: Step response of balanced model truncated to order four
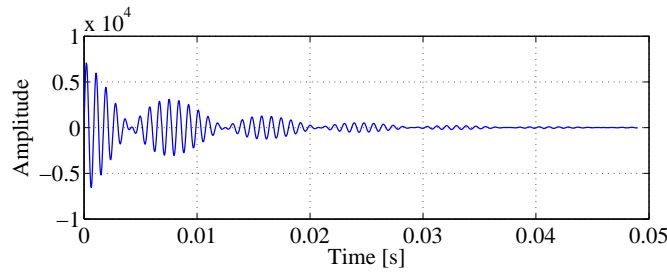
Figure 2.18: Impulse response of balanced model truncated to order four

2.5.2 Numerical Errors of the Reduced Models

The absolute errors of the reduced models considered so far are summarized in Table 2.6. The Euclidean norm defined as $\|\mathbf{x} - \hat{\mathbf{x}}\|_2 = (\sum_{i=1}^{n}(x_i - \hat{x}_i)^2)^{1/2}$ is used as the metric

for comparison. $\mathbf{x}$ represents the response vector of the original model and $\hat{\mathbf{x}}$ represents the response vector of a reduced-order model. Both the step and impulse inputs are considered for the fast subsystems only since it was shown that the approximation based on the slow subsystem gave very poor results. In Table 2.6, $Response_{orig}$ represents the response vector of the full order model, $Response_{residueFast}$ represents the vector of the fast subsystem when the original is residualized, $Response_{fastChang}$ represents the response vector of the fast subsystem obtained via the Chang transformation (see (2.8)-(2.9)), $Response_{fastBased}$ represents the response vector of the approximation based on the fast subsystem as given in (2.15)-(2.17), and finally, $Response_{bal_{DT}}$ represents the response vector of the reduced model via balancing transformation (2.29).

Table 2.6: Numerical errors of reduced-order models

	Step Response	Impulse Response
$\|\text{Response}_{full} - \text{Response}_{residueFast}\|_2$	9.75×10^{-2}	1.78×10^2
$\|\text{Response}_{full} - \text{Response}_{fastChang}\|_2$	3.01×10^{-4}	1.12×10^{-1}
$\|\text{Response}_{full} - \text{Response}_{fastBased}\|_2$	4.69	3.27×10^4
$\|\text{Response}_{full} - \text{Response}_{bal_{DT}}\|_2$	3.01×10^{-4}	1.12×10^{-1}

Note that the responses of the residualized system and the slow subsystem based on the Chang transformation are not compared to the original responses since the approximation was very poor as observed in the simulations.

From Table 2.6 we can see that the step response performs better than the impulse response. For the latter, the largest error occurs when the reduced model based on the fast subsystem is compared to the full-order model. Intuitively, we would not expect an accurate representation of the original model since we are letting $\dot{x}_1 = 0$ which violates the principle of classical singular perturbation theory. Nonetheless, as the simulations showed, the response based on the fast subsystem was closer to the original model's counterpart than the corresponding response of the residualized model.

The approximation of the fast subsystem of the residualized model based on the impulse response shows a large error as well. For the step response, we notice that the approximation based on the fast subsytem contains the largest error. On the other

hand, the fast subsystem obtained using the Chang transformation and the truncated model are equally accurate. These results agree with previous observations based on simulations.

2.6   Frequency Response of the Reduced Models

As we observed earlier in this chapter, singular perturbation techniques were not able to successfully obtain a reduced-order model of the IM system. What is interesting about the model under investigation is that it is highly oscillatory and highly damped. We showed that for these types of systems, large imaginary parts contribute to faster time-scale even though the real parts are classified as slow. For these reasons, further investigation in frequency domain is carried out in this section for the reduced-order models . We initially start with the six-order model [48] in balanced form. Four cases are investigated.

1. Model reduced to order four using DT and residualization. [85], [33]

2. Model reduced to order two using DT and residualization.

3. Model reduced to order four using DT and then to order two using residualization.

4. Model reduced to order four using residualization and then to order two using DT.

The Bode plots (magnitude and frequency) are shown below for each case.

Case 1
In *Case 1*, the balanced system has been directly truncated and reduced using the residualization technique. The model has been reduced from order six to order four. The magnitude and frequency plots for the two cases and the full order model are shown in Fig. 2.19.

The responses are practically the same in all three cases.
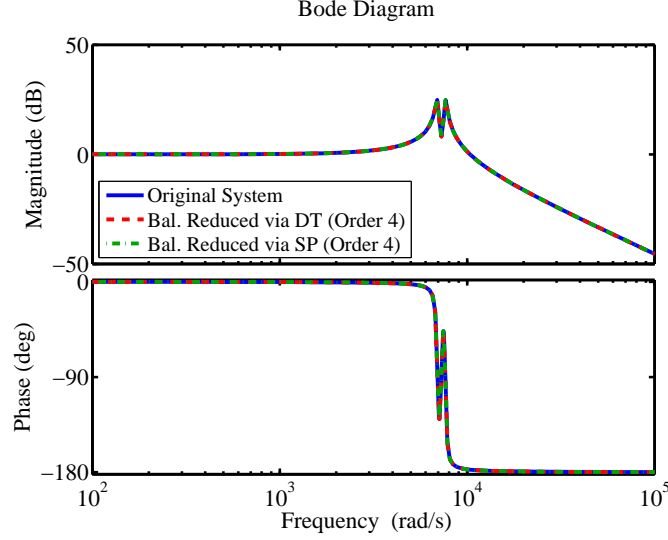
Figure 2.19: Frequency response of original and reduced models (To order 4)

Case 2

Case 2 is similar to *Case 1* with the only difference being that the models have been reduced to order two instead of four. Fig. 2.20 shows the results. The frequency response using DT is almost the same as that of the full order model while using residualization we can notice some differences. At $\omega = 7 \times 10^3$ $[rad/sec]$ the magnitude plot of the residualized reduced model is missing a notch that is present in both DT-reduced and original models. In addition, when $\omega = 4 \times 10^5$ $[rad/sec]$, the error of the magnitude plot of the residualization method starts increasing. Similar observations can be made about the phase plot.

Case 3

DT provides better accuracy for higher frequencies while residualization performs better at lower frequencies [33]. Combining these two techniques then should provide a good approximation of the frequency response. Fig. 2.21 shows the frequency response when the model is initially reduced to order four via DT and then to order two using the residualization method. The response is similar to that of *Case 2*.
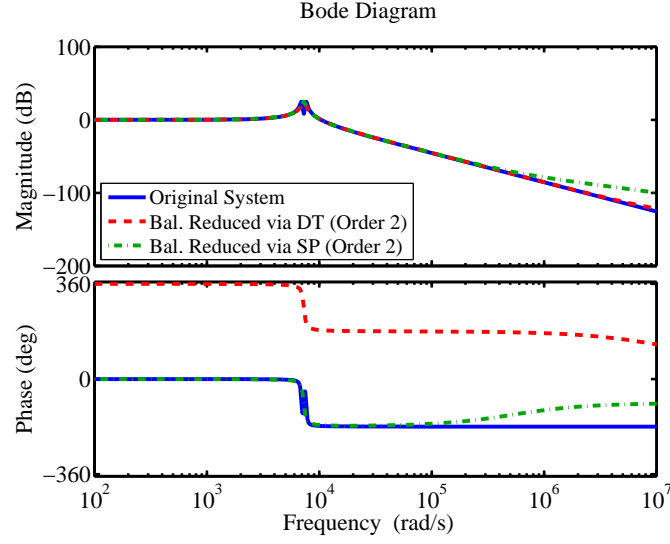
Figure 2.20: Frequency response of original and reduced models (To order 2)

Case 4

Case 4 is also a combination of both techniques but residualization has been performed first to reduce the model to order four then DT is used to further reduce the model to order two. The results can be seen in Fig. 2.22. The only difference exhibited in both the magnitude and phase responses is the missing notch at $\omega = 7 \times 10^3 \ [rad/sec]$. Otherwise the frequency responses match.
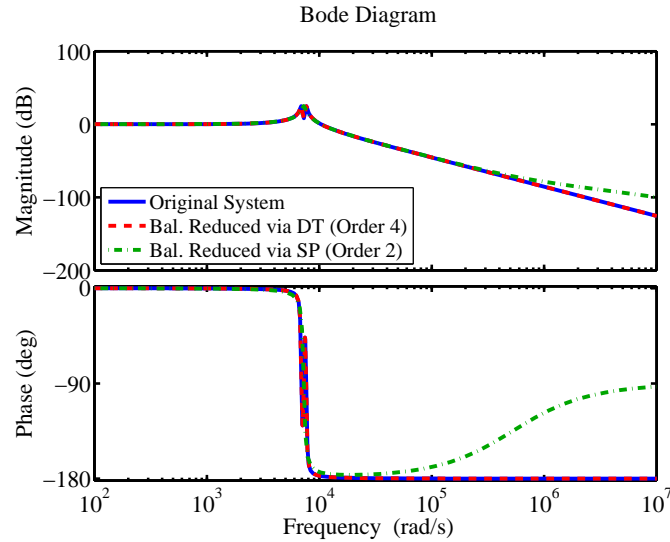
Figure 2.21: Frequency response of original and reduced models (DT/Residualization)
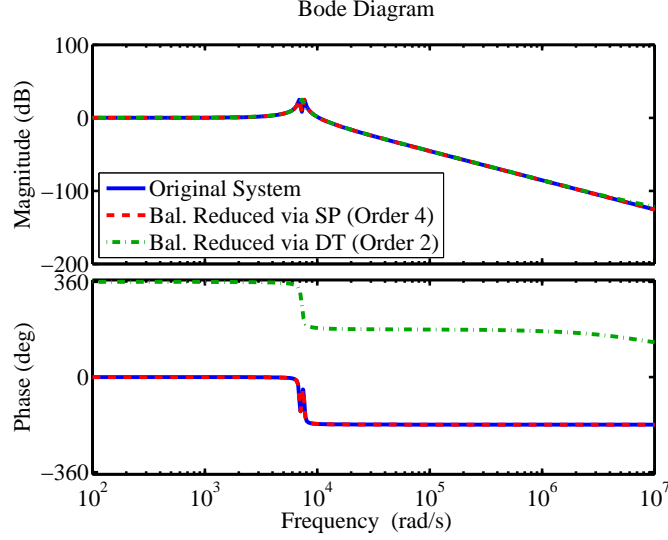
Figure 2.22: Frequency response of original and reduced models (Residualization/DT)

Case 3 and *Case 4* provide two cases where the model is reduced twice. While the final reduced models in both cases miss the notch at $\omega = 7 \times 10^3$ [rad/sec], *Case 4* (Residualization/DT) does not contain any errors at higher frequencies unlike *Case 3* (DT/Residualization). This observation agrees with theory since DT is the final step of model reduction and as mentioned above, it performs better than residualization at higher frequencies [33].

From the simulations above we see that the results agree with conclusions we reached in the time domain. Specifically, reduction of the model to order four (using balancing or singular perturbations), leads to an accurate approximation of the original model. On the other hand, if the model is reduced to order two, we notice discrepancies in both magnitude and phase.

2.7   Conclusion

In this chapter we studied order reduction methods applied to an IM model. Theoretically, the singular perturbation method should provide a good approximation of the model when it is reduced to order two (corresponding to the slow subsystem) in combination with the gain of the fast subsystem. It is observed that the latter is not the case. It is was shown explicitly that this system containing both lightly and highly

damped, highly oscillatory modes does not posses any slow dynamics, hence the slow subsystem obtained via singular perturbations does not approximate the original system and that for such a system, very fast modes must be included in the reduced-order models. In addition, the model is also reduced by truncating the balanced system based on the HSV. The reduced model in this case has an almost identical response as the original model. Combinations of DT and singular perturbations in frequency domain were also investigated. The observations in this chapter are very important and serve as guidelines to the designer who would be considering controller or filter design for highly oscillatory systems.

Chapter 3

Optimal Control for a New Class of Singularly Perturbed Linear Systems

THE model investigated earlier as well as other models of real physical systems used in power grids [87], [88] serve as motivation for the work in this chapter. Such models exhibit two time-scale properties and have a specially partitioned input matrix structure that makes it more effective for the system to have two inputs controlling the slow and fast subsystems individually. For example, hardware or events within a microgrid, while being part of the same system operate at different sampling times ranging from milliseconds to seconds [89]-[90]. One control input might be very effective for one subsystem however it could impact the performance of the other. With this in mind, we develop a new class of singularly perturbed systems with two control inputs that individually control each time-scale. Motivated by models of real physical systems, we also investigate the case when weak coupling exists between inputs and when the fast subsystem is weakly controlled. We focus on the optimal control problem, both the LQR and the LQG, and develop algorithms based on fixed-point iteration methods to solve the LQR and the LQG while avoiding ill-conditioning and improving on computational efficiency. Similar work has been considered in [67], [59] and [60] however, what distinguishes this work is the fact that both slow and fast subsystems are controlled by individual inputs instead of a universal one.

The purpose of this chapter is to analyze and solve the LQR and LQG problems for this new class of singularly perturbed systems. Inspired by models of real physical systems, we explore three different input matrix structures. For each of them we consider the optimal control problem and show how to efficiently obtain the solution in terms of reduced-order sub-problems. The rest of this chapter is organized as follows.

In Section 3.1 the problem is formulated. Recursive reduced-order methods for the new classes of singularly perturbed systems are described in Section 3.2. The problem is extended to linear stochastic filtering in Section 3.3. A case study is investigated in Section 3.4 and finally Section 3.5 concludes the chapter.

3.1   Problem Formulation

The singularly perturbed structure (2.1) that corresponds to a model of a real physical system with one input was considered in [60] for three cases namely, strongly controlled slow modes and weakly controlled fast modes, strongly controlled slow modes, weakly controlled fast modes respectively. It is important to emphasize that input matrices in (2.1) apply to one input vector that controls both the slow and fast state variables. Motivated by models of real physical systems [87]-[88], [91], we have found that a more general and efficient structure of singularly perturbed systems can be obtained by using two vector inputs: one that controls the slow subsystem and the other for controlling the fast subsystem. The state-space form of such control systems is given by

$$
\begin{aligned}
\dot{x}_1(t) &= \mathbf{A}_1 x_1(t) + \mathbf{A}_2 x_2(t) + \mathbf{B}_1 u_1(t) \\
\varepsilon \dot{x}_2(t) &= \mathbf{A}_3 x_1(t) + \mathbf{A}_4 x_2(t) + \mathbf{B}_4 u_2(t)
\end{aligned}
\tag{3.1}
$$

It is important to note that using the classical singular perturbation approach in (2.1), will lead to *complications* while forming the reduced-order slow and approximate fast subsystems. Namely, by setting $\varepsilon = 0$ [46], we have

$$
\dot{x}_{1s}(t) = \mathbf{A}_1 x_{1s}(t) + \mathbf{A}_2 x_{2s}(t) + \mathbf{B}_1 u_1(t) \tag{3.2a}
$$

$$
0 = \mathbf{A}_3 x_{1s}(t) + \mathbf{A}_4 x_{2s}(t) + \mathbf{B}_4 u_2(t) \tag{3.2b}
$$

Subsituting $x_{2s}(t)$ from (3.2b) into (3.2a), we obtain

$$
\dot{x}_{1s}(t) = (\mathbf{A}_1 - \mathbf{A}_2 \mathbf{A}_4^{-1} \mathbf{A}_3) x_{1s}(t) + \mathbf{B}_1 u_1(t) - \mathbf{A}_2 \mathbf{A}_4^{-1} \mathbf{B}_4 u_2(t) \tag{3.3}
$$

Equation (3.3) implies that the slow approximate subsystem is now controlled by both the slow and the fast ($u_1(t)$ and $u_2(t)$ respectively) control inputs. Similarly, the fast

approximate subsystem $x_{2f}(t) = x_2(t) - x_{2s}(t)$ will be controlled by both inputs. Furthermore, employing the most common technique based on the Chang transformation [52] to decouple the system into slow and fast subsystems will also lead to each individual system being controlled by both control inputs. The drawback of having $u_1(t)$ and $u_2(t)$ concurrently control both subsystems is that controller design and analysis will be considerably more complicated. A more concrete example of what was discussed earlier would be an electromechanical system that has mechanical components that operate in seconds and electrical circuitry that operates in milliseconds. Intuitively, two inputs would be more effective. To rectify this issue, we consider a state-space model where $u_1(t)$ and $u_2(t)$ are present and consider the optimal control problem and approach its solution using reduced-order equations which also avoids possible numerical ill-conditioning. In this dissertation we are considering three special cases for the state-space input matrix $\mathbf{B}$. These cases seem to be common occurrences in models of physical system (see earlier references). Other structures are possible and can be easily obtained under different assumptions. The three matrix structures are as follows.

$$(i)\ \mathbf{B} = \begin{bmatrix} \mathbf{B}_1 & \mathbf{0} \\ \mathbf{0} & \frac{1}{\varepsilon}\mathbf{B}_4 \end{bmatrix}, \ (ii)\ \mathbf{B} = \begin{bmatrix} \mathbf{B}_1 & \varepsilon\mathbf{B}_2 \\ \mathbf{B}_3 & \frac{1}{\varepsilon}\mathbf{B}_4 \end{bmatrix}$$
$$(iii)\ \mathbf{B} = \begin{bmatrix} \mathbf{B}_1 & \mathbf{0} \\ \mathbf{0} & \mathbf{B}_4 \end{bmatrix} \tag{3.4}$$

We start the problem with a standard cost function associated with the infinite horizon LQR problem of the singularly perturbed system as in (3.5) that has to be minimized.

$$J = \frac{1}{2} \int_0^\infty (x^T(t)\mathbf{Q}x(t) + u^T(t)\mathbf{R}u(t))dt \tag{3.5}$$

where $\mathbf{R} > 0$ and without loss of generality we assume that it is partitioned as

$$\mathbf{R} = \begin{bmatrix} \mathbf{R}_1 & \mathbf{0} \\ \mathbf{0} & \mathbf{R}_4 \end{bmatrix} \tag{3.6}$$

$\mathbf{Q} \geq 0$ and its structure is partitioned as in (3.7).

$$\mathbf{Q} = \begin{bmatrix} \mathbf{Q}_1 & \varepsilon\mathbf{Q}_2 \\ \varepsilon\mathbf{Q}_2^T & \varepsilon\mathbf{Q}_3 \end{bmatrix} \tag{3.7}$$

Then, the optimal solution $u(t)$ subject to $x(t)$ is

$$u(t) = \begin{bmatrix} u_1(t) & u_2(t) \end{bmatrix}^T$$
$$= -\mathbf{R}^{-1}\mathbf{B}^T\mathbf{P}x(t) \tag{3.8}$$

where matrix $\mathbf{B}$ is given by

$$\mathbf{B} = \begin{bmatrix} \mathbf{B}_1 & \mathbf{0} \\ \mathbf{0} & \frac{1}{\varepsilon}\mathbf{B}_4 \end{bmatrix} \tag{3.9}$$

Matrix $\mathbf{P}$ is the solution of the CARE given in (3.10).

$$\mathbf{A}^T\mathbf{P} + \mathbf{P}\mathbf{A} + \mathbf{Q} - \mathbf{P}\mathbf{B}\mathbf{R}^{-1}\mathbf{B}^T\mathbf{P} = 0 \tag{3.10}$$

The required structure of the solution matrix $\mathbf{P}$ comes from the nature of the solution of (3.10) and is given as

$$\mathbf{P} = \begin{bmatrix} \mathbf{P}_1 & \varepsilon\mathbf{P}_2 \\ \varepsilon\mathbf{P}_2^T & \varepsilon\mathbf{P}_3 \end{bmatrix} \tag{3.11}$$

Comments: Two-vector input multi-parameter singularly perturbed systems were considered within the multi-modeling concept that originated in [92] – deterministic, and in [93] – stochastic (see also [94]-[95] and references therein). The multi-modeling has been studied in different setup by Mukaidani and his colleagues (see for example [96], [97] and references therein). The input matrix for the multimodeling structures is given in terms of two small positive singular perturbation parameters ε_1 and ε_2 of the same order of magnitude. This structure of the input matrix is different from the input matrix structures considered in this dissertation and leads to completely different problems solvable under different assumptions that require dynamic game theory problem formulations involving the use of Nash and Pareto optimal control strategies.

Comments: While in this chapter we only consider two time-scales, the theoretical framework can be extended to the multi-time-scale case (more on multi-time-scale systems in the next chapter). That is, we would need to introduce as many inputs as the number of time-scales available. In that case, the derivations would be more involved and new assumptions will have to be imposed.

Remark 3.1 *Ill-conditioning is quite common in singularly perturbed system due to the presence of ε. In [60] a case study of a hydro power plant model revealed that available methods were not able to solve the CARE associated with the LQR problem. Popular algorithms such as Laub's method (used in MATLAB$^{\circledR}$) [98] or the MacFarlane-Potter algorithm [99], utilize transformation matrices under the assumption that they are non-singular to obtain the CARE solution. In [60], these transformation matrices happen to be near singular hence current algorithms failed to solve the CARE. However, reduced-order algorithms such as the ones used in this chapter were able to obtain an accurate solution.*

In the next sections, we show how to solve (3.10) efficiently in terms of reduced-order problems and eliminate possible numerical ill-conditioning associated with the original full-order problem for each case.

3.2 Reduced-Order Methods for the New Class of Singularly Perturbed Systems

This section presents detailed derivations and imposes the required assumptions for the new class of singularly perturbed linear systems for all three cases. We will refer to case (i), case (ii), and case (iii) as decoupled inputs case, weakly coupled inputs case, and weakly controlled fast subsystem case respectively.

3.2.1 Decoupled Inputs Case

The input matrix structure considered in this section is encountered frequently in models of real physical system as mentioned earlier. The singularly perturbed state-space model for this case is as follows.

$$\begin{aligned}
\dot{x}_1(t) &= \mathbf{A}_1 x_1(t) + \mathbf{A}_2 x_2(t) + \mathbf{B}_1 u_1(t) \\
\varepsilon \dot{x}_2(t) &= \mathbf{A}_3 x_1(t) + \mathbf{A}_4 x_2(t) + \mathbf{B}_4 u_2(t)
\end{aligned} \tag{3.12}$$

Substituting the appropriate matrix $\mathbf{B}$ as well as using (3.7) and (3.11) in (3.10), we obtain the following matrix algebraic equations (note that due to the symmetry of

CARE only three equations are needed).

$$\mathbf{A}_1^T\mathbf{P}_1 + \mathbf{A}_3^T\mathbf{P}_2^T + \mathbf{P}_1\mathbf{A}_1 + \mathbf{P}_2\mathbf{A}_3 + \mathbf{Q}_1 - \mathbf{P}_1\mathbf{S}_1\mathbf{P}_1 - \mathbf{P}_2\mathbf{S}_4\mathbf{P}_2^T = 0 \qquad (3.13a)$$

$$\varepsilon\mathbf{A}_1^T\mathbf{P}_2 + \mathbf{A}_3^T\mathbf{P}_3 + \mathbf{P}_1\mathbf{A}_2 + \mathbf{P}_2\mathbf{A}_4 + \mathbf{Q}_2 - \varepsilon\mathbf{P}_1\mathbf{S}_1\mathbf{P}_2 - \mathbf{P}_2\mathbf{S}_4\mathbf{P}_3 = 0 \qquad (3.13b)$$

$$\varepsilon\mathbf{A}_2^T\mathbf{P}_2 + \mathbf{A}_4^T\mathbf{P}_3 + \varepsilon\mathbf{P}_2^T\mathbf{A}_2 + \mathbf{P}_3\mathbf{A}_4 + \mathbf{Q}_3 - \varepsilon^2\mathbf{P}_2^T\mathbf{S}_1\mathbf{P}_2 - \mathbf{P}_3\mathbf{S}_4\mathbf{P}_3 = 0 \qquad (3.13c)$$

where $\mathbf{S}$ is defined as

$$\mathbf{S} = \mathbf{B}\mathbf{R}^{-1}\mathbf{B}^T = \begin{bmatrix} \mathbf{B}_1\mathbf{R}_1^{-1}\mathbf{B}_1^T & 0 \\ 0 & \frac{1}{\varepsilon^2}\mathbf{B}_4\mathbf{R}_4^{-1}\mathbf{B}_4^T \end{bmatrix}$$
$$= \begin{bmatrix} \mathbf{S}_1 & 0 \\ 0 & \frac{1}{\varepsilon^2}\mathbf{S}_4 \end{bmatrix} \qquad (3.14)$$

Next, we find the zero-order approximation of (3.13). For $\varepsilon \approx 0$, the zero-order approximation of (3.13) becomes

$$\mathbf{A}_1^T\mathbf{P}_1^{(0)} + \mathbf{A}_3^T\mathbf{P}_2^{(0)T} + \mathbf{P}_1^{(0)}\mathbf{A}_1 + \mathbf{P}_2^{(0)}\mathbf{A}_3 + \mathbf{Q}_1 - \mathbf{P}_1^{(0)}\mathbf{S}_1\mathbf{P}_1^{(0)} \qquad (3.15a)$$
$$- \mathbf{P}_2^{(0)}\mathbf{S}_4\mathbf{P}_2^{(0)T} = 0$$

$$\mathbf{A}_3^T\mathbf{P}_3^{(0)} + \mathbf{P}_1^{(0)}\mathbf{A}_2 + \mathbf{P}_2^{(0)}\mathbf{A}_4 - \mathbf{P}_2^{(0)}\mathbf{S}_4\mathbf{P}_3^{(0)} = 0 \qquad (3.15b)$$

$$\mathbf{A}_4^T\mathbf{P}_3^{(0)} + \mathbf{P}_3^{(0)}\mathbf{A}_4 - \mathbf{P}_3^{(0)}\mathbf{S}_4\mathbf{P}_3^{(0)} = 0 \qquad (3.15c)$$

The superscript (0) denotes an approximate quantity. Approximate solutions (3.15) differ from the original CARE by $\mathcal{O}(\varepsilon)$. The zero-order equations (3.15) can be further simplified by initially obtaining the solution of (3.15c), that is $\mathbf{P}_3^{(0)} = 0$. The latter leads to the solution of (3.15b). Substituting $\mathbf{P}_2^{(0)}$ in (3.15a) we obtain a CARE whose solution is $\mathbf{P}_1^{(0)}$. The equations for $\mathbf{P}_1^{(0)}$, $\mathbf{P}_2^{(0)}$, and $\mathbf{P}_3^{(0)}$ are as follows.

$$\mathbf{A}_0^T\mathbf{P}_1^{(0)} + \mathbf{P}_1^{(0)}\mathbf{A}_0 + \mathbf{Q}_1 - \mathbf{P}_1^{(0)}(\mathbf{S}_1 + \mathbf{A}_2\mathbf{A}_4^{-1}\mathbf{S}_4\mathbf{A}_4^{-T}\mathbf{A}_2^T)\mathbf{P}_1^{(0)} = 0 \qquad (3.16a)$$

$$\mathbf{P}_2^{(0)} + \mathbf{P}_1^{(0)}\mathbf{A}_2\mathbf{A}_4^{-1} = 0 \qquad (3.16b)$$

$$\mathbf{P}_3^{(0)} = 0 \qquad (3.16c)$$

where

$$\mathbf{A}_0 = \mathbf{A}_1 - \mathbf{A}_2\mathbf{A}_4^{-1}\mathbf{A}_3$$

To be able to solve (3.16a), we need the following assumption [32]

Assumption 3.1 Pairs (A_0, B_1) and $(A_0, \text{Chol}\{Q_1\})$ are stabilizable and detectable respectively.

In Assumption 3.1, $\text{Chol}\{\cdot\}$ stands for the Cholesky factorization.

Remark 3.2 *Equations* (3.16) *show that a reduced-order CARE of order n and a matrix algebraic equation can be used to obtain an approximate solution $P = P^{(0)} + \mathcal{O}(\varepsilon)$ of what used to be the CARE of order $n + m$. This is an advantage since the original full-order CARE is numerically ill-conditioned due to the presence of $\frac{1}{\varepsilon}$ element in matrix A.*

Remark 3.3 *Note that while formulating the slow reduced-order decoupled algebraic equations* (3.16), *the coefficients of the fast subsystem (A_4 and B_4) appropriately modify the coefficients of the reduced-order slow algebraic equation* (3.16a) *which has been the case also in the classical formulation of the singularly perturbed linear-quadratic (LQ) optimal control problem [46]. The method proposed in this section achieves control inputs that are dynamically decoupled, and with slow and fast controls controlling only the slow and fast subsystems respectively. This is realized by utilizing the solution of the corresponding slow and fast equations. That has not been the case in the classical formulation of the optimal LQ-problem.*

In the rest of this section, the error of matrix $\mathbf{P}$ for the approximation introduced above is investigated. The approximate CARE solution $\mathbf{P}^{(0)}$ obtained in (3.16) can be written in terms of the original CARE solution $\mathbf{P}$. In essence we have

$$\mathbf{P} = \mathbf{P}^{(0)} + \mathcal{O}(\varepsilon) = \begin{bmatrix} \mathbf{P}_1^{(0)} & \varepsilon\mathbf{P}_2^{(0)} \\ \varepsilon\mathbf{P}_2^{(0)T} & \varepsilon\mathbf{P}_3^{(0)} \end{bmatrix} \tag{3.17}$$

Defining an error matrix $\mathbf{E}$

$$\mathbf{E} = \begin{bmatrix} \mathbf{E}_1 & \mathbf{E}_2 \\ \mathbf{E}_2^T & \mathbf{E}_3 \end{bmatrix} \tag{3.18}$$

the solution $\mathbf{P}_j$, $j = 1, 2, 3$ in terms of the approximation errors becomes

$$\mathbf{P}_i = \mathbf{P}_j^{(0)} + \varepsilon \mathbf{E}_j, \quad j = 1, 2, 3 \tag{3.19}$$

The error equations are obtained by subtracting (3.15) from (3.13) after (3.19) has been substituted in the latter. This leads to

$$\mathbf{D}_1^T \mathbf{E}_1 + \mathbf{E}_1 \mathbf{D}_1 + \mathbf{D}_2^T \mathbf{E}_2^T + \mathbf{E}_2 \mathbf{D}_2 = \varepsilon \mathbf{H}_1 \tag{3.20a}$$

$$\mathbf{E}_2 \mathbf{A}_4 + \mathbf{E}_1 \mathbf{A}_2 + \mathbf{D}_2^T \mathbf{E}_3 + \mathbf{Q}_2 = \mathbf{H}_2 + \varepsilon \mathbf{H}_3 \tag{3.20b}$$

$$\mathbf{E}_3 \mathbf{A}_4 + \mathbf{A}_4^T \mathbf{E}_3 + \mathbf{Q}_3 + \mathbf{P}_2^{(0)T} \mathbf{A}_2 + \mathbf{A}_2^T \mathbf{P}_2^{(0)} = -\varepsilon(\mathbf{A}_2^T \mathbf{E}_2 + \mathbf{E}_2^T \mathbf{A}_2) + \varepsilon \mathbf{H}_4 \tag{3.20c}$$

where

$$\begin{aligned}
\mathbf{D}_1 &= \mathbf{A}_1 - \mathbf{S}_1 \mathbf{P}_1^{(0)} \\
\mathbf{D}_2 &= \mathbf{A}_3 - \mathbf{S}_4 \mathbf{P}_2^{(0)T} \\
\mathbf{H}_1 &= \mathbf{E}_1 \mathbf{S}_1 \mathbf{E}_1 + \mathbf{E}_2 \mathbf{S}_4 \mathbf{E}_2^T \\
\mathbf{H}_2 &= \mathbf{P}_1^{(0)} \mathbf{S}_1 \mathbf{P}_2^{(0)} - \mathbf{A}_1^T (\mathbf{P}_2^{(0)} + \varepsilon \mathbf{E}_2) \\
\mathbf{H}_3 &= \mathbf{P}_1^{(0)} \mathbf{S}_1 \mathbf{E}_2 + \mathbf{E}_1 \mathbf{S}_1 \mathbf{P}_2^{(0)} + \mathbf{E}_2 \mathbf{S}_4 \mathbf{E}_3 + \varepsilon \mathbf{E}_1 \mathbf{S}_1 \mathbf{E}_2 \\
\mathbf{H}_4 &= \mathbf{P}_2^{(0)T} \mathbf{S}_1 \mathbf{P}_2^{(0)} + \varepsilon \mathbf{P}_2^{(0)T} \mathbf{S}_1 \mathbf{E}_2 + \varepsilon \mathbf{E}_2^T \mathbf{S}_1 \mathbf{P}_2^{(0)} + \varepsilon^2 \mathbf{E}_2^T \mathbf{S}_1 \mathbf{E}_2 + \mathbf{E}_3 \mathbf{S}_4 \mathbf{E}_3
\end{aligned} \tag{3.21}$$

By inspecting (3.20), we observe that the cross-coupling terms and non-linear terms are multiplied by ε. Using these facts, a reduced-order fixed-point parallel algorithm is proposed to solve (3.20). Fixed-point iteration methods are usually good candidates to solve equations of the type $F(x) = 0$ iteratively. $F(x) = 0$ can be rewritten as $x = x - F(x)$ or $x = G(x)$. The latter is used to define the fixed-point iteration problem as

$$x^{(i)} = G^{(i)}(x) \tag{3.22}$$

Eq. (3.22) is guaranteed to converge given

$$\|x^{(i)} - x^{(i-1)}\| \le \rho \|G^{(i)}(x) - G^{(i-1)}(x)\| \tag{3.23}$$

where ρ is a constant that must be less than one. For the singularly perturbed problem under consideration, ρ is equivalent to ε. Since we defined $0 < \varepsilon \ll 1$, convergence is guaranteed.

Other iterative algorithms have been used to solve the CARE for singularly perturbed systems. Among the most common are those originating from the Newton method. For example in [61], the CARE of the corresponding guaranteed cost control problem of uncertain singularly perturbed systems is solved via a Newton method-based algorithm. While the Newton method is generally very effective when a good initial guess is used for the first iteration, for certain problems, the solution might not converge at all as it was shown in [59]. Note that unlike in this dissertation where only the symmetric case of the CARE has been considered, in [61] the CARE is non-symmetric. The symmetric CARE case solved via fixed-point iterations in this dissertation can also been solved via the hybrid Newton fixed-point algorithm presented in [62] (pp. 72-76). In addition, techniques such as power series methods, Taylor series, and asymptotic expansions have also been successfully used to acquire the solution of the CARE [63]-[66]. However, to obtain a very accurate solution or when the perturbation parameter is not sufficiently small, these methods can be computationally complex due to their non-recursive nature. Comparisons between the aforementioned techniques and fixed-point iteration methods are presented in [59] and [63] where it was shown that the performance of fixed-point iteration methods is superior.

The next step in the design of the algorithm would be to obtain the initial conditions of the errors. $\mathbf{E}_1^{(0)}$, $\mathbf{E}_2^{(0)}$, $\mathbf{E}_3^{(0)}$ are obtained by solving (3.20) after setting $\varepsilon = 0$.

$$\mathbf{D}_1^T \mathbf{E}_1^{(0)} + \mathbf{E}_1^{(0)} \mathbf{D}_1 + \mathbf{D}_2^T \mathbf{E}_2^{(0)T} + \mathbf{E}_2^{(0)} \mathbf{D}_2 = \mathbf{0} \tag{3.24a}$$

$$\mathbf{E}_2^{(0)} \mathbf{A}_4 + \mathbf{E}_1^{(0)} \mathbf{A}_2 + \mathbf{D}_2^T \mathbf{E}_3^{(0)} + \mathbf{Q}_2 = \mathbf{H}_2 \tag{3.24b}$$

$$\mathbf{E}_3^{(0)} \mathbf{A}_4 + \mathbf{A}_4^T \mathbf{E}_3^{(0)} + \mathbf{Q}_3 + \mathbf{P}_2^{(0)T} \mathbf{A}_2 + \mathbf{A}_2^T \mathbf{P}_2^{(0)} = \mathbf{0} \tag{3.24c}$$

Initially, (3.24c) is solved as a Lyapunov equation to obtain $\mathbf{E}_3^{(0)}$. Then, $\mathbf{E}_2^{(0)}$ is isolated from (3.24b) leading to

$$\mathbf{E}_2^{(0)} = (\mathbf{H}_2 - \mathbf{E}_1^{(0)} \mathbf{A}_2 - \mathbf{D}_2^T \mathbf{E}_3^{(0)} - \mathbf{Q}_2) \mathbf{A}_4^{-1} \tag{3.25}$$

Then, $\mathbf{E}_1^{(0)}$ is obtained from (3.24a) after the expression for $\mathbf{E}_2^{(0)}$ is substituted from (3.25) (likewise for $\mathbf{E}_2^{(0)T}$). Lastly, (3.24a) is solved algebraically to get $\mathbf{E}_2^{(0)}$ in terms of $\mathbf{E}_1^{(0)}$ and $\mathbf{E}_3^{(0)}$.

Conversely, the initial conditions can be taken as $\mathbf{E}_1^{(0)} = 0, \quad \mathbf{E}_2^{(0)} = 0, \quad \mathbf{E}_3^{(0)} = 0$ but the trade-off would be the number of iterations to achieve the desired solution. After some algebra, the algorithm for the new class of singularly perturbed systems follows.

$$\mathbf{E}_1^{(i+1)}\mathbf{A}_s + \mathbf{A}_s^T\mathbf{E}_1^{(i+1)} = \mathbf{D}_3\mathbf{A}_4^{-1}\mathbf{D}_2 + \mathbf{D}_2^T\mathbf{A}_4^{-T}\mathbf{D}_3^T + \varepsilon\mathbf{H}_1^{(i)} \tag{3.26a}$$

$$\mathbf{E}_2^{(i+1)}\mathbf{A}_4 + \mathbf{E}_1^{(i+1)}\mathbf{A}_2 + \mathbf{D}_2^T\mathbf{E}_3^{(i+1)} + \mathbf{Q}_2 = \mathbf{H}_2^{(i)} + \varepsilon\mathbf{H}_3^{(i,i+1)} \tag{3.26b}$$

$$\mathbf{E}_3^{(i+1)}\mathbf{A}_4 + \mathbf{A}_4^T\mathbf{E}_3^{(i+1)} + \mathbf{A}_2^T\mathbf{P}_2^{(0)} + \mathbf{P}_2^{(0)T}\mathbf{A}_2 = -\varepsilon(\mathbf{A}_2^T\mathbf{E}_2^{(i)} + \mathbf{E}_2^{T(i)}\mathbf{A}_2) \tag{3.26c}$$
$$+ \varepsilon\mathbf{H}_4^{(i)}$$

where $\mathbf{A}_s = \mathbf{D}_1 - \mathbf{A}_2\mathbf{A}_4^{-1}\mathbf{D}_2$ and $\mathbf{D}_3 = \mathbf{D}_2^T\mathbf{E}_3^{(i+1)} + \mathbf{Q}_2 - \mathbf{H}_2^{(i)} - \varepsilon\mathbf{H}_3^{(i,i+1)}$. $\mathbf{P}_j^{(i)} = \mathbf{P}_j^{(0)} + \varepsilon\mathbf{E}_j^{(i)}, j = 1, 2, 3$ and matrices $\mathbf{H}_k, \ k = 1, 2, 3, 4$ in (3.21) are updated in each iteration as follows.

$$\mathbf{H}_1^{(i)} = \mathbf{E}_1^{(i)}\mathbf{S}_1\mathbf{E}_1^{(i)} + \mathbf{E}_2^{(i)}\mathbf{S}_4\mathbf{E}_2^{T(i)}$$

$$\mathbf{H}_2^{(i)} = \mathbf{P}_1^{(0)}\mathbf{S}_1\mathbf{P}_2^{(0)} - \mathbf{A}_1^T(\mathbf{P}_2^{(0)} + \varepsilon\mathbf{E}_2^{(i)})$$

$$\mathbf{H}_3^{(i)} = \mathbf{P}_1^{(0)}\mathbf{S}_1\mathbf{E}_2^{(i)} + \mathbf{E}_1^{(i)}\mathbf{S}_1\mathbf{P}_2^{(0)} + \mathbf{E}_2^{(i)}\mathbf{S}_4\mathbf{E}_3^{(i)} + \varepsilon\mathbf{E}_1^{(i)}\mathbf{S}_1\mathbf{E}_2^{(i)}$$

$$\mathbf{H}_4^{(i,i+1)} = \mathbf{P}_2^{(0)T}\mathbf{S}_1\mathbf{P}_2^{(0)} + \varepsilon\mathbf{P}_2^{(0)T}\mathbf{S}_1\mathbf{E}_2^{(i)} + \varepsilon\mathbf{E}_2^{T(i)}\mathbf{S}_1\mathbf{P}_2^{(0)} + \varepsilon^2\mathbf{E}_2^{T(i)}\mathbf{S}_1\mathbf{E}_2^{(i)}$$
$$+ \mathbf{E}_3^{(i+1)}\mathbf{S}_4\mathbf{E}_3^{(i+1)}$$

Solution of recursive equations similar to (3.26) are discussed in [67], [82]-[83]. Essentially the solution is obtained by initially solving (3.26c) then (3.26a) and lastly (3.26b). The pseudocode containing the steps of the solution is presented in Algorithm 1.

Algorithm 1 Evaluate $\mathbf{E}^{(i)}$

1: **procedure** SOLVE RECURSIVE EQUATIONS
2:     **while** solution of $\mathbf{E}^{(i)}$ converges **do**
3:         solve (3.26c) as Lyapunov to obtain $\mathbf{E}_3^{(i)}$
4:         update: $\mathbf{P}_3^{(i)} \leftarrow \mathbf{P}_3^{(0)} + \varepsilon\mathbf{E}_3^{(i)}$
5:         solve (3.26a) as Lyapunov to obtain $\mathbf{E}_1^{(i)}$
6:         update: $\mathbf{P}_1^{(i)} \leftarrow \mathbf{P}_1^{(0)} + \varepsilon\mathbf{E}_1^{(i)}$
7:         solve (3.26b) algebraically to obtain $\mathbf{E}_2^{(i)}$
8:         update: $\mathbf{P}_2^{(i)} \leftarrow \mathbf{P}_2^{(0)} + \varepsilon\mathbf{E}_2^{(i)}$

The rate of convergence of this algorithm is summarized by the following theorem

Theorem 3.1 Under assumption 1, (3.26) converges to the exact solution of the error with convergence rate $\mathcal{O}(\varepsilon)$ [59].

$$\|\mathbf{E}_j - \mathbf{E}_j^{(i)}\| = \mathcal{O}(\varepsilon^i), \ i = 1, 2, 3, \cdots; \ j = 1, 2, 3 \tag{3.27}$$

Proof. The proof starts by showing the existence of a bounded solution of $\mathbf{E}_1$, $\mathbf{E}_2$, and $\mathbf{E}_3$ in the neighborhood of $\varepsilon^* \in [\varepsilon_{min}, \varepsilon_{max}]$. It is sufficient to show that the corresponding Jacobian in (3.28) is non-singular at $\varepsilon = 0$ [59].

$$J(\varepsilon) = \begin{bmatrix} \dfrac{\partial \mathbf{F}_1}{\partial \mathbf{E}_1} & \dfrac{\partial \mathbf{F}_1}{\partial \mathbf{E}_2} & \dfrac{\partial \mathbf{F}_1}{\partial \mathbf{E}_3} \\ \dfrac{\partial \mathbf{F}_2}{\partial \mathbf{E}_1} & \dfrac{\partial \mathbf{F}_2}{\partial \mathbf{E}_2} & \dfrac{\partial \mathbf{F}_2}{\partial \mathbf{E}_3} \\ \dfrac{\partial \mathbf{F}_3}{\partial \mathbf{E}_1} & \dfrac{\partial \mathbf{F}_3}{\partial \mathbf{E}_2} & \dfrac{\partial \mathbf{F}_3}{\partial \mathbf{E}_3} \end{bmatrix} \tag{3.28}$$

$\mathbf{F}_i$, $i = 1, 2, 3$ in (3.28) represents each of the equations in (3.20). The complete Jacobian, after (3.26a) has been algebraically manipulated into a more explicit form (see Appendix A for more details), becomes

$$\mathbf{J}(\varepsilon) \triangleq \begin{bmatrix} \mathbf{J}_{11} & \mathbf{0} & \mathbf{0} \\ \mathbf{J}_{21} & \mathbf{J}_{22} & \mathbf{J}_{23} \\ \mathbf{0} & \mathbf{0} & \mathbf{J}_{33} \end{bmatrix} + \begin{bmatrix} \mathcal{O}(\varepsilon) & \mathcal{O}(\varepsilon) & \mathbf{0} \\ \mathbf{0} & \mathcal{O}(\varepsilon) & \mathcal{O}(\varepsilon) \\ \mathbf{0} & \mathcal{O}(\varepsilon) & \mathbf{0} \end{bmatrix} \tag{3.29}$$

The entries in the second matrix come from elements containing the ε term in (3.20). To guarantee that $J(\varepsilon)$ is non-singular, we have to show that the diagonal blocks are non-singular as well. They can be represented by using a Kronecker product

$$\mathbf{J}_{11} = \mathbf{A}_s^T \otimes \mathbf{I}_n + \mathbf{I}_n \otimes \mathbf{A}_s^T$$

$$\mathbf{J}_{22} = \mathbf{A}_4^T \otimes \mathbf{I}_m \tag{3.30}$$

$$\mathbf{J}_{33} = \mathbf{A}_4^T \otimes \mathbf{I}_m + \mathbf{I}_m \otimes \mathbf{A}_4^T$$

where $\mathbf{I}_n$ and $\mathbf{I}_m$ are identity matrices of corresponding dimensions. $\mathbf{J}_{22}$ and $\mathbf{J}_{33}$ are both dependent on $\mathbf{A}_4$ therefore they are invertible by Assumption 2.1. $\mathbf{A}_s$ is the feedback matrix of the slow subsystem hence asymptotically stable. Therefore, a bounded solution for the error matrix $\mathbf{E}$ is guaranteed. The convergence rate can be found by

subtracting the error equations (3.20) from the proposed algorithm (3.26) for $i = 0$. The norm of this difference for the third equation becomes

$$(\mathbf{E}_3 - \mathbf{E}_3^{(1)})\mathbf{A}_4 + \mathbf{A}_4^T(\mathbf{E}_3 - \mathbf{E}_3^{(1)}) = \varepsilon\mathcal{F}(\mathbf{E}_2, \mathbf{E}_3, \varepsilon) \tag{3.31}$$

Feedback matrix $\mathbf{A}_4$ is asymptotically stable and $\mathbf{E}_2$ and $\mathbf{E}_3$ are bounded implying

$$\|\mathbf{E}_3 - \mathbf{E}_3^{(1)}\| = \mathcal{O}(\varepsilon) \tag{3.32}$$

Similar results are obtained for the remaining two equations resulting in

$$\|\mathbf{E}_j - \mathbf{E}_j^{(1)}\| = \mathcal{O}(\varepsilon), \ j = 1, 2, 3 \tag{3.33}$$

Repeating this procedure for $i = 2, 3, \ldots$, and using (3.33) and (3.21) it can be shown that

$$\|\mathbf{H}_j - \mathbf{H}_j^{(i-1)}\| = \mathcal{O}(\varepsilon^i), \ i = 1, 2, 3, \cdots \tag{3.34}$$

and

$$\|\mathbf{E} - \mathbf{E}^{(i)}\| = \mathcal{O}(\varepsilon^i), \ i = 1, 2, 3, \cdots \tag{3.35}$$

The proof is complete. $\square$

Equation (3.35) suggests that the algorithm has linear convergence, implying that the accuracy improves in each iteration by $\mathcal{O}(\varepsilon)$. Having knowledge of the error matrix for each iteration, the approximate solution P of the CARE is then given by

$$\mathbf{P}^{(i)} = \begin{bmatrix} \mathbf{P}_1^{(0)} + \varepsilon\mathbf{E}_1^{(i)} & \varepsilon(\mathbf{P}_2^{(0)} + \varepsilon\mathbf{E}_2^{(i)}) \\ \varepsilon(\mathbf{P}_2^{(0)T} + \varepsilon\mathbf{E}_2^{T(i)}) & \varepsilon(\mathbf{P}_3^{(0)} + \varepsilon\mathbf{E}_3^{(i)}) \end{bmatrix} \tag{3.36}$$

The static feedback gain is then

$$\mathbf{G}^{(i)} = -\mathbf{R}^{-1}\mathbf{B}^T\mathbf{P}^{(i)} \tag{3.37}$$

Under this feedback the cost function becomes

$$J^{(i)} = \int_0^\infty [x^T(t)(\mathbf{Q} + \mathbf{G}^{(i)T}\mathbf{R}\mathbf{G}^{(i)})x(t)]dt \tag{3.38}$$

The integral in (3.38) is evaluated by finding the solution of the following Lyapunov equation [32]

$$(\mathbf{A} - \mathbf{S}\mathbf{P}^{(i)})^T\mathbf{V}^{(i)} + \mathbf{V}^{(i)}(\mathbf{A} - \mathbf{S}\mathbf{P}^{(i)}) + \mathbf{Q} + \mathbf{P}^{(i)T}\mathbf{S}\mathbf{P}^{(i)} = 0 \tag{3.39}$$

We assume that the system initial conditions are distributed on the unit sphere therefore $J^{(i)}$ is simply evaluated as

$$J^{(i)} = \mathrm{tr}\{\mathbf{V}^{(i)}\} \tag{3.40}$$

Convergence of the approximate optimal cost (3.40) is related to the convergence of the approximate solution $\mathbf{P}^{(i)}$ and the corresponding feedback gain $\mathbf{G}^{(i)}$ [101]. If $\mathbf{P}^{(i)} - \mathbf{P} = \mathcal{O}(\varepsilon^i)$, where i is a positive integer, then $\mathbf{J}^{(i)} - \mathbf{J}_{opt} = \mathcal{O}(\varepsilon^{2i})$. This indicates that convergence to the exact solution is reached in only a few iterations when ε is sufficiently small.

3.2.2 Weakly Coupled Inputs Case

A more general case of what was considered earlier is when the input matrix does not contain any zero partitions causing the singularly perturbed system input matrix to be weakly coupled. Likewise, this matrix structure has been known to occur in models of real physical systems such as the ones stated in the introduction and is generally common. The state-space model corresponding to this case is now given by

$$
\begin{aligned}
\dot{x}_1(t) &= \mathbf{A}_1 x_1(t) + \mathbf{A}_2 x_2(t) + \mathbf{B}_1 u_1(t) + \varepsilon \mathbf{B}_2 u_2(t) \\
\varepsilon \dot{x}_2(t) &= \mathbf{A}_3 x_1(t) + \mathbf{A}_4 x_2(t) + \varepsilon \mathbf{B}_3 u_1(t) + \mathbf{B}_4 u_2(t)
\end{aligned}
\tag{3.41}
$$

Note that input $u_2(t)$ in the first equation and input $u_1(t)$ in the second equation are multiplied by ε. This creates the weak coupling between the inputs. Due the structure of the input matrix, the algebra in this case is more involved but the procedure is no different than the earlier case.

To obtain the individual CAREs, we start by substituting the corresponding matrix $\mathbf{B}$, matrices $\mathbf{R}$ and $\mathbf{Q}$ defined in (3.6)-(3.7) and matrix (3.11) in (3.10).

$$\mathbf{A}_1^T \mathbf{P}_1 + \mathbf{A}_3^T \mathbf{P}_2^T + \mathbf{P}_1 \mathbf{A}_1 + \mathbf{P}_2 \mathbf{A}_3 + \mathbf{Q}_1 - \mathbf{P}_1 \mathbf{S}_1 \mathbf{P}_1 - \mathbf{P}_2 \mathbf{S}_4 \mathbf{P}_2^T - \varepsilon \mathbf{Z}_{11} \tag{3.42a}$$
$$- \varepsilon^2 \mathbf{Z}_{12} = \mathbf{0}$$

$$\varepsilon \mathbf{A}_1^T \mathbf{P}_2 + \mathbf{A}_3^T \mathbf{P}_3 + \mathbf{P}_1 \mathbf{A}_2 + \mathbf{P}_2 \mathbf{A}_4 + \varepsilon \mathbf{Q}_2 - \mathbf{P}_2 \mathbf{S}_4 \mathbf{P}_3 - \varepsilon \mathbf{Z}_{21} - \varepsilon^2 \mathbf{Z}_{22} \tag{3.42b}$$
$$- \varepsilon^3 \mathbf{Z}_{23} = \mathbf{0}$$

$$\varepsilon \mathbf{A}_2^T \mathbf{P}_2 + \mathbf{A}_4^T \mathbf{P}_3 + \varepsilon \mathbf{P}_2^T \mathbf{A}_2 + \mathbf{P}_3 \mathbf{A}_4 + \varepsilon \mathbf{Q}_3 - \mathbf{P}_3 \mathbf{S}_4 \mathbf{P}_3 - \varepsilon^2 \mathbf{Z}_{31} - \varepsilon^4 \mathbf{Z}_{32} = \mathbf{0} \tag{3.42c}$$

where $\mathbf{S}_1$ and $\mathbf{S}_4$ are defined in (3.14) and $\mathbf{Z}_{ij}$, $i, j = 1, 2, 3$ are defined as follows.

$$\mathbf{Z}_{11} = \mathbf{P}_2\mathbf{B}_3\mathbf{R}_1^{-1}\mathbf{B}_1^T\mathbf{P}_1 + \mathbf{P}_1\mathbf{B}_1\mathbf{R}_1^{-1}\mathbf{B}_3^T\mathbf{P}_2^T + \mathbf{P}_2\mathbf{B}_4\mathbf{R}_4^{-1}\mathbf{B}_2^T\mathbf{P}_1 + \mathbf{P}_1\mathbf{B}_2\mathbf{R}_4^{-1}\mathbf{B}_4^T\mathbf{P}_2^T$$

$$\mathbf{Z}_{12} = \mathbf{P}_1\mathbf{B}_2\mathbf{R}_4^{-1}\mathbf{B}_2^T\mathbf{P}_1 + \mathbf{P}_2\mathbf{B}_3\mathbf{R}_1^{-1}\mathbf{B}_3^T\mathbf{P}_2^T$$

$$\mathbf{Z}_{21} = \mathbf{P}_1\mathbf{B}_1\mathbf{R}_1^{-1}\mathbf{B}_1^T\mathbf{P}_2 + \mathbf{P}_1\mathbf{B}_1\mathbf{R}_1^{-1}\mathbf{B}_3^T\mathbf{P}_3 + \mathbf{P}_1\mathbf{B}_2\mathbf{R}_4^{-1}\mathbf{B}_4^T\mathbf{P}_3$$

$$\mathbf{Z}_{22} = \mathbf{P}_2\mathbf{B}_3\mathbf{R}_1^{-1}\mathbf{B}_1^T\mathbf{P}_2 + \mathbf{P}_2\mathbf{B}_4\mathbf{R}_4^{-1}\mathbf{B}_2^T\mathbf{P}_2 + \mathbf{P}_2\mathbf{B}_3\mathbf{R}_1^{-1}\mathbf{B}_3^T\mathbf{P}_3$$

$$\mathbf{Z}_{23} = \mathbf{P}_1\mathbf{B}_2\mathbf{R}_4^{-1}\mathbf{B}_2^T\mathbf{P}_2$$

$$\mathbf{Z}_{31} = \mathbf{P}_2^T\mathbf{B}_1\mathbf{R}_1^{-1}\mathbf{B}_1^T\mathbf{P}_2 + \mathbf{P}_3\mathbf{B}_3\mathbf{R}_1^{-1}\mathbf{B}_1^T\mathbf{P}_2 + \mathbf{P}_3\mathbf{B}_4\mathbf{R}_4^{-1}\mathbf{B}_2^T\mathbf{P}_2 + \mathbf{P}_2^T\mathbf{B}_1\mathbf{R}_1^{-1}\mathbf{B}_3^T\mathbf{P}_3$$
$$+ \mathbf{P}_2^T\mathbf{B}_2\mathbf{R}_4^{-1}\mathbf{B}_4^T\mathbf{P}_3 + \mathbf{P}_3\mathbf{B}_3\mathbf{R}_1^{-1}\mathbf{B}_3^T\mathbf{P}_3$$

$$\mathbf{Z}_{32} = \mathbf{P}_2^T\mathbf{B}_2\mathbf{R}_4^{-1}\mathbf{B}_2^T\mathbf{P}_2$$

$$\tag{3.43}$$

For $\varepsilon = 0$, the zero-order approximation of (3.42) is the same as the decoupled inputs case discussed previously. The error equations are obtained by subtracting (3.15) from (3.42) after (3.19) has been substituted in (3.42) and the fixed-point iteration algorithm is designed the same way as the case presented in the previous section. The error equation are as follows.

$$\mathbf{E}_1\mathbf{D}_1 + \mathbf{D}_1^T\mathbf{E}_1 + \mathbf{E}_2\mathbf{D}_2 + \mathbf{D}_2^T\mathbf{E}_2^T - \mathbf{Y}_1 = \varepsilon\mathbf{H}_5 \tag{3.44a}$$

$$\mathbf{E}_2\mathbf{A}_4 + \mathbf{E}_1\mathbf{A}_2 + \mathbf{A}_1^T\mathbf{P}_2^{(0)} + \varepsilon\mathbf{A}_1^T\mathbf{E}_2 + \mathbf{A}_3^T\mathbf{E}_3 + \mathbf{Q}_2 = \mathbf{H}_6 + \varepsilon\mathbf{H}_7 \tag{3.44b}$$

$$\mathbf{E}_3\mathbf{A}_4 + \mathbf{A}_4^T\mathbf{E}_3 + \mathbf{A}_2^T\mathbf{P}_2^{(0)} + \mathbf{P}_2^{(0)T}\mathbf{A}_2 + \varepsilon\mathbf{E}_2\mathbf{A}_2 + \varepsilon\mathbf{A}_2^T\mathbf{E}_2 + \mathbf{Q}_3 = \mathbf{H}_8 + \varepsilon\mathbf{H}_9 \tag{3.44c}$$

As in the decoupled inputs case, error equations (3.44) have non-linear terms and cross-coupling terms multiplied by ε hence fixed-point iteration methods are great candidates to obtain their accurate solution. In addition, error equations (3.44) have a familiar structure hinting that the algorithm for this case would follow the same steps. That is, the first and last equations in (3.44) are Lyapunov equations that can easily be solved, and the solution of the second equation for $\mathbf{E}_2$ is obtained algebraically after all other quantities are known.

Matrix $\mathbf{D}_1$ and $\mathbf{D}_2$ were defined in the previous section and the rest of unknown matrices are defined as follows.

$$\mathbf{Y}_1 = \mathbf{P}_2^{(0)}\mathbf{B}_3\mathbf{R}_1^{-1}\mathbf{B}_1^T\mathbf{P}_1^{(0)} + \mathbf{P}_1^{(0)}\mathbf{B}_1\mathbf{R}_1^{-1}\mathbf{B}_3^T\mathbf{P}_2^{(0)T} + \mathbf{P}_2^{(0)}\mathbf{B}_4\mathbf{R}_4^{-1}\mathbf{B}_2^T\mathbf{P}_1^{(0)}$$
$$+ \mathbf{P}_1^{(0)}\mathbf{B}_2\mathbf{R}_4^{-1}\mathbf{B}_4^T\mathbf{P}_2^{(0)T}$$

$$\mathbf{H}_5 = \mathbf{E}_1\mathbf{S}_1\mathbf{E}_1 + \mathbf{E}_2\mathbf{S}_4\mathbf{E}_2^T + \varepsilon\bar{\mathbf{Z}}_{12} + \mathbf{P}_2^{(0)}\mathbf{B}_3\mathbf{R}_1^{-1}\mathbf{B}_1^T\mathbf{E}_1 + \mathbf{E}_2\mathbf{B}_3\mathbf{R}_1^{-1}\mathbf{B}_1^T\mathbf{P}_1^{(0)}$$
$$+ \varepsilon\mathbf{E}_2\mathbf{B}_3\mathbf{R}_1^{-1}\mathbf{B}_1^T\mathbf{E}_1 + \mathbf{P}_1^{(0)}\mathbf{B}_1\mathbf{R}_1^{-1}\mathbf{B}_3^T\mathbf{E}_2^T + \mathbf{E}_1\mathbf{B}_1\mathbf{R}_1^{-1}\mathbf{B}_3^T\mathbf{P}_2^{(0)T}$$
$$+ \varepsilon\mathbf{E}_1\mathbf{B}_1\mathbf{R}_1^{-1}\mathbf{B}_3^T\mathbf{E}_2^T + \mathbf{P}_2^{(0)}\mathbf{B}_4\mathbf{R}_4^{-1}\mathbf{B}_2^T\mathbf{E}_1 + \mathbf{E}_2\mathbf{B}_4\mathbf{R}_4^{-1}\mathbf{B}_2^T\mathbf{P}_1^{(0)}$$
$$+ \varepsilon\mathbf{E}_2\mathbf{B}_4\mathbf{R}_4^{-1}\mathbf{B}_2^T\mathbf{E}_1 + \mathbf{P}_1^{(0)}\mathbf{B}_2\mathbf{R}_4^{-1}\mathbf{B}_4^T\mathbf{E}_2 + \mathbf{E}_1\mathbf{B}_2\mathbf{R}_4^{-1}\mathbf{B}_4^T\mathbf{P}_2^{(0)T}$$
$$+ \varepsilon\mathbf{E}_1\mathbf{B}_2\mathbf{R}_4^{-1}\mathbf{B}_4^T\mathbf{E}_2$$

$$\mathbf{H}_6 = \mathbf{P}_2^{(0)}\mathbf{S}_4\mathbf{E}_3 + \mathbf{E}_2\mathbf{S}_4\mathbf{P}_3^{(0)} + \mathbf{P}_1^{(0)}\mathbf{B}_1\mathbf{R}_1^{-1}\mathbf{B}_1^T\mathbf{P}_2^{(0)} + \mathbf{P}_1^{(0)}\mathbf{B}_1\mathbf{R}_1^{-1}\mathbf{B}_3^T\mathbf{P}_3^{(0)}$$
$$+ \mathbf{P}_1^{(0)}\mathbf{B}_2\mathbf{R}_4^{-1}\mathbf{B}_4^T\mathbf{P}_3^{(0)}$$

$$\mathbf{H}_7 = \mathbf{E}_2\mathbf{S}_4\mathbf{E}_3 + \bar{\mathbf{Z}}_{22} + \varepsilon\bar{\mathbf{Z}}_{33} + \mathbf{P}_1^{(0)}\mathbf{B}_1\mathbf{R}_1^{-1}\mathbf{B}_1^T\mathbf{E}_2 + \mathbf{E}_1\mathbf{B}_1\mathbf{R}_1^{-1}\mathbf{B}_1^T\mathbf{P}_2^{(0)}$$
$$+ \varepsilon\mathbf{E}_1\mathbf{B}_1\mathbf{R}_1^{-1}\mathbf{B}_1^T\mathbf{E}_2 + \mathbf{P}_1^{(0)}\mathbf{B}_1\mathbf{R}_1^{-1}\mathbf{B}_3^T\mathbf{E}_3 + \mathbf{E}_1\mathbf{B}_1\mathbf{R}_1^{-1}\mathbf{B}_3^T\mathbf{P}_3^{(0)}$$
$$+ \varepsilon\mathbf{E}_1\mathbf{B}_1\mathbf{R}_1^{-1}\mathbf{B}_3^T\mathbf{E}_3 + \mathbf{P}_1^{(0)}\mathbf{B}_2\mathbf{R}_4^{-1}\mathbf{B}_4^T\mathbf{E}_3 + \mathbf{E}_1\mathbf{B}_2\mathbf{R}_4^{-1}\mathbf{B}_4^T\mathbf{P}_3^{(0)}$$
$$+ \varepsilon\mathbf{E}_1\mathbf{B}_2\mathbf{R}_4^{-1}\mathbf{B}_4^T\mathbf{E}_3$$

$$\mathbf{H}_8 = \mathbf{P}_3^{(0)}\mathbf{S}_4\mathbf{E}_3 + \mathbf{E}_3\mathbf{S}_4\mathbf{P}_3^{(0)}$$

$$\mathbf{H}_9 = \mathbf{E}_3\mathbf{S}_4\mathbf{E}_3 + \mathbf{Z}_{31}^{(0)} + \varepsilon\bar{\mathbf{Z}}_{32} + \varepsilon^2\bar{\mathbf{Z}}_{33}$$

where $\bar{\mathbf{Z}}_{ij}, i, j = 1, 2, 3$ are updated quantities after (3.19) has been substituted. The initial conditions for the errors are evaluated from the equations below.

$$\mathbf{E}_1^{(0)}\mathbf{A}_1 + \mathbf{E}_2^{(0)}\mathbf{A}_3 + \mathbf{A}_1^T\mathbf{E}_1^{(0)} + \mathbf{A}_3^T\mathbf{E}_2^{(0)T} = \bar{\mathbf{H}}_5 \tag{3.45a}$$

$$\mathbf{E}_2^{(0)}\mathbf{A}_4 + \mathbf{E}_1^{(0)}\mathbf{A}_2 + \mathbf{A}_1^T\mathbf{P}_2^{(0)} + \mathbf{A}_3^T\mathbf{E}_3^{(0)} + \mathbf{Q}_2 = \mathbf{H}_6 \tag{3.45b}$$

$$\mathbf{E}_3^{(0)}(\mathbf{A}_4 - \mathbf{S}_4\mathbf{P}_3^{(0)}) + (\mathbf{A}_4^T - \mathbf{P}_3^{(0)}\mathbf{S}_4)\mathbf{E}_3^{(0)} + \mathbf{A}_2^T\mathbf{P}_2^{(0)} + \mathbf{P}_2^{(0)T}\mathbf{A}_2 + \mathbf{Q}_3 = \mathbf{0} \tag{3.45c}$$

where $\bar{\mathbf{H}}_5$ is the same as $\mathbf{H}_5$ except that all the terms containing ε are set to zero. The solution of the error equations is easily obtained by initially solving (3.45c) as a Lyapunov equation for $\mathbf{E}_3^{(0)}$. Then, $\mathbf{E}_1^{(0)}$ is obtained from (3.45a) after $\mathbf{E}_2^{(0)}$ is substituted from (3.45b). Finally, $\mathbf{E}_2^{(0)}$ is obtained from (3.45b). After the initial conditions for the

errors are obtained, the parallel algorithm is as follows.

$$\mathbf{A}_L^T \mathbf{E}_1^{(i+1)} + \mathbf{E}_1^{(i+1)} \mathbf{A}_L + \mathbf{H}_R^{(i,i+1)} \mathbf{A}_F^{-1} \mathbf{A}_3 + \mathbf{A}_3^T \mathbf{A}_F^{-T} \mathbf{H}_R^{T(i,i+1)} - \mathbf{H}_5 = \mathbf{0} \qquad (3.46a)$$

$$\mathbf{E}_2^{(i+1)} \mathbf{A}_F + \mathbf{E}_1^{(i+1)} \mathbf{A}_2 + \mathbf{A}_1^T \mathbf{P}_2^{(0)} + \varepsilon \mathbf{A}_1^T \mathbf{E}_2^{(i)} + (\mathbf{A}_3^T - \mathbf{P}_2^{(0)} \mathbf{S}_4) \mathbf{E}_3^{(i+1)} \qquad (3.46b)$$
$$+ \mathbf{Q}_2 = \mathbf{Z}_{21}^{(0)} + \varepsilon \mathbf{H}_7^{(i)}$$

$$\mathbf{E}_3^{(i+1)} \mathbf{A}_F + \mathbf{A}_F^T \mathbf{E}_3^{(i+1)} + \mathbf{A}_2^T \mathbf{P}_2^{(0)} + \mathbf{P}_2^{(0)T} \mathbf{A}_2 + \varepsilon \mathbf{E}_2^{(i)} \mathbf{A}_2 + \varepsilon \mathbf{A}_2^T \mathbf{E}_2^{(i)} \qquad (3.46c)$$
$$+ \mathbf{Q}_3 = \varepsilon \mathbf{H}_9^{(i+1)}$$

where $\mathbf{A}_L = \mathbf{A}_1 - \mathbf{A}_2 \mathbf{A}_F^{-1} \mathbf{A}_3$, $\mathbf{H}_R = \mathbf{Z}_{21}^{(0)} + \varepsilon \mathbf{H}_7^{(i)} - \mathbf{A}_1^T \mathbf{P}_2^{(0)} - \varepsilon \mathbf{A}_1^T \mathbf{E}_2^{(i)} - (\mathbf{A}_3^T - \mathbf{P}_2^{(0)} \mathbf{S}_4) \mathbf{E}_3^{(i+1)} - \mathbf{Q}_2$, and $\mathbf{A}_F = \mathbf{A}_4 - \mathbf{S}_4 \mathbf{P}_3^{(0)}$. The solution of the algorithm follows the same steps as Algorithm 1, namely (3.46c) is initially solved, then the solution of (3.46a) is obtained after $\mathbf{E}_2$ is substituted and lastly, (3.46b) is solved algebraically to obtain $\mathbf{E}_2^{(i)}$. The rate of convergence of the algorithm is the same as in the decoupled inputs case, that is $\mathcal{O}(\varepsilon)$ per iteration. Matrix $\mathbf{P}^{(i)}$, which is used to determine the approximate optimal gain is given by (3.36) and the approximate cost function is evaluated using (3.40).

3.2.3 Weakly Controlled Fast Subsystem

In this section, the case when the input matrix is not affected by the perturbation parameter is considered. The structure of matrix $\mathbf{B}$ in this case gives the following state-space model.

$$\dot{x}_1(t) = \mathbf{A}_1 x_1(t) + \mathbf{A}_2 x_2(t) + \mathbf{B}_1 u_1(t)$$
$$\varepsilon \dot{x}_2(t) = \mathbf{A}_3 x_1(t) + \mathbf{A}_4 x_2(t) + \varepsilon \mathbf{B}_4 u_2(t) \qquad (3.47)$$

After the matrices have been substituted in (3.10), the reduced-order CAREs now become

$$\mathbf{A}_1^T \mathbf{P}_1 + \mathbf{A}_3^T \mathbf{P}_2^T + \mathbf{P}_1 \mathbf{A}_1 + \mathbf{P}_2 \mathbf{A}_3 + \mathbf{Q}_1 - \mathbf{P}_1 \mathbf{S}_1 \mathbf{P}_1 - \varepsilon^2 \mathbf{P}_2 \mathbf{S}_4 \mathbf{P}_2^T = \mathbf{0} \qquad (3.48a)$$

$$\varepsilon \mathbf{A}_1^T \mathbf{P}_2 + \mathbf{A}_3^T \mathbf{P}_3 + \mathbf{P}_1 \mathbf{A}_2 + \mathbf{P}_2 \mathbf{A}_4 + \varepsilon \mathbf{Q}_2 - \varepsilon \mathbf{P}_1 \mathbf{S}_1 \mathbf{P}_2 - \varepsilon^2 \mathbf{P}_2 \mathbf{S}_4 \mathbf{P}_3 = \mathbf{0} \qquad (3.48b)$$

$$\varepsilon \mathbf{A}_2^T \mathbf{P}_2 + \mathbf{A}_4^T \mathbf{P}_3 + \varepsilon \mathbf{P}_2^T \mathbf{A}_2 + \mathbf{P}_3 \mathbf{A}_4 + \varepsilon \mathbf{Q}_3 - \varepsilon^2 \mathbf{P}_2^T \mathbf{S}_1 \mathbf{P}_2 - \varepsilon^2 \mathbf{P}_3 \mathbf{S}_4 \mathbf{P}_3 = \mathbf{0} \qquad (3.48c)$$

The zero-order approximation of (3.48) is simply

$$\mathbf{A}_1^T \mathbf{P}_1^{(0)} + \mathbf{A}_3^T \mathbf{P}_2^{(0)T} + \mathbf{P}_1^{(0)} \mathbf{A}_1 + \mathbf{P}_2^{(0)} \mathbf{A}_3 + \mathbf{Q}_1 - \mathbf{P}_1^{(0)} \mathbf{S}_1 \mathbf{P}_1^{(0)} = \mathbf{0} \tag{3.49a}$$

$$\mathbf{A}_3^T \mathbf{P}_3^{(0)} + \mathbf{P}_1^{(0)} \mathbf{A}_2 + \mathbf{P}_2^{(0)} \mathbf{A}_4 = \mathbf{0} \tag{3.49b}$$

$$\mathbf{A}_4^T \mathbf{P}_3^{(0)} + \mathbf{P}_3^{(0)} \mathbf{A}_4 = \mathbf{0} \tag{3.49c}$$

(3.49a) and (3.49b) are the same as in the other previously discussed cases. The only difference are the last two terms on the left-hand side of (3.49a). Nonetheless, the simplification of (3.49) follows the same steps as the first two cases and one CARE and an algebraic equation are obtained as shown in (3.50).

$$\mathbf{A}_0^T \mathbf{P}_1^{(0)} + \mathbf{P}_1^{(0)} \mathbf{A}_0 + \mathbf{Q}_1 - \mathbf{P}_1^{(0)} \mathbf{S}_1 \mathbf{P}_1^{(0)} = \mathbf{0} \tag{3.50a}$$

$$\mathbf{P}_2^{(0)} + \mathbf{P}_1^{(0)} \mathbf{A}_2 \mathbf{A}_4^{-1} = \mathbf{0} \tag{3.50b}$$

$$\mathbf{P}_3^{(0)} = \mathbf{0} \tag{3.50c}$$

The error equations for this case are as follows.

$$\mathbf{E}_1 \mathbf{D}_1 + \mathbf{D}_1^T \mathbf{E}_1 + \mathbf{A}_3^T \mathbf{E}_2^T + \mathbf{E}_2 \mathbf{A}_3 = \varepsilon \mathbf{H}_{10} \tag{3.51a}$$

$$\mathbf{E}_2 \mathbf{A}_4 + \mathbf{A}_3^T \mathbf{E}_3 + \mathbf{E}_1 \mathbf{A}_2 + \mathbf{A}_1^T \mathbf{P}_2^{(0)} = \mathbf{H}_{11} + \varepsilon \mathbf{H}_{12} \tag{3.51b}$$

$$\mathbf{E}_3 \mathbf{A}_4 + \mathbf{A}_4^T \mathbf{E}_3 + \mathbf{A}_2^T \mathbf{P}_2^{(0)} + \mathbf{P}_2^{(0)T} \mathbf{A}_2 + \mathbf{Q}_3 = \varepsilon \mathbf{H}_{13} - \varepsilon(\mathbf{A}_2^T \mathbf{E}_2 + \mathbf{E}_2^T \mathbf{A}_2)$$

where

$$\mathbf{D}_1 = \mathbf{A}_1 - \mathbf{S}_1 \mathbf{P}_1^{(0)}$$

$$\mathbf{H}_{10} = \mathbf{E}_1 \mathbf{S}_1 \mathbf{E}_1 + \mathbf{P}_2^{(0)} \mathbf{S}_4 \mathbf{P}_2^{(0)T} + \varepsilon \mathbf{P}_2^{(0)} \mathbf{S}_4 \mathbf{E}_2^T + \varepsilon \mathbf{E}_2 \mathbf{S}_4 \mathbf{P}_2^{(0)T} + \varepsilon^2 \mathbf{E}_2 \mathbf{S}_4 \mathbf{E}_2^T$$

$$\mathbf{H}_{11} = \mathbf{P}_1^{(0)} \mathbf{S}_1 \mathbf{P}_2^{(0)} - \varepsilon \mathbf{A}_1^T \mathbf{E}_2 - \mathbf{Q}_2$$

$$\mathbf{H}_{12} = \mathbf{P}_1^{(0)} \mathbf{S}_1 \mathbf{E}_2 + \mathbf{E}_1 \mathbf{S}_1 \mathbf{P}_2^{(0)} + \varepsilon \mathbf{E}_1 \mathbf{S}_1 \mathbf{E}_2 + \mathbf{P}_2^{(0)} \mathbf{S}_4 \mathbf{P}_3^{(0)} + \mathbf{P}_2^{(0)} \mathbf{S}_4 \mathbf{E}_3 \tag{3.52}$$

$$\qquad + \varepsilon \mathbf{E}_2 \mathbf{S}_4 \mathbf{P}_3^{(0)} + \varepsilon^2 \mathbf{E}_2 \mathbf{S}_4 \mathbf{E}_3$$

$$\mathbf{H}_{13} = \mathbf{P}_2^{(0)T} \mathbf{S}_1 \mathbf{P}_2^{(0)} + \varepsilon \mathbf{P}_2^{(0)T} \mathbf{S}_1 \mathbf{E}_2 + \varepsilon \mathbf{E}_2^T \mathbf{S}_1 \mathbf{P}_2^{(0)} + \varepsilon^2 \mathbf{E}_2^T \mathbf{S}_1 \mathbf{E}_2 + \mathbf{P}_3^{(0)} \mathbf{S}_4 \mathbf{P}_3^{(0)}$$

$$\qquad + \varepsilon \mathbf{P}_3^{(0)} \mathbf{S}_4 \mathbf{E}_3 + \varepsilon \mathbf{E}_3 \mathbf{S}_4 \mathbf{P}_3^{(0)} + \varepsilon^2 \mathbf{E}_3 \mathbf{S}_4 \mathbf{E}_3$$

The zero-order error equations needed to obtain the initial conditions of the algorithm

are

$$\mathbf{E}_1^{(0)}\mathbf{D}_1 + \mathbf{D}_1^T\mathbf{E}_1^{(0)} + \mathbf{A}_3^T\mathbf{E}_2^{(0)T} + \mathbf{E}_2^{(0)}\mathbf{A}_3 = \mathbf{0} \tag{3.53a}$$

$$\mathbf{E}_2^{(0)}\mathbf{A}_4 + \mathbf{A}_3^T\mathbf{E}_3^{(0)} + \mathbf{E}_1^{(0)}\mathbf{A}_2 + \mathbf{A}_1^T\mathbf{P}_2^{(0)} = \mathbf{P}_1^{(0)}\mathbf{S}_1\mathbf{P}_2^{(0)} - \mathbf{Q}_2 \tag{3.53b}$$

$$\mathbf{E}_3^{(0)}\mathbf{A}_4 + \mathbf{A}_4^T\mathbf{E}_3^{(0)} + \mathbf{A}_2^T\mathbf{P}_2^{(0)} + \mathbf{P}_2^{(0)T}\mathbf{A}_2 + \mathbf{Q}_3 = \mathbf{0} \tag{3.53c}$$

As in the last two cases, (3.53c) and (3.53a) are solved as Lyapunov equations to obtain $\mathbf{E}_3^{(0)}$ and $\mathbf{E}_1^{(0)}$ (after $\mathbf{E}_2^{(0)}$ has been substituted in (3.53a)). Lastly, $\mathbf{E}_2^{(0)}$ is obtained by solving (3.53b) algebraically.

The proposed algorithm to obtain the errors follows.

$$\mathbf{E}_1^{(i+1)}\mathbf{D}_0 + \mathbf{D}_0^T\mathbf{E}_1^{(i+1)} + \mathbf{A}_3^T\mathbf{A}_4^{-T}\mathbf{H}_0^{T(i,i+1)} + \mathbf{H}_0^{(i,i+1)}\mathbf{A}_4^{-1}\mathbf{A}_3 = \varepsilon\mathbf{H}_{10}^{(i)} \tag{3.54a}$$

$$\mathbf{E}_2^{(i+1)}\mathbf{A}_4 + \mathbf{A}_3^T\mathbf{E}_3^{(i+1)} + \mathbf{E}_1^{(i+1)}\mathbf{A}_2 + \mathbf{A}_1^T\mathbf{P}_2^{(0)} = \mathbf{H}_{11}^{(i)} + \varepsilon\mathbf{H}_{12}^{(i,i+1)} \tag{3.54b}$$

$$\mathbf{E}_3^{(i+1)}\mathbf{A}_4 + \mathbf{A}_4^T\mathbf{E}_3^{(i+1)} + \mathbf{A}_2^T\mathbf{P}_2^{(0)} + \mathbf{P}_2^{T(0)}\mathbf{A}_2 + \mathbf{Q}_3 = \varepsilon\mathbf{H}_{13}^{(i)} \tag{3.54c}$$

$$- \varepsilon(\mathbf{A}_2^T\mathbf{E}_2^{(i)} + \mathbf{E}_2^{T(i)}\mathbf{A}_2)$$

where $\mathbf{D}_0 = \mathbf{D}_1 - \mathbf{A}_2\mathbf{A}_4^{-1}\mathbf{A}_3$ and $\mathbf{H}_0 = \mathbf{H}_{11} + \varepsilon\mathbf{H}_{12} - \mathbf{A}_1^T\mathbf{P}_2^{(0)} - \mathbf{A}_3^T\mathbf{E}_3$.

Similarly, the solution of (3.54) follows the same steps as Algorithm 1. The approximate matrix $\mathbf{P}^{(i)}$ is defined in (3.36). Just like in the decoupled inputs and the weakly coupled inputs cases, Theorem 3.1 holds and the approximate cost function is evaluated using (3.40).

Remark 3.4 *By investigating all three cases we see that there is an additional advantage. The solution of the zero-order approximation for all three cases is simplified to a CARE and an matrix algebraic equation. For the first and second cases, the solution is exactly the same. The CARE in the third case has less terms terms compared to the other two. This is very advantageous from a computational perspective when large scale models are considered (see [102]) as well as for avoiding possible ill-conditioning that could occur.*

Example 3.1 To illustrate the efficiency of the algorithm proposed in this section, we look at an example. The following fourth-order stable singularly perturbed model

corresponds to the decoupled inputs case.

$$
\mathbf{A} = \begin{bmatrix} 0 & 1 & 0 & 0 \\ 0 & 0 & 1 & 0 \\ 0 & 0 & 0 & 100 \\ -150 & -505 & -470 & -125 \end{bmatrix}, \ \mathbf{B} = \begin{bmatrix} 1 & 0 \\ 2 & 0 \\ 0 & 100 \\ 0 & 100 \end{bmatrix}, \ \mathbf{Q} = \begin{bmatrix} 1 & 0 & 0.01 & 0.02 \\ 0 & 2 & 0.01 & 0.03 \\ 0.01 & 0.01 & 0.02 & 0 \\ 0.02 & 0.03 & 0 & 0.02 \end{bmatrix}, \ \mathbf{R} = 1
$$

The eigenvalues of the model are $-0.538 \pm 0.174j$ and $-61.962 \pm 207.429j$. Using the ratio of the real part of the eigenvalue of the fast cluster with the real part of the eigenvalue of the slow cluster, the singular perturbation parameter is $\varepsilon = 0.01$. The results of the approximate CARE solution $\mathbf{P}^{(i)}$ versus the original $\mathbf{P}$ are shown in Table 3.1. It is evident that in a few iterations, the approximate solution approaches the original one[1].

Table 3.1: Convergence of approximate CARE solution to the actual value.

Iteration (i)	$||P^{(i)} - P||$	$|J^{(i)} - J_{opt}|$
0	6.3338162×10^{-3}	3.7268571×10^{-4}
1	7.8903535×10^{-7}	$9.4213526 \times 10^{-13}$
2	3.3152804×10^{-8}	$1.0214052 \times 10^{-14}$
3	1.0518355×10^{-9}	$1.7541524 \times 10^{-14}$
4	$3.0019249 \times 10^{-11}$	$2.3092639 \times 10^{-14}$
5	$8.8380134 \times 10^{-13}$	$2.2870594 \times 10^{-14}$
6	$3.7457814 \times 10^{-14}$	$2.6201263 \times 10^{-14}$
7	$2.2773932 \times 10^{-14}$	$2.4424907 \times 10^{-15}$
8	$2.3022198 \times 10^{-14}$	$6.6613381 \times 10^{-15}$

3.3 Linear Stochastic Filtering for the New Class of Singularly Perturbed Systems

As a follow-up of the above work, we extend the problem when noise is added to the model. The presence of disturbance is a realistic representation of physical systems. As an example, we can consider a microgrid setup where events such as geomagnetic influence, load demands, or interconnection of multiple components cause unwanted

---

[1]In this dissertation $\mathcal{O}(10^{-13})$ or less is considered zero to computer accuracy.

disturbances [103]-[105]. The latter are usually modeled as white noise.

Linear stochastic filtering, and more specifically the iterative solution of the LQG problem is considered for the three different input matrix structures discussed previously. The general LTI stochastic system in state-space form now has the following form

$$
\begin{aligned}
\dot{x}(t) &= \mathbf{A}x(t) + \mathbf{B}u(t) + \mathcal{F}w(t) \\
y(t) &= \mathbf{C}x(t) + \mathbf{D}u(t) + v(t)
\end{aligned}
\tag{3.55}
$$

where $x \in \mathbb{R}^{n+m}$ are the state variables, $u \in \mathbb{R}^p$ is the control vector input, and $y \in \mathbb{R}^q$ is the system output. $w \in \mathbb{R}^{r_1}$ and $v \in \mathbb{R}^{r_2}$ are zero-mean stationary Gaussian white noise processes ($\mathcal{N}(0, \mu_1)$ and $\mathcal{N}(0, \mu_2)$ respectively) and their intensities are positive definite i.e. $\mathbf{W} > 0$ and $\mathbf{V} > 0$.

3.3.1 Decoupled Inputs Case

The matrices of the decoupled input case are partitioned as follows.

$$
\mathbf{B} = \begin{bmatrix} \mathbf{B}_1 & \mathbf{0} \\ \mathbf{0} & \frac{1}{\varepsilon}\mathbf{B}_4 \end{bmatrix}, \quad
\mathbf{C} = \begin{bmatrix} \mathbf{C}_1 & \mathbf{0} \\ \mathbf{0} & \mathbf{C}_4 \end{bmatrix}, \quad
\mathcal{F} = \begin{bmatrix} \mathcal{F}_1 & \mathbf{0} \\ \mathbf{0} & \frac{1}{\varepsilon}\mathcal{F}_4 \end{bmatrix}
\tag{3.56}
$$

Note the similar structure of matrices $\mathbf{B}$ and $\mathbf{C}$ due to duality.

Substitution of these matrices in the singularly perturbed system (3.55) leads to

$$
\begin{aligned}
\dot{x}_1(t) &= \mathbf{A}_1 x_1(t) + \mathbf{A}_2 x_2(t) + \mathbf{B}_1 u_1(t) + \mathcal{F}_1 w_1(t) \\
\varepsilon \dot{x}_2(t) &= \mathbf{A}_3 x_1(t) + \mathbf{A}_4 x_2(t) + \mathbf{B}_4 u_2(t) + \mathcal{F}_4 w_2(t) \\
y_1(t) &= \mathbf{C}_1 x_1(t) + v_1(t) \\
y_2(t) &= \mathbf{C}_4 x_2(t) + v_2(t)
\end{aligned}
\tag{3.57}
$$

Next, we consider a performance measure given in (3.58).

$$
J = \lim_{t_f \to \infty} \frac{1}{t_f} \mathcal{E} \left\{ \int_0^{t_f} \left[x(t)^T \mathbf{Q} x(t) + u^T(t) \mathbf{R} u(t) \right] dt \right\}
\tag{3.58}
$$

The optimal control $u(t)$ for (3.58) is given as [46]

$$
\begin{bmatrix} u_1(t) \\ u_2(t) \end{bmatrix} = - \begin{bmatrix} \mathbf{F}_1 \hat{x}_1(t) + \mathbf{F}_2 \hat{x}_2(t) \\ \mathbf{F}_3 \hat{x}_1(t) + \mathbf{F}_4 \hat{x}_2(t) \end{bmatrix}
\tag{3.59}
$$

where the regulator gains $\mathbf{F}_i, i = 1, 2, 3, 4$ are given by

$$\mathbf{F}_1 := \mathbf{R_1}^{-1}\mathbf{B}_1^T\mathbf{P}_1$$

$$\mathbf{F}_2 := \varepsilon\mathbf{R_1}^{-1}\mathbf{B}_1^T\mathbf{P}_2$$

$$\mathbf{F}_3 := \mathbf{R_4}^{-1}\mathbf{B}_4^T\mathbf{P}_2^T \tag{3.60}$$

$$\mathbf{F}_4 := \mathbf{R_4}^{-1}\mathbf{B}_4^T\mathbf{P}_3$$

and $\mathbf{P}_i$, $i = 1, 2, 3$ are the solution of the regulator-type CARE. Optimal estimated states $\hat{x}_1$ and $\hat{x}_2$ of this stochastic singularly perturbed system are obtained from the Kalman filter [46]:

$$\dot{\hat{x}}_1(t) = \mathbf{A}_1\hat{x}_1(t) + \mathbf{A}_2\hat{x}_2(t) + \mathbf{B}_1u_1(t) + [\mathbf{K}_1\mathbf{C}_1\tilde{x}_1(t) + \mathbf{K}_2\mathbf{C}_4\tilde{x}_2(t)] \tag{3.61a}$$

$$\varepsilon\dot{\hat{x}}_2(t) = \mathbf{A}_3\hat{x}_1(t) + \mathbf{A}_4\hat{x}_2(t) + \mathbf{B}_4u_2(t) + \varepsilon[\mathbf{K}_3\mathbf{C}_1\tilde{x}_1(t) + \mathbf{K}_4\mathbf{C}_4\tilde{x}_2(t)] \tag{3.61b}$$

where $\tilde{x}_1(t) = x_1(t) - \hat{x}_1(t)$ and $\tilde{x}_2(t) = x_2(t) - \hat{x}_2(t)$ denote the slow and the fast state errors respectively. $\mathbf{K}_i, i = 1, 2, 3, 4$ are the filter's gain matrices given as follows.

$$\mathbf{K}_1 := \boldsymbol{\Sigma}_1\mathbf{C}_1^T\mathbf{V}_1^{-1}$$

$$\mathbf{K}_2 := \boldsymbol{\Sigma}_2\mathbf{C}_4^T\mathbf{V}_4^{-1}$$

$$\mathbf{K}_3 := \varepsilon\boldsymbol{\Sigma}_2^T\mathbf{C}_1^T\mathbf{V}_1^{-1} \tag{3.62}$$

$$\mathbf{K}_4 := \boldsymbol{\Sigma}_3\mathbf{C}_4^T\mathbf{V}_4^{-1}$$

where $\mathbf{K}$ is partitioned as

$$\mathbf{K} = \begin{bmatrix} \mathbf{K}_1 & \mathbf{K}_2 \\ \frac{1}{\varepsilon}\mathbf{K}_3 & \frac{1}{\varepsilon}\mathbf{K}_4 \end{bmatrix}$$

Matrix $\mathbf{V}$ has the same structure as matrix $\mathbf{R}$ and $\boldsymbol{\Sigma}_i, i = 1, 2, 3$ are solutions of the filter-type CAREs

$$\mathbf{A}\boldsymbol{\Sigma} + \mathcal{F}\mathbf{W}\mathcal{F}^T + \boldsymbol{\Sigma}\mathbf{A}^T - \boldsymbol{\Sigma}\mathbf{C}^T\mathbf{V}^{-1}\mathbf{C}\boldsymbol{\Sigma} = 0 \tag{3.63}$$

Due to the nature of the solution, the steady-state error covariance matrix $\boldsymbol{\Sigma}$ is partitioned as in (3.64).

$$\boldsymbol{\Sigma} = \begin{bmatrix} \boldsymbol{\Sigma}_1 & \boldsymbol{\Sigma}_2 \\ \boldsymbol{\Sigma}_2^T & \frac{1}{\varepsilon}\boldsymbol{\Sigma}_3 \end{bmatrix} \tag{3.64}$$

Substituting the inputs from (3.59) into the Kalman filters (3.61) we obtain

$$\dot{\hat{x}}_1(t) = (\mathbf{A}_1 - \mathbf{B}_1\mathbf{F}_1)\hat{x}_1(t) + (\mathbf{A}_2 - \mathbf{B}_1\mathbf{F}_2)\hat{x}_2(t) + \mathbf{K}_1\bar{\nu}_1(t) + \mathbf{K}_2\bar{\nu}_2(t) \quad (3.65a)$$

$$\varepsilon\dot{\hat{x}}_2(t) = (\mathbf{A}_3 - \mathbf{B}_4\mathbf{F}_3)\hat{x}_1(t) + (\mathbf{A}_4 - \mathbf{B}_4\mathbf{F}_4)\hat{x}_2(t) + \mathbf{K}_3\bar{\nu}_1(t) + \mathbf{K}_4\bar{\nu}_2(t) \quad (3.65b)$$

where $\bar{\nu}_1(t) = \mathbf{C}_1\tilde{x}_1(t)$ and $\bar{\nu}_2(t) = \mathbf{C}_4\tilde{x}_2(t)$ are the innovation processes driving (3.65a) and (3.65b) respectively. The filtering structure in (3.65) contains both slow and fast dynamics and as it will be evident later when the complete solution of the LQG is considered, it is necessary to decouple the filter into slow and fast subsystems. To decouple the filter's dynamics, the invariant transformation in (2.7) is used to obtain exactly slow and fast subsystems.

After the decoupling, the filter in new coordinates becomes

$$\dot{\hat{\xi}}(t) = [(\mathbf{A}_1 - \mathbf{B}_1\mathbf{F}_1) - (\mathbf{A}_2 - \mathbf{B}_1\mathbf{F}_2)\mathbf{L}]\hat{\xi}(t) + (\mathbf{K}_1 - \varepsilon\mathbf{MLK}_1 - \varepsilon\mathbf{MK}_3)\nu_1(t) \quad (3.66a)$$
$$+ (\mathbf{K}_2 - \varepsilon\mathbf{MLK}_2 - \varepsilon\mathbf{MK}_4)\nu_2(t)$$

$$\varepsilon\dot{\hat{\eta}}(t) = [(\mathbf{A}_4 - \mathbf{B}_4\mathbf{F}_4) + \varepsilon\mathbf{L}(\mathbf{A}_2 - \mathbf{B}_1\mathbf{F}_2)]\hat{\eta}(t) + (\mathbf{K}_3 + \varepsilon\mathbf{LK}_1)\nu_1(t) \quad (3.66b)$$
$$+ (\mathbf{K}_4 + \varepsilon\mathbf{LK}_2)\nu_2(t)$$

The innovation processes after the transformation become

$$\nu_1(t) = y_1(t) - \mathbf{C}_1\hat{\xi}(t) - \varepsilon\mathbf{C}_1\mathbf{M}\hat{\eta}(t)$$
$$\nu_2(t) = y_2(t) + \mathbf{C}_4\mathbf{L}\hat{\xi}(t) - (\mathbf{C}_4 - \varepsilon\mathbf{C}_4\mathbf{LM})\hat{\eta}(t)$$
$$(3.67)$$

and the optimal control in new coordinates is now given by

$$u_1(t) = -(\mathbf{F}_1 - \mathbf{F}_2\mathbf{L})\hat{\xi}(t) - [\mathbf{F}_2 + \varepsilon(\mathbf{F}_1 - \mathbf{F}_2\mathbf{L})\mathbf{M}]\hat{\eta}(t) \quad (3.68a)$$

$$u_2(t) = -(\mathbf{F}_3 - \mathbf{F}_4\mathbf{L})\hat{\xi}(t) - [\mathbf{F}_4 + \varepsilon(\mathbf{F}_3 - \mathbf{F}_4\mathbf{L})\mathbf{M}]\hat{\eta}(t) \quad (3.68b)$$

Matrices $\mathbf{M}$ and $\mathbf{L}$ needed to obtain the solution of the decoupled filter (3.66) are evaluated by solving a weakly non-linear and a linear equation

$$(\mathbf{A}_4 - \mathbf{B}_4\mathbf{F}_4)\mathbf{L} - (\mathbf{A}_3 - \mathbf{B}_4\mathbf{F}_3) - \varepsilon\mathbf{L}[(\mathbf{A}_1 - \mathbf{B}_1\mathbf{F}_1) - (\mathbf{A}_2 - \mathbf{B}_1\mathbf{F}_2)\mathbf{L}] = \mathbf{0} \quad (3.69a)$$

$$\mathbf{M}(\mathbf{A}_4 - \mathbf{B}_4\mathbf{F}_4) - (\mathbf{A}_2 - \mathbf{B}_1\mathbf{F}_2) - \varepsilon[(\mathbf{A}_1 - \mathbf{B}_1\mathbf{F}_1) - (\mathbf{A}_2 - \mathbf{B}_1\mathbf{F}_2)\mathbf{L}]\mathbf{M} \quad (3.69b)$$
$$+ \varepsilon\mathbf{ML}(\mathbf{A}_2 - \mathbf{B}_1\mathbf{F}_2) = \mathbf{0}$$

An iterative separation technique to solve for $\mathbf{M}$ and $\mathbf{L}$ follows. The technique developed in [106] is used to obtain both $\mathbf{L}$ and $\mathbf{M}$.

$$\mathbf{L}^{(i+1)} = (\mathbf{A}_4 - \mathbf{B}_4\mathbf{F}_4^{(N)})^{-1}(\mathbf{A}_3 - \mathbf{B}_4\mathbf{F}_3^{(N)}) + \varepsilon(\mathbf{A}_4 - \mathbf{B}_4\mathbf{F}_4^{(N)})^{-1}\mathbf{L}^{(i)}[(\mathbf{A}_1 - \mathbf{B}_1\mathbf{F}_1^{(N)})$$
$$- (\mathbf{A}_2 - \mathbf{B}_1\mathbf{F}_2^{(N)})\mathbf{L}^{(i)}] \qquad (3.70a)$$

$$\mathbf{M}^{(i+1)} = \varepsilon\{[(\mathbf{A}_1 - \mathbf{B}_1\mathbf{F}_1^{(N)}) - (\mathbf{A}_2 - \mathbf{B}_1\mathbf{F}_2^{(N)})\mathbf{L}^{(N)}]\mathbf{M}_s^{(i)} - \mathbf{M}^{(i)}\mathbf{L}^{(N)}(\mathbf{A}_2 - \mathbf{B}_1\mathbf{F}_2^{(N)})\}$$
$$\times (\mathbf{A}_4 - \mathbf{B}_4\mathbf{F}_4^{(N)})^{-1} + (\mathbf{A}_2 - \mathbf{B}_1\mathbf{F}_2^{(N)})(\mathbf{A}_4 - \mathbf{B}_4\mathbf{F}_4^{(N)})^{-1}$$

$$(3.70b)$$

for $i = 1, 2, \ldots, N$. $\mathbf{F}_1^{(N)}$, $\mathbf{F}_2^{(N)}$, $\mathbf{F}_3^{(N)}$, $\mathbf{F}_4^{(N)}$ are determined by substituting the last iteration of the corresponding partition of (3.36) in (3.60). Likewise, $\mathbf{L}^{(N)}$ is the value of the last iteration of (3.70a). The initial conditions of the algorithm are

$$\mathbf{L}^{(0)} = (\mathbf{A}_4 - \mathbf{B}_4\mathbf{F}_4^{(0)})^{-1}(\mathbf{A}_3 - \mathbf{B}_4\mathbf{F}_3^{(0)})$$
$$\mathbf{M}^{(0)} = (\mathbf{A}_2 - \mathbf{B}_1\mathbf{F}_2^{(0)})(\mathbf{A}_4 - \mathbf{B}_4\mathbf{F}_4^{(0)})^{-1}$$

Theorem 3.2 Under the conditions of Theorem 3.1, (3.70a) and (3.70b) converge to the exact solution $\mathbf{L}$ and $\mathbf{M}$ with convergence rate $\mathcal{O}(\varepsilon)$

$$\|\mathbf{L} - \mathbf{L}^{(i)}\| = \mathcal{O}(\varepsilon^i), \; i = 1, 2, \cdots, n$$
$$\|\mathbf{M} - \mathbf{M}^{(i)}\| = \mathcal{O}(\varepsilon^i), \; i = 1, 2, \cdots, n$$

Proof We prove this theorem by following similar steps as the proof for Theorem 3.1. We initially form the difference of the first iteration with the zero-order approximation (initial conditions) for both $\mathbf{L}$ and $\mathbf{M}$. We can see by observing (3.70) and the initial conditions that the resulting difference is $\mathcal{O}(\varepsilon)$ in both cases i.e.

$$\|\mathbf{L}^{(1)} - \mathbf{L}^{(0)}\| = \mathcal{O}(\varepsilon)$$
$$\|\mathbf{M}^{(1)} - \mathbf{M}^{(0)}\| = \mathcal{O}(\varepsilon)$$

Continuing in this fashion for other iterations, we conclude that after each iteration the accuracy improves by $\mathcal{O}(\varepsilon)$. For ε sufficiently small, both $\mathbf{L}$ and $\mathbf{M}$ converge in just a few iterations. $\square$

At this point we observe that for a complete solution of the LQG problem, both recursive solutions of the regulator and filter-type CAREs are needed. We already

obtained the solutions of the regulator-type CARE in the previous section. Here, we give a detailed solution of the filter-type CARE only for the first case. The steps to obtain the solution for the other two cases are very similar. Likewise, solution can be obtained by making use of the duality of the regulator and filter.

After all the matrices have been substituted in (3.63) we obtain

$$\mathbf{A}_1\boldsymbol{\Sigma}_1 + \mathbf{A}_2\boldsymbol{\Sigma}_2^T + \boldsymbol{\Sigma}_1\mathbf{A}_1^T + \boldsymbol{\Sigma}_2\mathbf{A}_2^T + \mathcal{F}_1\mathbf{W}_1\mathcal{F}_1^T - \boldsymbol{\Sigma}_1\mathcal{S}_1\boldsymbol{\Sigma}_1 - \boldsymbol{\Sigma}_2\mathcal{S}_4\boldsymbol{\Sigma}_2^T \;=\; \mathbf{0} \qquad (3.71a)$$

$$\varepsilon\mathbf{A}_1\boldsymbol{\Sigma}_2 + \mathbf{A}_2\boldsymbol{\Sigma}_3 + \boldsymbol{\Sigma}_1\mathbf{A}_3^T + \boldsymbol{\Sigma}_2\mathbf{A}_4^T + -\varepsilon\boldsymbol{\Sigma}_1\mathcal{S}_1\boldsymbol{\Sigma}_2 - \boldsymbol{\Sigma}_2\mathcal{S}_4\boldsymbol{\Sigma}_3 \;=\; \mathbf{0} \qquad (3.71b)$$

$$\varepsilon\mathbf{A}_3\boldsymbol{\Sigma}_2 + \mathbf{A}_4\boldsymbol{\Sigma}_3 + \varepsilon\boldsymbol{\Sigma}_2^T\mathbf{A}_3^T + \boldsymbol{\Sigma}_3\mathbf{A}_4^T + \mathcal{F}_4\mathbf{W}_4\mathcal{F}_4^T - \varepsilon^2\boldsymbol{\Sigma}_2^T\mathcal{S}_1\boldsymbol{\Sigma}_2 \qquad (3.71c)$$

$$- \;\boldsymbol{\Sigma}_3\mathcal{S}_4\boldsymbol{\Sigma}_3 \;=\; \mathbf{0}$$

where $\mathcal{S}_1 = \mathbf{C}_1^T\mathbf{V}_1^{-1}\mathbf{C}_1$ and $\mathcal{S}_4 = \mathbf{C}_4^T\mathbf{V}_4^{-1}\mathbf{C}_4$. The zero-order approximation of (3.71) becomes

$$\mathbf{A}_1\boldsymbol{\Sigma}_1^{(0)} + \mathbf{A}_2\boldsymbol{\Sigma}_2^{(0)T} + \boldsymbol{\Sigma}_1^{(0)}\mathbf{A}_1^T + \boldsymbol{\Sigma}_2^{(0)}\mathbf{A}_2^T + \mathcal{F}_1\mathbf{W}_1\mathcal{F}_1^T - \boldsymbol{\Sigma}_1^{(0)}\mathcal{S}_1\boldsymbol{\Sigma}_1^{(0)} \qquad (3.72a)$$

$$- \;\boldsymbol{\Sigma}_2^{(0)}\mathcal{S}_4\boldsymbol{\Sigma}_2^{(0)T} \;=\; \mathbf{0}$$

$$\mathbf{A}_2\boldsymbol{\Sigma}_3^{(0)} + \boldsymbol{\Sigma}_1^{(0)}\mathbf{A}_3^T + \boldsymbol{\Sigma}_2^{(0)}\mathbf{A}_4^T - \boldsymbol{\Sigma}_2^{(0)}\mathcal{S}_4\boldsymbol{\Sigma}_3^{(0)} \;=\; \mathbf{0} \qquad (3.72b)$$

$$\mathbf{A}_4\boldsymbol{\Sigma}_3^{(0)} + \boldsymbol{\Sigma}_3^{(0)}\mathbf{A}_4^T + \mathcal{F}_4\mathbf{W}_1\mathcal{F}_4^T - \boldsymbol{\Sigma}_3^{(0)}\mathcal{S}_4\boldsymbol{\Sigma}_3^{(0)} \;=\; \mathbf{0} \qquad (3.72c)$$

The zero-order equations (3.72) can be further simplified by initially obtaining the solution of Lyapunov equation (3.72c). The latter leads to the solution of (3.72b). Substituting $\boldsymbol{\Sigma}_2^{(0)}$ in (3.72a) we obtain a CARE whose solution is $\boldsymbol{\Sigma}_1^{(0)}$. The equations for $\boldsymbol{\Sigma}_1^{(0)}$, $\boldsymbol{\Sigma}_2^{(0)}$, and $\boldsymbol{\Sigma}_3^{(0)}$ are as follows.

$$\mathcal{D}_2\boldsymbol{\Sigma}_1^{(0)} + \boldsymbol{\Sigma}_1^{(0)}\mathcal{D}_2^T - \boldsymbol{\Sigma}_1^{(0)}\mathcal{D}_3\boldsymbol{\Sigma}_1^{(0)} + \mathcal{Q}_1 = \mathbf{0} \qquad (3.73a)$$

$$\boldsymbol{\Sigma}_2^{(0)} = -\mathbf{A}_2\boldsymbol{\Sigma}_3^{(0)}\mathcal{D}_1^{-T} - \boldsymbol{\Sigma}_1^{(0)}\mathbf{A}_3^T\mathcal{D}_1^{-T} \qquad (3.73b)$$

$$\mathbf{A}_4\boldsymbol{\Sigma}_3^{(0)} + \boldsymbol{\Sigma}_3^{(0)}\mathbf{A}_4^T + \mathcal{F}_4\mathbf{W}_4\mathcal{F}_4^T - \boldsymbol{\Sigma}_3^{(0)}\mathcal{S}_4\boldsymbol{\Sigma}_3^{(0)} \;=\; \mathbf{0} \qquad (3.73c)$$

where

$$\mathcal{D}_1 = \mathbf{A}_4 - \Sigma_3^{(0)}\mathcal{S}_4$$

$$\mathcal{D}_2 = \mathbf{A}_1 - \mathbf{A}_2\mathcal{D}_1^{-1}\mathbf{A}_3 - \mathbf{A}_2\mathbf{\Sigma_3}^{(0)}\mathcal{D}_1^{-T}\mathcal{S}_4\mathcal{D}_1^{-1}\mathbf{A}_3$$

$$\mathcal{D}_3 = \mathcal{S}_1 + \mathbf{A}_3^T\mathcal{D}_1^{-T}\mathcal{S}_4\mathcal{D}_1^{-1}\mathbf{A}_3$$

$$\mathcal{Q}_1 = \mathcal{F}_1\mathbf{W}_1\mathcal{F}_1^T - \mathbf{A}_2\mathcal{D}_1^{-1}\mathbf{\Sigma}_3^{(0)}\mathbf{A}_2^T - \mathbf{A}_2\mathbf{\Sigma}_3^{(0)}\mathcal{D}_1^{-T}\mathbf{A}_2^T - \mathbf{A}_2\mathbf{\Sigma_3}^{(0)}\mathcal{D}_1^{-T}\mathcal{S}_4\mathcal{D}_1^{-1}\mathbf{\Sigma}_3\mathbf{A}_2^T$$

To be able to solve (3.73a), we need the following assumption [46].

Assumption 3.2 The triple $(\mathcal{D}_2, \mathbf{C}_1^T, \mathrm{Chol}\{\mathcal{Q}_1\})$ is stabilizable-detectable respectively.

Equations (3.73) show that a reduced-order CARE of order n and a Lyapunov equation of order m are used to obtain an approximate solution $\mathbf{\Sigma} = \mathbf{\Sigma}^{(0)} + \mathcal{O}(\varepsilon)$ of what used to be the CARE of order $n + m$. This is an advantage since the original full-order filter-type CARE can be numerically ill-conditioned due to the presence of $\frac{1}{\varepsilon}$ element in matrix $\mathbf{A}$.

As in the regulator-type case discussed earlier, equations (3.73) are just an $\mathcal{O}(\varepsilon)$ approximation of the actual CARE solution. Namely, we have the following.

$$\mathbf{\Sigma} = \mathbf{\Sigma}^{(0)} + \mathcal{O}(\varepsilon) = \begin{bmatrix} \mathbf{\Sigma}_1^{(0)} & \mathbf{\Sigma}_2^{(0)} \\ \mathbf{\Sigma}_2^{(0)T} & \frac{1}{\varepsilon}\mathbf{\Sigma}_3^{(0)} \end{bmatrix} + \mathcal{O}(\varepsilon) \tag{3.74}$$

To improve the approximation, we start by defining an error matrix $\mathbf{E}s$.

$$\mathbf{E}s = \begin{bmatrix} \mathbf{E}s_1 & \mathbf{E}s_2 \\ \mathbf{E}s_2^T & \mathbf{E}s_3 \end{bmatrix} \tag{3.75}$$

The actual CARE solution can now be written in terms of the error defined in (3.75).

$$\mathbf{\Sigma}_i = \mathbf{\Sigma}_i^{(0)} + \varepsilon\mathbf{E}s_i, \quad i = 1, 2, 3 \tag{3.76}$$

To obtain the error equations, corresponding (3.76) are substituted in (3.71). Then,

(3.72) is subtracted from the result.

$$\mathcal{D}_4 \mathbf{E} s_1 + \mathbf{E} s_1 \mathcal{D}_4^T + \mathbf{A}_2 \mathbf{E} s_2^T + \mathbf{E} s_2 \mathbf{A}_2^T - \varepsilon(\mathbf{E} s_1 \mathcal{S}_1 \mathbf{E} s_1 + \mathbf{E} s_2 \mathcal{S}_4 \mathbf{E} s_2^T) \tag{3.77a}$$
$$- \mathbf{\Sigma}_2^{(0)} \mathcal{S}_4 \mathbf{E} s_2^T - \mathbf{E} s_2 \mathcal{S}_4 \mathbf{\Sigma}_2^{(0)T} = \mathbf{0}$$

$$\mathbf{A}_1 \mathbf{\Sigma}_2^{(0)} + \varepsilon \mathbf{A}_1 \mathbf{E} s_2 + \mathbf{A}_2 \mathbf{E} s_3 + \mathbf{E} s_1 \mathbf{A}_3^T + \mathbf{E} s_2 \mathbf{A}_4^T - \mathbf{\Sigma}_1^{(0)} \mathcal{S}_1 \mathbf{\Sigma}_2^{(0)} - \mathbf{\Sigma}_2^{(0)} \mathcal{S}_4 \mathbf{E} s_3 \tag{3.77b}$$
$$- \mathbf{E} s_2 \mathcal{S}_4 \mathbf{\Sigma}_3^{(0)} = \varepsilon \mathcal{H}_1$$

$$\mathcal{D}_1 \mathbf{E} s_3 + \mathbf{E} s_3 \mathcal{D}_1^T + \mathbf{A}_3 \mathbf{\Sigma}_2^{(0)} + \varepsilon \mathbf{A}_3 \mathbf{E} s_2 + \mathbf{\Sigma}_2^{(0)T} \mathbf{A}_3^T + \varepsilon \mathbf{E} s_2^T \mathbf{A}_3^T = \varepsilon \mathcal{H}_2 \tag{3.77c}$$

where

$$\mathcal{D}_4 = \mathbf{A}_1 - \mathbf{\Sigma}_1 \mathcal{S}_1$$

$$\mathcal{H}_1 = \mathbf{\Sigma}_1^{(0)} \mathcal{S}_1 \mathbf{E} s_2 + \mathbf{E} s_1 \mathcal{S}_1 \mathbf{\Sigma}_2^{(0)} + \varepsilon \mathbf{E} s_1 \mathcal{S}_1 \mathbf{E} s_2 + \mathbf{E} s_2 \mathcal{S}_4 \mathbf{E} s_3 \tag{3.78}$$

$$\mathcal{H}_2 = \mathbf{\Sigma}_2^{(0)T} \mathcal{S}_1 \mathbf{\Sigma}_2^{(0)} + \varepsilon \mathbf{\Sigma}_2^{(0)T} \mathcal{S}_1 \mathbf{E} s_2^{(0)} + \varepsilon \mathbf{E} s_2^T \mathcal{S}_1 \mathbf{\Sigma}_2^{(0)} + \varepsilon^2 \mathbf{E} s_2^T \mathcal{S}_1 \mathbf{E} s_2 + \mathbf{E} s_3 \mathcal{S}_4 \mathbf{E} s_3$$

Cross-coupling terms and all the non-linear terms are multiplied by ε in (3.77) hinting that a reduced-order fixed-point algorithm can be used to obtain the solution. The initial conditions namely $\mathbf{E} s_1^{(0)}$, $\mathbf{E} s_2^{(0)}$, $\mathbf{E} s_3^{(0)}$ are obtained by solving (3.77) after setting $\varepsilon = 0$. Initially (3.77c) is solved as a Lyapunov equation to obtain $\mathbf{E} s_3^{(0)}$. Then, $\mathbf{E} s_1^{(0)}$ is obtained from (3.77a) after the expression for $\mathbf{E} s_2^{(0)}$ is substituted from (3.77b). Lastly, (3.77b) is solved algebraically to get $\mathbf{E} s_2^{(0)}$. The proposed recursive algorithm to obtain the error is as follows.

$$\mathcal{D}_5 \mathbf{E}_1^{(i+1)} + \mathbf{E}_1^{(i+1)} \mathcal{D}_5^T + \mathcal{D}_6 = \varepsilon \mathcal{H}_3 \tag{3.79a}$$

$$\mathbf{E} s_2^{(i+1)} \mathcal{D}_1^T + \mathbf{A}_1 \mathbf{\Sigma}_2^{(0)} + \varepsilon \mathbf{A}_1 \mathbf{E} s_2^{(i)} + \mathbf{A}_2 \mathbf{E} s_3^{(i+1)} + \mathbf{E} s_1^{(i)} \mathbf{A}_3^T - \mathbf{\Sigma}_1^{(0)} \mathcal{S}_1 \mathbf{\Sigma}_2^{(0)} \tag{3.79b}$$
$$- \mathbf{\Sigma}_2^{(0)} \mathcal{S}_4 \mathbf{E} s_3^{(i+1)} = \varepsilon \mathcal{H}_1^{(i,i+1)}$$

$$\mathcal{D}_1 \mathbf{E} s_3^{(i+1)} + \mathbf{E} s_3^{(i+1)} \mathcal{D}_1^T + \mathbf{A}_3 \mathbf{\Sigma}_2^{(0)} + \varepsilon \mathbf{A}_3 \mathbf{E} s_2 + \mathbf{\Sigma}_2^{(0)T} \mathbf{A}_3^T + \varepsilon \mathbf{E} s_2^T \mathbf{A}_3^T = \varepsilon \mathcal{H}_2^{(i)} \tag{3.79c}$$

where

$$\mathcal{D}_5 = \mathbf{A}_1 - \mathbf{A}_2 \mathcal{D}_1^{-1} \mathbf{A}_3 - \mathbf{\Sigma}_1^{(0)} \mathcal{S}_1 + \mathbf{\Sigma}_2^{(0)} \mathcal{S}_4 \mathcal{D}_1^{-1} \mathbf{A}_3$$

$$\mathcal{D}_6 = \mathbf{A}_2 \mathcal{D}_1^{-1} \Gamma + \Gamma \mathcal{D}_1^{-T} \mathbf{A}_2^T - \mathbf{\Sigma}_2^{(0)} \mathcal{S}_4 \mathcal{D}_1^{-1} \Gamma^T - \Gamma \mathcal{D}_1^{-T} \mathcal{S}_4 \mathbf{\Sigma}_2^{(0)T}$$

$$\mathcal{H}_3 = \mathbf{E} s_1^{(i)} \mathcal{S}_4 \mathbf{E} s_1^{(i)} + \mathbf{\Sigma}_2^{(0)} \mathcal{S}_4 \mathcal{D}_1^{-1} \Gamma^T + \mathbf{\Sigma}_2^{(0)} \mathcal{S}_4 \mathcal{D}_1^{-1} \Pi^T + \Pi \mathcal{D}_1^{-T} \mathcal{S}_4 \mathbf{\Sigma}_2^{(0)T} \tag{3.80}$$
$$+ \mathbf{E} s_2^{(i)} \mathcal{S}_4 \mathbf{E} s_2^{(i)T} - \mathbf{A}_2 \mathcal{D}_1^{-1} \Pi^T - \Pi \mathcal{D}_1^{-T} \mathbf{A}_2^T$$

Γ and Π are respectively defined as $\Gamma = \boldsymbol{\Sigma}_1^{(0)} \mathcal{S}_1 \boldsymbol{\Sigma}_2^{(0)} + \boldsymbol{\Sigma}_2^{(0)} \mathcal{S}_4 \mathbf{E}s_3^{(i+1)} - \mathbf{A}_1 \Sigma_2^{(0)} - \mathbf{A}_2 \mathbf{E}s_3^{(i+1)}$
and $\Pi = \boldsymbol{\Sigma}_1^{(0)} \mathcal{S}_1 \mathbf{E}s_2^{(i)} + \mathbf{E}s_1^{(i)} \mathcal{S}_1 \boldsymbol{\Sigma}_2^{(0)} + \varepsilon \mathbf{E}s_1^{(i)} \mathcal{S}_1 \mathbf{E}s_2^{(i)} + \mathbf{E}s_2^{(i)} \mathcal{S}_4 \mathbf{E}s_3^{(i+1)}$. Matrices $\boldsymbol{\Sigma}_j^{(i)} = \boldsymbol{\Sigma}_j^{(0)} + \varepsilon \mathbf{E}s_j^{(i)}, j = 1, 2, 3$ and matrices $\mathcal{H}_k$, $k = 1, 2, 3$, Γ, and Π are updated accordingly in each iteration.

The solution follows similar steps as for the regulator-type CARE. Namely, (3.79c) is solved, then (3.79a) after $\mathbf{E}s_2^{(i)}$ is substituted, and lastly the solution of (3.79b) is obtained. The steps of the solution are presented in Algorithm 2.

Algorithm 2 Evaluate $\mathbf{E}s^{(i)}$

1: **procedure** SOLVE RECURSIVE EQUATIONS
2:     **while** solution of $\mathbf{E}s^{(i)}$ converges **do**
3:         solve Lyapunov (3.79c) to obtain $\mathbf{E}s_3^{(i)}$
4:         $\boldsymbol{\Sigma}_3^{(i)} \leftarrow \boldsymbol{\Sigma}_3^{(0)} + \varepsilon \mathbf{E}s_3^{(i)}$
5:         solve Lyapunov (3.79a) to obtain $\mathbf{E}s_1^{(i)}$
6:         $\boldsymbol{\Sigma}_1^{(i)} \leftarrow \boldsymbol{\Sigma}_1^{(0)} + \varepsilon \mathbf{E}s_1^{(i)}$
7:         solve (3.79b) algebraically to obtain $\mathbf{E}s_2^{(i)}$
8:         $\boldsymbol{\Sigma}_2^{(i)} \leftarrow \boldsymbol{\Sigma}_2^{(0)} + \varepsilon \mathbf{E}s_2^{(i)}$

The following theorem summarizes the rate of convergence of the error.

Theorem 3.3 Under Assumption 2.1, (3.79) converges to the exact solution of the error with convergence rate $\mathcal{O}(\varepsilon)$.

$$\|\mathbf{E}s_j - \mathbf{E}s_j^{(i)}\| = \mathcal{O}(\varepsilon^i), \; i = 1, 2, 3, \cdots; \; j = 1, 2, 3 \tag{3.81}$$

Proof. The proof is similar to that of Theorem 3.2. The existence of a bounded solution of $\mathbf{E}s_1$, $\mathbf{E}s_2$, and $\mathbf{E}s_3$ is guaranteed if the corresponding Jacobian of the error equations is non-singular. Due to the duality between the regulator and filter-type CARE, we are guaranteed non-singularity since it was proved before that the Jacobian for the regulator-type CARE is non-singular. Next, to find the rate of convergence, the difference of the proposed algorithm for $i = 0$ and the error equations is obtained. For the third equation this becomes.

$$(\mathbf{E}s_3 - \mathbf{E}s_3^{(1)})\mathcal{D}_1 + \mathcal{D}_1^T(\mathbf{E}s_3 - \mathbf{E}s_3^{(1)}) = \varepsilon \mathcal{F}(\mathbf{E}s_2, \mathbf{E}s_3, \varepsilon) \tag{3.82}$$

Similarly, this can be shown for the other equations. Repeating this procedure leads to

$$\|\mathbf{E}s - \mathbf{E}s^{(i)}\| = \mathcal{O}(\varepsilon^i), \; i = 1, 2, 3, \cdots \tag{3.83}$$

The proof is complete. $\square$

Next, we consider the complete solution of the LQG. It is well-known that the solution of the LQG is divided into two parts collectively known as the *separation theorem* [107]. First, the optimal control law $u(t) = -\mathbf{G}\hat{x}(t)$ is obtained by solving the LQ problem (i.e. solving the regulator-type CARE to evaluate $\mathbf{G}$) and then, the Kalman filter is used to obtain the optimal estimated states. The Kalman filter gain is evaluated by utilizing the solution of the filter-type CARE. The iterative solution of the regulator and filter-type CARE were discussed earlier therefore we now focus on the complete solution of the LQG.

To do so, we rewrite the cost functional in terms of the trace and make use of the co-variance matrices of both, the original states and the estimated states after decoupling. An augmented system is then formed to obtain the numerical values of the variances of the original and optimal estimated decoupled states which are then used to calculate the cost functional. Details on how the solution is achieved iteratively follow.

For notational convenience and to simplify the algebra, we rewrite the inputs, filter equations, and innovation processes. Starting with the approximate inputs, we have

$$u^{(i)}(t) = -\phi_1^{(i)}\hat{\xi}^{(i)}(t) - \phi_2^{(i)}\hat{\eta}^{(i)}(t) \tag{3.84a}$$

$$u^{(i)}(t) = -\phi_3^{(i)}\hat{\xi}^{(i)}(t) - \phi_4^{(i)}\hat{\eta}^{(i)}(t) \tag{3.84b}$$

Likewise, the approximate filter equations can be simplified as

$$\dot{\hat{\xi}}^{(i)}(t) = \alpha_1^{(i)}\hat{\xi}^{(i)}(t) + \gamma_1^{(i)}\nu_1^{(i)}(t) + \gamma_2^{(i)}\nu_2^{(i)}(t) \tag{3.85a}$$

$$\varepsilon\dot{\hat{\eta}}^{(i)}(t) = \alpha_2^{(i)}\hat{\eta}^{(i)}(t) + \gamma_3^{(i)}\nu_1^{(i)}(t) + \gamma_4^{(i)}\nu_2^{(i)}(t) \tag{3.85b}$$

where the approximate innovation processes are given by

$$\nu_1^{(i)}(t) = y_1(t) - \rho_1^{(i)}\hat{\xi}^{(i)}(t) - \rho_2^{(i)}\hat{\eta}^{(i)}(t)$$

$$\nu_2^{(i)}(t) = y_2(t) - \rho_3^{(i)}\hat{\xi}^{(i)}(t) - \rho_4^{(i)}\hat{\eta}^{(i)}(t)$$

Quantities $\alpha_j, j = 1, 2$, $\gamma_j, j = 1, 2, 3, 4$, $\rho_j, j = 1, 2, 3, 4$, and $\phi_j, j = 1, 2, 3, 4$ are equivalent to corresponding approximate expressions in (3.66), (3.67), and (3.68).

The solution of the suboptimal criterion

$$J^{(i)} = \lim_{t_f \to \infty} \frac{1}{t_f} E \left\{ \int_0^{t_f} \left[x^{(i)T}(t) \mathbf{Q} x^{(i)}(t) + u^{(i)T}(t) \mathbf{R} u^{(i)}(t) \right] dt \right\} \qquad (3.86)$$

is given in terms of the trace as [108]

$$J^{(i)} = \mathrm{tr}\{ \mathbf{Q} q_{11}^{(i)} + \phi^{(i)T} \mathbf{R} \phi^{(i)} q_{22}^{(i)} \} \qquad (3.87)$$

where

$$\phi^{(i)} = \begin{bmatrix} \phi_1^{(i)} & \phi_2^{(i)} \\ \phi_3^{(i)} & \phi_4^{(i)} \end{bmatrix}$$

and matrix $q^{(i)}$ is evaluated from the covariance matrix of the original and estimated states. Namely,

$$Cov(x_1(t), x_2(t)) = \begin{bmatrix} \mathrm{Cov}(x_1^T(t)x_1(t)) & \mathrm{Cov}(x_1^T(t)x_2(t)) \\ \mathrm{Cov}(x_2^T(t)x_1(t)) & \mathrm{Cov}(x_2^T(t)x_2(t)) \end{bmatrix} \qquad (3.88a)$$

$$Cov(\hat{\xi}(t), \hat{\eta}(t)) = \begin{bmatrix} \mathrm{Cov}(\hat{\xi}^T(t)\hat{\xi}(t)) & \mathrm{Cov}(\hat{\xi}^T(t)\hat{\eta}(t)) \\ \mathrm{Cov}(\hat{\eta}^T(t)\hat{\xi}(t)) & \mathrm{Cov}(\hat{\eta}^T(t)\hat{\eta}(t)) \end{bmatrix} \qquad (3.88b)$$

The unknown quantities are then given as follows.

$$q_{11}^{(i)} = \mathrm{Var} \begin{bmatrix} x_1^{(i)}(t) \\ x_2^{(i)}(t) \end{bmatrix}, \quad q_{22}^{(i)} = \mathrm{Var} \begin{bmatrix} \hat{\xi}^{(i)}(t) \\ \hat{\eta}^{(i)}(t) \end{bmatrix}$$

The numerical values of q_{11} and q_{22} are obtained by using the augmented system in (3.89) which is driven by white noise.

$$\begin{bmatrix} \dot{x}_1^{(i)}(t) \\ \varepsilon \dot{x}_2^{(i)}(t) \\ \dot{\hat{\xi}}^{(i)}(t) \\ \varepsilon \dot{\hat{\eta}}^{(i)}(t) \end{bmatrix} = \begin{bmatrix} \mathbf{A}_1 & \mathbf{A}_2 & -\mathbf{B}_1 \phi_1^{(i)} & -\mathbf{B}_1 \phi_2^{(i)} \\ \mathbf{A}_3 & \mathbf{A}_4 & -\mathbf{B}_4 \phi_3^{(i)} & -\mathbf{B}_4 \phi_4^{(i)} \\ \gamma_1^{(i)} \mathbf{C}_1 & \gamma_2^{(i)} \mathbf{C}_4 & \alpha_1^{(i)} - \gamma_1^{(i)} \rho_1^{(i)} - \gamma_2^{(i)} \rho_3^{(i)} & -\gamma_1^{(i)} \rho_2^{(i)} - \gamma_2^{(i)} \rho_4^{(i)} \\ \gamma_3^{(i)} \mathbf{C}_1 & \gamma_4^{(i)} \mathbf{C}_4 & -\gamma_3^{(i)} \rho_1^{(i)} - \gamma_4^{(i)} \rho_3^{(i)} & \alpha_2^{(i)} - \gamma_3^{(i)} \rho_2^{(i)} - \gamma_4^{(i)} \rho_4^{(i)} \end{bmatrix} \begin{bmatrix} x_1^{(i)}(t) \\ x_2^{(i)}(t) \\ \hat{\xi}^{(i)}(t) \\ \hat{\eta}^{(i)}(t) \end{bmatrix}$$

$$+ \begin{bmatrix} \mathcal{F}_1 & \mathbf{0} & \mathbf{0} & \mathbf{0} \\ \mathbf{0} & \mathcal{F}_4 & \mathbf{0} & \mathbf{0} \\ \mathbf{0} & \mathbf{0} & \gamma_1^{(i)} & \gamma_2^{(i)} \\ \mathbf{0} & \mathbf{0} & \gamma_3^{(i)} & \gamma_4^{(i)} \end{bmatrix} \begin{bmatrix} w_1(t) \\ w_2(t) \\ v_1(t) \\ v_2(t) \end{bmatrix}$$

$$(3.89)$$

We rewrite the overall augmented system as

$$\dot{Z}^{(i)}(t) = \mathcal{A}^{(i)} Z^{(i)}(t) + \mathcal{G}^{(i)} \tilde{w}(t) \tag{3.90}$$

where the matrices and vectors in (3.90) represent quantities of the augmented system. It is well-known that in steady state, the covariance matrix of the augmented state $Z^{(i)}$ is given by the solution of the following Lyapunov equation [108].

$$\mathcal{A}^{(i)} q^{(i)} + q^{(i)} \mathcal{A}^{(i)T} + \mathcal{G}^{(i)} \widetilde{W} \mathcal{G}^{(i)T} = 0 \tag{3.91}$$

where $\widetilde{W} = \text{diag}(\mathbf{W} \quad \mathbf{V})$ and matrix $q^{(i)}$ is partitioned as

$$q^{(i)} = \begin{bmatrix} q_{11}^{(i)} & q_{12}^{(i)} \\ q_{12}^{(i)T} & q_{22}^{(i)} \end{bmatrix}$$

With all the quantities known, the solution of the LQG can be obtained iteratively until the algorithm converges $(i = 0, 1, 2, \cdots)$ i.e.

$$\phi_j^{(i)} \to \phi_j^{actual}; \ j = 1, 2, 3, 4$$

$$\alpha_j^{(i)} \to \alpha_j^{actual}; \ j = 1, 2$$

$$\gamma_j^{(i)} \to \gamma_j^{actual}; \ j = 1, 2, 3, 4$$

$$\rho_j^{(i)} \to \rho_j^{actual}; \ j = 1, 2, 3, 4$$

$$J^{(i)} \to J^{opt}$$

where *actual* quantities denote values when actual solutions of the regulator and filter-type CARE are used to evaluate ϕ_j, α_j, γ_j, and ρ_j.

The optimal performance cost is evaluated as follows [108].

$$\begin{aligned} J^{opt} &= \text{tr}(\mathbf{P}\mathcal{F}\mathbf{W}\mathbf{P}^T + \mathbf{\Sigma}\mathbf{F}^T\mathbf{R}\mathbf{F}) \\ &= \text{tr}(\mathbf{P}\mathbf{K}\mathbf{V}\mathbf{K}^T + \mathbf{\Sigma}\mathbf{Q}) \end{aligned} \tag{3.92}$$

3.3.2 Weakly Coupled Inputs

Due to similarities with the decoupled inputs case, in this section as well as the next, the recursive solution of the filter-type CARE will be skipped. Instead, we assume that the solution of both the regulator and filter-type CAREs are already obtained and focus on the solution of the LQG.

Matrices C and $\mathcal{F}$ have the following structure for this case.

$$\mathbf{C} = \begin{bmatrix} \mathbf{C}_1 & \mathbf{C}_2 \\ \mathbf{C}_3 & \mathbf{C}_4 \end{bmatrix}, \quad \mathcal{F} = \begin{bmatrix} \mathcal{F}_1 & \varepsilon\mathcal{F}_2 \\ \mathcal{F}_3 & \frac{1}{\varepsilon}\mathcal{F}_4 \end{bmatrix} \tag{3.93}$$

After substitutions, the state-space system becomes

$$\begin{aligned}
\dot{x}_1(t) &= \mathbf{A}_1 x_1(t) + \mathbf{A}_2 x_2(t) + \mathbf{B}_1 u_1(t) + \varepsilon\mathbf{B}_2 u_2(t) + \mathcal{F}_1 w_1(t) + \varepsilon\mathcal{F}_2 w_2(t) \\
\varepsilon\dot{x}_2(t) &= \mathbf{A}_3 x_1(t) + \mathbf{A}_4 x_2(t) + \varepsilon\mathbf{B}_3 u_1(t) + \mathbf{B}_4 u_2(t) + \varepsilon\mathcal{F}_3 w_1(t) + \mathcal{F}_4 w_2(t) \\
y_1(t) &= \mathbf{C}_1 x_1(t) + \mathbf{C}_2 x_2(t) + v_1(t) \\
y_2(t) &= \mathbf{C}_3 x_1(t) + \mathbf{C}_4 x_2(t) + v_2(t)
\end{aligned} \tag{3.94}$$

The optimal control in this case is the same as (3.59) but the expressions for the gains differ. The regulator gains are as follows.

$$\begin{aligned}
\mathbf{F}_1 &:= \mathbf{R_1}^{-1}\mathbf{B}_1^T\mathbf{P}_1 + \varepsilon\mathbf{R_1}^{-1}\mathbf{B}_3^T\mathbf{P}_2^T \\
\mathbf{F}_2 &:= \varepsilon\mathbf{R_1}^{-1}\mathbf{B}_1^T\mathbf{P}_2 + \varepsilon\mathbf{R_1}^{-1}\mathbf{B}_3^T\mathbf{P}_3 \\
\mathbf{F}_3 &:= \varepsilon\mathbf{R_4}^{-1}\mathbf{B}_2^T\mathbf{P}_1 + \mathbf{R_4}^{-1}\mathbf{B}_4^T\mathbf{P}_2^T \\
\mathbf{F}_4 &:= \varepsilon^2\mathbf{R_4}^{-1}\mathbf{B}_2^T\mathbf{P}_2 + \mathbf{R_4}^{-1}\mathbf{B}_4^T\mathbf{P}_3
\end{aligned} \tag{3.95}$$

As before, the optimal state is estimated via the Kalman filter and its structure is given in (3.96).

$$\dot{\hat{x}}_1(t) = \mathbf{A}_1\hat{x}_1(t) + \mathbf{A}_2\hat{x}_2(t) + \mathbf{B}_1 u_1(t) + \varepsilon\mathbf{B}_2 u_2(t) + [\mathbf{K}_1\mathbf{C}_1 + \mathbf{K}_2\mathbf{C}_3]\tilde{x}_1(t) \tag{3.96a}$$
$$+ [\mathbf{K}_1\mathbf{C}_2 + \mathbf{K}_2\mathbf{C}_4]\tilde{x}_2(t)$$

$$\varepsilon\dot{\hat{x}}_2(t) = \mathbf{A}_3\hat{x}_1(t) + \mathbf{A}_4\hat{x}_2(t) + \varepsilon\mathbf{B}_3 u_1(t) + \mathbf{B}_4 u_2(t) + \varepsilon[\mathbf{K}_3\mathbf{C}_1 + \mathbf{K}_4\mathbf{C}_3]\tilde{x}_1(t) \tag{3.96b}$$
$$+ [\mathbf{K}_3\mathbf{C}_2 + \mathbf{K}_4\mathbf{C}_4]\tilde{x}_2(t)$$

$\tilde{x}_1(t) = x_1(t) - \hat{x}_1(t)$ and $\tilde{x}_2(t) = x_2(t) - \hat{x}_2(t)$ denote the slow and the fast state errors respectively. Filter gains $\mathbf{K}_i, i = 1, 2, 3, 4$ are given as follows.

$$\begin{aligned}
\mathbf{K}_1 &:= \mathbf{\Sigma}_1\mathbf{C}_1^T\mathbf{V}_1^{-1} + \mathbf{\Sigma}_2\mathbf{C}_2^T\mathbf{V}_1^{-1} \\
\mathbf{K}_2 &:= \mathbf{\Sigma}_2\mathbf{C}_4^T\mathbf{V}_4^{-1} + \mathbf{\Sigma}_1\mathbf{C}_3^T\mathbf{V}_4^{-1} \\
\mathbf{K}_3 &:= \varepsilon\mathbf{\Sigma}_2^T\mathbf{C}_1^T\mathbf{V}_1^{-1} + \mathbf{\Sigma}_3\mathbf{C}_2^T\mathbf{V}_1^{-1} \\
\mathbf{K}_4 &:= \varepsilon\mathbf{\Sigma}_2^T\mathbf{C}_3^T\mathbf{V}_4^{-1} + \mathbf{\Sigma}_3\mathbf{C}_4^T\mathbf{V}_4^{-1}
\end{aligned} \tag{3.97}$$

After (3.96) is decoupled into exactly slow and fast subsystems and the corresponding substitutions for the inputs are made, the structure of the filter in new coordinates becomes

$$\dot{\hat{\xi}}(t) = [(\mathbf{A}_1 - \mathbf{B}_1\mathbf{F}_1 - \varepsilon\mathbf{B}_2\mathbf{F}_3) - (\mathbf{A}_2 - \mathbf{B}_1\mathbf{F}_2 - \varepsilon\mathbf{B}_2\mathbf{F}_4)\mathbf{L}]\hat{\xi}(t) \tag{3.98a}$$

$$+ (\mathbf{K}_1 - \varepsilon\mathbf{MLK}_1 - \varepsilon\mathbf{MK}_3)\nu_1(t) + (\mathbf{K}_2 - \varepsilon\mathbf{MLK}_2 - \varepsilon\mathbf{MK}_4)\nu_2(t)$$

$$\varepsilon\dot{\hat{\eta}}(t) = [(\mathbf{A}_4 - \mathbf{B}_4\mathbf{F}_4 - \varepsilon\mathbf{B}_3\mathbf{F}_2) + \varepsilon\mathbf{L}(\mathbf{A}_2 - \mathbf{B}_1\mathbf{F}_2) - \varepsilon\mathbf{B}_2\mathbf{F}_4]\hat{\eta}(t) \tag{3.98b}$$

$$+ (\mathbf{K}_3 + \varepsilon\mathbf{LK}_1)\nu_1(t) + (\mathbf{K}_4 + \varepsilon\mathbf{LK}_2)\nu_2(t)$$

The innovation processes after the transformation become

$$\nu_1(t) = y_1(t) - (\mathbf{C}_1 - \mathbf{C}_2\mathbf{L})\hat{\xi}(t) - (\varepsilon\mathbf{C}_1\mathbf{M} + \mathbf{C}_2[\mathbf{I} - \varepsilon\mathbf{LM}])\hat{\eta}(t)$$
$$\tag{3.99}$$
$$\nu_2(t) = y_2(t) - (\mathbf{C}_3 - \mathbf{C}_4\mathbf{L})\hat{\xi}(t) - (\varepsilon\mathbf{C}_3\mathbf{M} + \mathbf{C}_4[\mathbf{I} - \varepsilon\mathbf{LM}])\hat{\eta}(t)$$

Since the optimal control in new coordinates is only dependent on $\mathbf{F}_i, i = 1, 2, 3, 4$, it is the same as (3.68). Matrices $\mathbf{L}$ and $\mathbf{M}$ satisfy the following equations.

$$(\mathbf{A}_4 - \mathbf{B}_4\mathbf{F}_4 - \varepsilon\mathbf{B}_3\mathbf{F}_2)\mathbf{L} - (\mathbf{A}_3 - \mathbf{B}_4\mathbf{F}_3 - \varepsilon\mathbf{B}_4\mathbf{F}_3) \tag{3.100a}$$

$$- \varepsilon\mathbf{L}[(\mathbf{A}_1 - \mathbf{B}_1\mathbf{F}_1 - \varepsilon\mathbf{B}_2\mathbf{F}_3) - (\mathbf{A}_2 - \mathbf{B}_1\mathbf{F}_2 - \varepsilon\mathbf{B}_2\mathbf{F}_4)\mathbf{L}] = \mathbf{0}$$

$$\mathbf{M}(\mathbf{A}_4 - \mathbf{B}_4\mathbf{F}_4 - \varepsilon\mathbf{B}_3\mathbf{F}_2) - (\mathbf{A}_2 - \mathbf{B}_1\mathbf{F}_2 - \varepsilon\mathbf{B}_2\mathbf{F}_4) \tag{3.100b}$$

$$- \varepsilon[(\mathbf{A}_1 - \mathbf{B}_1\mathbf{F}_1 - \varepsilon\mathbf{B}_2\mathbf{F}_3) - (\mathbf{A}_2 - \mathbf{B}_1\mathbf{F}_2 - \varepsilon\mathbf{B}_2\mathbf{F}_4)\mathbf{L}]\mathbf{M}$$

$$+ \varepsilon\mathbf{ML}(\mathbf{A}_2 - \mathbf{B}_1\mathbf{F}_2 - \varepsilon\mathbf{B}_2\mathbf{F}_4) = \mathbf{0}$$

The algorithm used in (3.70) can be used to solve (3.100) after corresponding substitutions.

At this point, we are able to obtain the LQG solution iteratively. The only differences from the previous section are the quantities in (3.84), (3.85), and the quantities of the innovation processes. The new augmented system now becomes

$$\begin{bmatrix} \dot{x}_1^{(i)}(t) \\ \varepsilon\dot{x}_2^{(i)}(t) \\ \dot{\hat{\xi}}^{(i)}(t) \\ \varepsilon\dot{\hat{\eta}}^{(i)}(t) \end{bmatrix} = \mathcal{A} \begin{bmatrix} x_1^{(i)}(t) \\ x_2^{(i)}(t) \\ \hat{\xi}^{(i)}(t) \\ \hat{\eta}^{(i)}(t) \end{bmatrix} + \begin{bmatrix} \mathcal{F}_1 & \varepsilon\mathcal{F}_2 & \mathbf{0} & \mathbf{0} \\ \varepsilon\mathcal{F}_3 & \mathcal{F}_4 & \mathbf{0} & \mathbf{0} \\ \mathbf{0} & \mathbf{0} & \gamma_1^{(i)} & \gamma_2^{(i)} \\ \mathbf{0} & \mathbf{0} & \gamma_3^{(i)} & \gamma_4^{(i)} \end{bmatrix} \begin{bmatrix} w_1(t) \\ w_2(t) \\ v_1(t) \\ v_2(t) \end{bmatrix} \tag{3.101}$$

where $\mathcal{A}$ is defined as

$\mathcal{A} =$

$$
\begin{bmatrix}
\mathbf{A}_1 & \mathbf{A}_2 & -(\mathbf{B}_1\phi_1^{(i)} + \varepsilon\mathbf{B}_2\phi_3^{(i)}) & -(\mathbf{B}_1\phi_2^{(i)} + \varepsilon\mathbf{B}_2\phi_4^{(i)}) \\
\mathbf{A}_3 & \mathbf{A}_4 & -(\mathbf{B}_4\phi_3^{(i)} + \varepsilon\mathbf{B}_3\phi_1^{(i)}) & -(\mathbf{B}_4\phi_4^{(i)} + \varepsilon\mathbf{B}_3\phi_2^{(i)}) \\
\gamma_1^{(i)}\mathbf{C}_1 + \gamma_2^{(i)}\mathbf{C}_3 & \gamma_1^{(i)}\mathbf{C}_2 + \gamma_2^{(i)}\mathbf{C}_4 & \alpha_1^{(i)} - \gamma_1^{(i)}\rho_1^{(i)} - \gamma_2^{(i)}\rho_3^{(i)} & -\gamma_1^{(i)}\rho_2^{(i)} - \gamma_2^{(i)}\rho_4^{(i)} \\
\gamma_3^{(i)}\mathbf{C}_1 + \gamma_4^{(i)}\mathbf{C}_3 & \gamma_4^{(i)}\mathbf{C}_4 + \gamma_3^{(i)}\mathbf{C}_2 & -\gamma_3^{(i)}\rho_1^{(i)} - \gamma_4^{(i)}\rho_3^{(i)} & \alpha_2^{(i)} - \gamma_3^{(i)}\rho_2^{(i)} - \gamma_4^{(i)}\rho_4^{(i)}
\end{bmatrix}
$$

$$(3.102)$$

In each iteration, the quantities in $\mathcal{A}$ tend to their actual values as in the previous case. Namely,

$$\phi_j^{(i)} \to \phi_j^{actual}; \; j = 1, 2, 3, 4$$

$$\alpha_j^{(i)} \to \alpha_j^{actual}; \; j = 1, 2$$

$$\gamma_j^{(i)} \to \gamma_j^{actual}; \; j = 1, 2, 3, 4$$

$$\rho_j^{(i)} \to \rho_j^{actual}; \; j = 1, 2, 3, 4$$

$$J^{(i)} \to J^{opt}$$

The optimal cost functional is given by (3.92).

3.3.3 Weakly Controlled Fast Subsystem

Matrices $\mathbf{C}$ and $\mathcal{F}$ are now partitioned as follows.

$$
\mathbf{C} = \begin{bmatrix} \mathbf{C}_1 & \mathbf{0} \\ \mathbf{0} & \mathbf{C}_4 \end{bmatrix}, \quad \mathcal{F} = \begin{bmatrix} \mathcal{F}_1 & \mathbf{0} \\ \mathbf{0} & \mathcal{F}_4 \end{bmatrix}
$$

$$(3.103)$$

Substitution of the matrices in the state-space representation of the stochastic singularly perturbed system (3.55) gives

$$
\begin{aligned}
\dot{x}_1(t) &= \mathbf{A}_1 x_1(t) + \mathbf{A}_2 x_2(t) + \mathbf{B}_1 u_1(t) + \mathcal{F}_1 w_1(t) \\
\varepsilon\dot{x}_2(t) &= \mathbf{A}_3 x_1(t) + \mathbf{A}_4 x_2(t) + \varepsilon\mathbf{B}_4 u_2(t) + \varepsilon\mathcal{F}_4 w_2(t) \\
y_1(t) &= \mathbf{C}_1 x_1(t) + v_1(t) \\
y_2(t) &= \mathbf{C}_4 x_2(t) + v_2(t)
\end{aligned}
$$

$$(3.104)$$

where the regulator gains $\mathbf{F}_i, i = 1, 2, 3, 4$ are given by (matrix $\mathbf{R}$ is partitioned as before)

$$\mathbf{F}_1 := \mathbf{R_1}^{-1}\mathbf{B}_1^T\mathbf{P}_1$$

$$\mathbf{F}_2 := \varepsilon\mathbf{R_1}^{-1}\mathbf{B}_1^T\mathbf{P}_2$$

$$\mathbf{F}_3 := \varepsilon\mathbf{R_4}^{-1}\mathbf{B}_4^T\mathbf{P}_2^T \qquad (3.105)$$

$$\mathbf{F}_4 := \varepsilon\mathbf{R_4}^{-1}\mathbf{B}_4^T\mathbf{P}_3$$

Optimal estimated states $\hat{x}_1$ and $\hat{x}_2$ of the singularly perturbed system are obtained from the Kalman filter [46]:

$$\dot{\hat{x}}_1(t) = \mathbf{A}_1\hat{x}_1(t) + \mathbf{A}_2\hat{x}_2(t) + \mathbf{B}_1u_1(t) + \mathbf{K}_1\mathbf{C}_1\tilde{x}_1(t) + \mathbf{K}_2\mathbf{C}_4\tilde{x}_2(t) \qquad (3.106a)$$

$$\varepsilon\dot{\hat{x}}_2(t) = \mathbf{A}_3\hat{x}_1(t) + \mathbf{A}_4\hat{x}_2(t) + \varepsilon\mathbf{B}_4u_2(t) + \mathbf{K}_3\mathbf{C}_1\tilde{x}_1(t) + \mathbf{K}_4\mathbf{C}_4\tilde{x}_2(t) \qquad (3.106b)$$

where $\tilde{x}_1(t) = x_1(t) - \hat{x}_1(t)$ and $\tilde{x}_2(t) = x_2(t) - \hat{x}_2(t)$ denote the slow and the fast state errors respectively. $\mathbf{K}_i, i = 1, 2, 3, 4$ are the filter's gain matrices and are defined as in (3.62). Matrix $\mathbf{V}$ has the same structure as matrix $\mathbf{R}$ and $\boldsymbol{\Sigma}_i$ are obtained from the solution of the filter-type CARE. Substituting the inputs into the Kalman filter (3.106), we obtain

$$\dot{\hat{x}}_1(t) = (\mathbf{A}_1 - \mathbf{B}_1\mathbf{F}_1)\hat{x}_1(t) + (\mathbf{A}_2 - \mathbf{B}_1\mathbf{F}_2)\hat{x}_2(t) + \mathbf{K}_1\nu_1(t) + \mathbf{K}_2\nu_2(t) \qquad (3.107a)$$

$$\varepsilon\dot{\hat{x}}_2(t) = (\mathbf{A}_3 - \varepsilon\mathbf{B}_4\mathbf{F}_3)\hat{x}_1(t) + (\mathbf{A}_4 - \varepsilon\mathbf{B}_4\mathbf{F}_4)\hat{x}_2(t) + \mathbf{K}_3\nu_1(t) + \mathbf{K}_4\nu_2(t) \qquad (3.107b)$$

where $\nu_1(t) = \mathbf{C}_1\tilde{x}_1(t)$ and $\nu_2(t) = \mathbf{C}_4\tilde{x}_2(t)$ are the innovation processes driving (3.107a) and (3.107b) respectively. The filtering structure in (3.107) contains both slow and fast dynamics and we need to decouple it to obtain exactly slow and fast subsystems.

The filter in new coordinates becomes

$$\dot{\hat{\xi}}(t) = [(\mathbf{A}_1 - \mathbf{B}_1\mathbf{F}_1) - (\mathbf{A}_2 - \mathbf{B}_1\mathbf{F}_2)\mathbf{L}]\hat{\xi}(t) + (\mathbf{K}_1 - \varepsilon\mathbf{MLK}_1 - \mathbf{MK}_3)\nu_1(t) \qquad (3.108a)$$

$$+ (\mathbf{K}_2 - \varepsilon\mathbf{MLK}_2 - \mathbf{MK}_4)\nu_2(t)$$

$$\varepsilon\dot{\hat{\eta}}(t) = [(\mathbf{A}_4 - \varepsilon\mathbf{B}_4\mathbf{F}_4) - \varepsilon\mathbf{L}(\mathbf{A}_2 - \mathbf{B}_1\mathbf{F}_2)]\hat{\eta}(t) + (\mathbf{K}_3 + \varepsilon\mathbf{LK}_1)\nu_1(t) \qquad (3.108b)$$

$$+ (\mathbf{K}_4 + \varepsilon\mathbf{LK}_2)\nu_2(t)$$

The innovation processes after the transformation become

$$\nu_1(t) = y_1(t) - \mathbf{C}_1\hat{\xi}(t) - \varepsilon\mathbf{C}_1\mathbf{M}\hat{\eta}(t)$$

$$\nu_2(t) = y_2(t) + \mathbf{C}_4\mathbf{L}\hat{\xi}(t) - (\mathbf{C}_4 - \varepsilon\mathbf{C}_4\mathbf{L}\mathbf{M})\hat{\eta}(t)$$

(3.109)

The optimal control in new coordinates is given by (3.68). Matrices $\mathbf{M}$ and $\mathbf{L}$ needed to obtain the solution of the decoupled filter are evaluated by solving a weakly non-linear and a linear equation

$$(\mathbf{A}_4 - \varepsilon\mathbf{B}_4\mathbf{F}_4)\mathbf{L} - (\mathbf{A}_3 - \varepsilon\mathbf{B}_4\mathbf{F}_3) - \varepsilon\mathbf{L}[(\mathbf{A}_1 - \mathbf{B}_1\mathbf{F}_1) - (\mathbf{A}_2 - \mathbf{B}_1\mathbf{F}_2)\mathbf{L}] = \mathbf{0} \quad (3.110\text{a})$$

$$\mathbf{M}(\mathbf{A}_4 - \varepsilon\mathbf{B}_4\mathbf{F}_4) - (\mathbf{A}_2 - \mathbf{B}_1\mathbf{F}_2) - \varepsilon[(\mathbf{A}_1 - \mathbf{B}_1\mathbf{F}_1) - (\mathbf{A}_2 - \mathbf{B}_1\mathbf{F}_2)\mathbf{L}]\mathbf{M} \quad (3.110\text{b})$$
$$+ \varepsilon\mathbf{M}\mathbf{L}(\mathbf{A}_2 - \mathbf{B}_1\mathbf{F}_2) = \mathbf{0}$$

Algorithm (3.70) can be used to solve for $\mathbf{L}$ and $\mathbf{M}$ after corresponding subsitutions. For simplicity, the approximate input and approximate filters can be written as in (3.84) and in (3.85). The same method is followed for the innovation processes. As before, the solution of the suboptimal criterion can be obtained from

$$J^{(i)} = \text{tr}\{\mathbf{Q}q_{11}^{(i)} + \phi^{(i)T}\mathbf{R}\phi^{(i)}q_{22}^{(i)}\}$$

(3.111)

where

$$\phi^{(i)} = \begin{bmatrix} \phi_1^{(i)} & \phi_2^{(i)} \\ \phi_3^{(i)} & \phi_4^{(i)} \end{bmatrix}$$

and $q_{11}^{(i)}$ and $q_{22}^{(i)}$ are the variances of the original and new coordinates respectively. The overall augmented system for the weakly controlled fast subsystem case is as follows.

$$\begin{bmatrix} \dot{x}_1^{(i)}(t) \\ \varepsilon\dot{x}_2^{(i)}(t) \\ \dot{\hat{\xi}}^{(i)}(t) \\ \varepsilon\dot{\hat{\eta}}^{(i)}(t) \end{bmatrix} = \begin{bmatrix} \mathbf{A}_1 & \mathbf{A}_2 & -\mathbf{B}_1\phi_1^{(i)} & -\mathbf{B}_1\phi_2^{(i)} \\ \mathbf{A}_3 & \mathbf{A}_4 & -\varepsilon\mathbf{B}_4\phi_3^{(i)} & -\varepsilon\mathbf{B}_4\phi_4^{(i)} \\ \gamma_1^{(i)}\mathbf{C}_1 & \gamma_2^{(i)}\mathbf{C}_4 & \alpha_1^{(i)} - \gamma_1^{(i)}\rho_1^{(i)} - \gamma_2^{(i)}\rho_3^{(i)} & -\gamma_1^{(i)}\rho_2^{(i)} - \gamma_2^{(i)}\rho_4^{(i)} \\ \gamma_3^{(i)}\mathbf{C}_1 & \gamma_4^{(i)}\mathbf{C}_4 & -\gamma_3^{(i)}\rho_1^{(i)} - \gamma_4^{(i)}\rho_3^{(i)} & \alpha_2^{(i)} - \gamma_3^{(i)}\rho_2^{(i)} - \gamma_4^{(i)}\rho_4^{(i)} \end{bmatrix} \begin{bmatrix} x_1^{(i)}(t) \\ x_2^{(i)}(t) \\ \hat{\xi}^{(i)}(t) \\ \hat{\eta}^{(i)}(t) \end{bmatrix}$$

$$+ \begin{bmatrix} \mathbf{G}_1 & \mathbf{0} & \mathbf{0} & \mathbf{0} \\ \mathbf{0} & \varepsilon\mathbf{G}_4 & \mathbf{0} & \mathbf{0} \\ \mathbf{0} & \mathbf{0} & \gamma_1^{(i)} & \gamma_2^{(i)} \\ \mathbf{0} & \mathbf{0} & \gamma_3^{(i)} & \gamma_4^{(i)} \end{bmatrix} \begin{bmatrix} w_1(t) \\ w_2(t) \\ v_1(t) \\ v_2(t) \end{bmatrix}$$

(3.112)

The iterative procedure to obtain (3.111) follows the same steps as before and is run until the approximate quantities approach the actual ones and the approximate cost functional approaches the optimal, that is:

$$\phi_j^{(i)} \rightarrow \phi_j^{actual}; \ j = 1, 2, 3, 4$$

$$\alpha_j^{(i)} \rightarrow \alpha_j^{actual}; \ j = 1, 2$$

$$\gamma_j^{(i)} \rightarrow \gamma_j^{actual}; \ j = 1, 2, 3, 4$$

$$\rho_j^{(i)} \rightarrow \rho_j^{actual}; \ j = 1, 2, 3, 4$$

$$J^{(i)} \rightarrow J^{opt}$$

where J^{opt} is evaluated using (3.92).

Example 3.2 Another example follows to illustrate the solution of the LQG using the proposed method. This example corresponds to the first considered case. The following fourth-order stable singularly perturbed model is considered.

$$\mathbf{A} = \begin{bmatrix} 0 & 1 & 0 & 0 \\ 0 & 0 & 1 & 0 \\ 0 & 0 & 0 & 100 \\ -208 & -216 & -122 & -80 \end{bmatrix}, \ \mathbf{B} = \begin{bmatrix} 1 & 0 \\ 2 & 0 \\ 0 & 100 \\ 0 & 100 \end{bmatrix}, \ \mathbf{C} = \begin{bmatrix} 1 & 1 & 0 & 0 \\ 0 & 0 & 1 & 1 \end{bmatrix}$$

The eigenvalues of the model are $-0.89 \pm 0.966j$ and $-39.11 \pm 102.61j$ leading to $\varepsilon = 0.02$. In addition, for this example we select the intensity matrices $\mathbf{V}$ and $\mathbf{W}$ to be $\mathbf{I}^{2 \times 2}$ and $\mathbf{I}^{2 \times 2}$ respectively. And finally, $\mathbf{G}_1 = \mathbf{B}_1$ and $\mathbf{G}_4 = \mathbf{B}_4$. Table 3.2 shows that in a few iterations, the approximate performance criterion approaches the original one. The difference is $\mathcal{O}(\varepsilon)$ in the zeroth iteration and eventually tends to zero (to computer accuracy).

3.4   Case Study

In this section, a case study follows to illustrate the iterative methods developed in this chapter to obtain the solution of the LQR and the LQG.

Table 3.2: Comparison of the optimal performance and approximate performance evaluated using proposed algorithm.

Iteration (i)	$|J^{(i)} - J|$
0	2.5086635×10^{-1}
1	3.0092710×10^{-6}
2	3.3886959×10^{-8}
3	1.6283028×10^{-9}
4	1.2251729×10^{-9}
5	$7.5612405 \times 10^{-11}$
6	$7.1089801 \times 10^{-12}$
7	$3.7125858 \times 10^{-13}$
8	$6.9277917 \times 10^{-14}$

3.4.1 Model Description

The model investigated is a fourth order RC ladder circuit used frequently for analog-to-digital conversion purposes including microgrids where the these type of circuits are used in the available electronics [88]. $x_1(t) \in \mathbb{R}^2$ and $x_2(t) \in \mathbb{R}^2$ represent slow and fast state variables respectively. The eigenvalues of this system are given as $\lambda_{RC} = \{-27.64, -72.36, -287.69, -1112.31\}$. Matrix $\mathbf{B}$ has a structure corresponding to the first case and for this example the natural choice for the perturbation parameter based on the eigenvalue separation is $\varepsilon = 0.05$. Matrix $\mathbf{R}$ is chosen to be identity and $\mathbf{G}$ is selected to be the same as $\mathbf{B}$. Matrix $\mathbf{Q}$ and the state-space matrices are as follows.

$$\mathbf{A} = \begin{bmatrix} -\frac{3}{2RC} & \frac{1}{RC} & 0 & 0 \\ \frac{1}{RC} & -\frac{2}{RC} & 0 & 0 \\ 0 & 0 & -\frac{2}{\varepsilon RC} & \frac{1}{\varepsilon RC} \\ 0 & 0 & \frac{1}{\varepsilon RC} & -\frac{3}{2\varepsilon RC} \end{bmatrix}, \mathbf{B} = \begin{bmatrix} \frac{1}{2RC} & 0 \\ 0 & 0 \\ 0 & 0 \\ 0 & \frac{1}{2\varepsilon RC} \end{bmatrix}$$

$$\mathbf{C} = \begin{bmatrix} \frac{1}{2RC} & 0 & 0 & 0 \\ 0 & 0 & 0 & \frac{1}{2RC} \end{bmatrix}, \mathbf{Q} = \begin{bmatrix} 1 & 0 & 0.01 & 0.02 \\ 0 & 2 & 0.01 & 0.03 \\ 0.01 & 0.01 & 0.02 & 0 \\ 0.02 & 0.03 & 0 & 0.02 \end{bmatrix}$$

where $R = 5 \times 10^3 \, \Omega$ and $C = 100 \times 10^{-6} \, F$.

The model is stable and matrix $\mathbf{A}_4$ is invertible. To test out the convergence and the accuracy of the algorithm proposed in (3.26), the norm of the difference of approximate and original solutions of the CARE is evaluated. In addition, the difference of the optimal and the approximate cost functions is obtained. Note that depending on the application, this model can be further modified to by introducing additional components leading to additional states.

3.4.2 Simulation Results

The results for the LQR case are shown in Table 3.3 for eleven iterations (the first iteration where $i = 0$ represents zero-order approximate quantities). It is evident that the difference becomes very small in both columns in only a few iterations of the algorithm eventually reaching zero (to computer accuracy).

Table 3.3: Norm of the difference of approximate and original CARE solutions and difference of optimal and approximate cost functions

Iteration (i)	$||P^{(i)} - P||_2$	$|J^{(i)} - J_{opt}|$
0	1.3273989×10^{-4}	6.8142844×10^{-6}
1	2.4812770×10^{-7}	$1.0401090 \times 10^{-11}$
2	4.3468860×10^{-8}	$3.1757930 \times 10^{-13}$
3	1.016505×10^{-8}	$1.7069679 \times 10^{-14}$
4	2.5504348×10^{-9}	$1.1241008 \times 10^{-15}$
5	$6.4928189 \times 10^{-10}$	$1.2490009 \times 10^{-16}$
6	$1.6592750 \times 10^{-10}$	$2.7755576 \times 10^{-17}$
7	$4.2455934 \times 10^{-11}$	$3.4694470 \times 10^{-17}$
8	$1.0868064 \times 10^{-11}$	$4.1633363 \times 10^{-17}$
9	$2.7825205 \times 10^{-12}$	$4.8572257 \times 10^{-17}$
10	$1.1262267 \times 10^{-13}$	$2.0258312 \times 10^{-17}$

In addition, Table 3.4 shows the solution of the LQG. In this case the intensity matrices $\mathbf{V}$ and $\mathbf{W}$ have been selected to be identity. Namely, $\mathbf{V} = \mathbf{I}^{2 \times 2}$ and $\mathbf{W} = \mathbf{I}^{2 \times 2}$. Both the solution of the filter-type CARE and the evaluation of the the cost function are presented. The error goes to zero very rapidly for the optimal cost function. For

this particular example, the lack of sub-matrices $\mathbf{A}_2$ and $\mathbf{A}_3$ aids the filter-type CARE solution to reach the actual value in the first iteration as shown in the second column of Table 3.4.

In both cases, the solution agrees with the results of *Theorem 3.1*. In addition, the solution of the $\mathbf{L}$ and $\mathbf{M}$ equations (needed for the decoupling of the Kalman filter) agrees with *Theorem 3.2* and with the work of [101] (the solution of the cost functional converges faster than the solution of CARE).

Table 3.4: Norm of the difference of approximate and original filter-type CARE solutions and difference of optimal and approximate cost functions

Iteration (i)	$\|\Sigma^{(i)} - \Sigma\|_2$	$\|J^{(i)} - J_{opt}\|$
0	$7.1070216 \times 10^{-15}$	1.3957807×10^{-3}
1	$7.1070216 \times 10^{-15}$	$7.0459238 \times 10^{-10}$
2	$7.1070216 \times 10^{-15}$	$2.1409985 \times 10^{-11}$
3	$7.1070216 \times 10^{-15}$	$1.2048140 \times 10^{-12}$
4	$7.1070216 \times 10^{-15}$	$8.7485574 \times 10^{-14}$
5	$7.1070216 \times 10^{-15}$	$2.8865799 \times 10^{-14}$
6	$7.1070216 \times 10^{-15}$	$2.7533531 \times 10^{-14}$
7	$7.1070216 \times 10^{-15}$	$2.3980817 \times 10^{-14}$
8	$7.1070216 \times 10^{-15}$	$2.3536728 \times 10^{-14}$
9	$7.1070216 \times 10^{-15}$	$2.4424907 \times 10^{-14}$
10	$7.1070216 \times 10^{-15}$	$4.2642772 \times 10^{-15}$

3.5   Conclusion

This chapter investigated the LQR and LQG control problems for a new class of singularly perturbed. Three cases were investigated namely, when two inputs control slow and fast subsystems independently, when the controls are weakly coupled, and when the fast subsystem is weakly controlled. We showed that the solution of three CARE of a system of size $m + n$ can be obtained by solving reduced CARE of size m and a matrix algebraic equation. This method has computational advantages as well

as avoids possible numerical ill-conditioning. In addition, we established recursive algorithms to evaluate the error of the approximation. The problem was then investigated when disturbances were present and the complete solution of the LQG was obtained accurately in a few iterations for all three cases. A case study of a real physical system (used in microgrid setups) demonstrated the efficiency of the proposed methods.

Chapter 4

Multi-Time-Scale Systems Control via Use of Combined Controllers

Previous chapters considered only the analysis of two-time-scale singularly perturbed systems. In this chapter we focus on system where multiple time scales might arise. While singular perturbation methods are commonly used to analyze systems containing slow and fast modes, in practice we are faced with problems that contain multiple time-scales. Such examples include fuel cell systems [49]-[50] where the electrochemical subsystem of the fuel cell operates in seconds, the chemical part (energy balance and mass balance) operates in minutes, and the electrical part evolves in milliseconds [109]. Other cases of real physical systems that are well-known to have multiple time-scales are heavy-water reactors [110]-[112], chemical reactions [113]-[114], aerospace systems [115], biological models [116], power systems [117], and road vehicles [118]. Given the multitude of physical systems that operate in different time-scales, it is important to extend the analysis of classical singular perturbation theory to include all the time-scale present in the system. Multi-time-scale singularly perturbed systems and multi-parameter singularly perturbed systems have been studied in different aspects in control such as time-scale decoupling [51], [119]-[120], game theory [121], [122], and linear systems [123]. Unlike previous research, in this chapter develop a method that can convert any *implicit singularly perturbed system* into explicit form. The term implicit singularly perturbed system refers to system such as the ones mentioned earlier that contain multiple separated eigenvalue clusters.

We present a numerically well-conditioned method that simplifies the implicit multi-time-scale singularly perturbed problem. The standard explicit form is obtained and it is decoupled into individual time-scales afterwards. This technique simplifies the

complex analysis of singularly perturbed model and leads to milder computational conditions for controller design simulations.

The method is based on an ordered Schur decomposition that orders the eigenvalues of the system in ascending order along the diagonal and since it is an invariant transformation, the properties of the original system are not affected. Singular perturbation parameters ε_i, $i = 1, 2, \cdots, N$ are extracted to obtain the standard explicit singular perturbation form. The Chang transformation (2.7) is then used sequentially to decouple the system into individual time-scales. Unlike in [51] where two algebraic equations have to be solved to obtain decoupled systems for each time-scale, our method entails only the solution of one Sylvester equation.

Next, two methods for controller design have been presented. Initially, controller design based on eigenvalue assignment where only states from individual subsystems are fed back is considered. The process is done sequentially until full-state feedback is accomplished. Afterward, a combined eigenvalue placement-linear quadratic controller is proposed. LQ is used for the fastest subsystem while eigenvalue assignment is used for the rest. This hybrid technique provides flexibility for the designer in that the LQ weights can be chosen depending on the problem. This chapter is organized as follows.

In Section 4.1, the motivation behind the research is discussed. The problem is formulated in Section 4.2 where the Schur decomposition is introduced. Singular perturbation parameter extraction and time-scale decoupling are discussed in Section 4.3 and 4.4 respectively. Controller design methods are considered in Section 4.5 and a case study is discussed in Section 4.6. Finally, Section 4.7 concludes the chapter.

4.1 Motivation

Classical singular perturbation techniques have been commonly used to successfully model and analyze systems whose eigenvalues are grouped into two disjoint clusters representing slow and fast modes. The eigenvalue distribution of such systems is shown in Fig. 4.1. The latter is the most researched variant of singular perturbation methods; see [46], [52], [85] and references therein for example. As an extension to this

work, research in multi-parameter and multi-time-scale singular perturbations techniques followed. The latter systems are characterized by multiple time-scales and their eigenvalues are typically distributed as shown in Fig. 4.2; see [120]-[122]. Note that in both cases the system either lacks oscillations or is lightly oscillatory. Another case
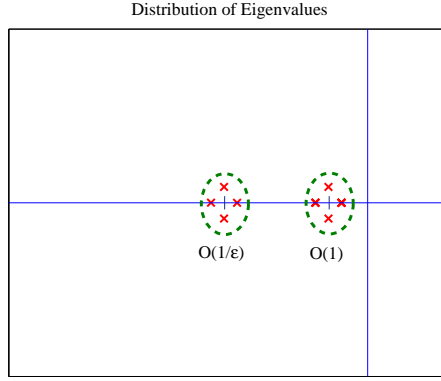
Figure 4.1: Classical singular perturbation eigenvalue distribution
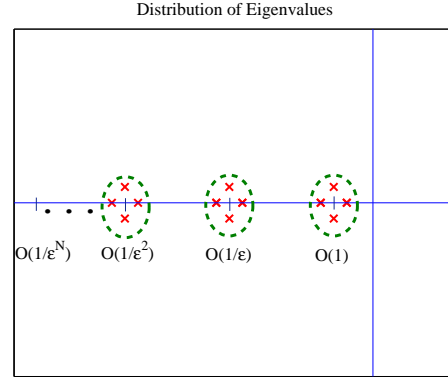
Figure 4.2: Eigenvalue distribution for multi-time-scale systems

is when the singularly perturbed system contains slightly damped, highly oscillatory modes. To the best of our knowledge, this case has only been discussed in [41]. Fig. 4.3 shows the eigenvalue distribution for these classes of systems. It is important to observe that the eigenvalues having imaginary part $\mathcal{O}(\frac{1}{\varepsilon})$ are classified as fast even though their corresponding real parts are $\mathcal{O}(\varepsilon)$.

As motivation, we return our attention to the IM model investigated in **Chapter 2**.
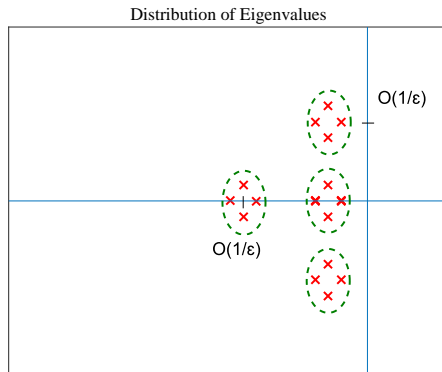
Figure 4.3: Highly oscillatory system eigenvalue distribution
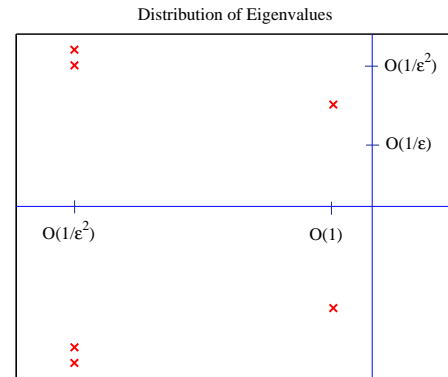
Figure 4.4: Eigenvalues of the microgrid model

Its eigenvalues are pictorially represented in Fig. 4.4. As stated earlier, (2.22) shows

explicitly that the original system does not contain any slow dynamics. In fact, state variable $z_1(\tau)$ is *fast* and $z_2(\tau)$ and $z_3(\tau)$ are *very fast*. Using only the fast modes which happen to the be the slowest modes in this model did not produce a good approximation. However, the fourth-order approximation based on the very fast modes represented by $z_2(\tau)$ and $z_3(\tau)$ produces an excellent approximation in the original coordinates.

The observations from the cases presented in Fig. 4.3 and Fig. 4.4 lead to the conclusion that when complex eigenvalues $\lambda_i := -\alpha_i \pm \beta_i j, \ i = 1, 2, \cdots, n$ with $\beta_i \gg \alpha_i$ are present, the imaginary part is essential in determining the time-scale the eigenvalue belongs to. Fig. 4.5 illustrates this concept. Eigenvalues enclosed within the green triangle belong to the slowest time-scale available. The area in between the red and green triangles contains eigenvalues belonging to the next fastest time-scale and this trend continues for all other time-scales available in the system. In this chapter, we
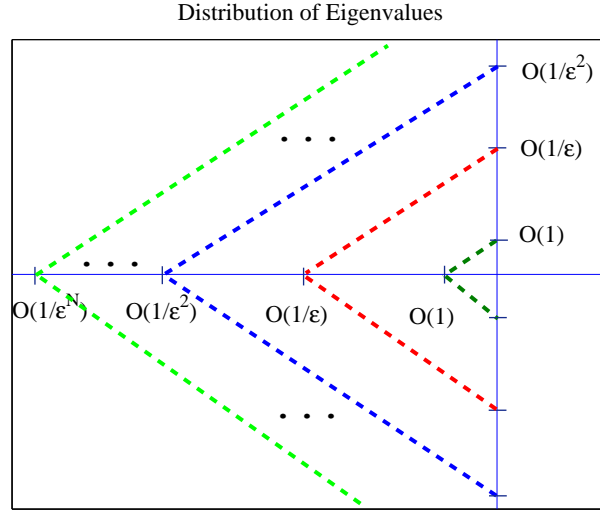
Figure 4.5: Time-scale spread for a multi-time-scale model

focus on asymptotically stable systems that can have eigenvalues distributed anywhere in the closed left-half plane. Apart from obtaining an explicit singularly perturbed form from an implicit multi-time-scale system, we also focus on controller design methods for such systems.

4.2 Problem Formulation

As noted in the earlier sections, many real physical systems contain small inherent parameters when they are modeled. This forces parts of the system to operate in different time-scales. Some of these systems are falsely classified as having only two time-scales and classical singular perturbation techniques are used for analysis and design. While literature on multi-time-scale singular perturbed systems exists, in this dissertation we develop a method that brings an implicit singularly perturbed system into the standard explicit form by extracting the perturbation parameters. The small separation parameters, $0 < \varepsilon_N \ll \varepsilon_{N-1} \ll \ldots \ll \varepsilon_1 = 1$, represent the multiple time scales with ε_1 being associated with the slowest state variable and the ε_N being associated with the fastest. We consider a general implicit multiple time scale no-input problem as shown in (4.1).

$$\dot{x}(t) = \mathbf{A}(\varepsilon)x(t) \tag{4.1}$$

where $x(t) = [x_1(t)\ x_2(t)\ \ldots\ x_N(t)]^T$ is the state vector. To simplify the problem we employ the *Schur decomposition* to transform the model into a well-conditioned form, extract the perturbation parameter, and then sequentially decouple it to obtain the individual time scales. Schur decomposition is an efficient method used to find the system's eigenvalues by utilizing the *QR* algorithm [54]. To introduce the Schur decomposition, we add two definitions.

Definition 4.1 For real matrices, a unitary matrix is a matrix $\mathbf{T}$ such that $\mathbf{T}^T = \mathbf{T}^{-1}$.

Definition 4.2 A Hessenberg matrix is an $n \times n$ matrix for which $a_{ij} = 0$ for $i > j+1$. A Hessenberg matrix has the following form.

$$\begin{bmatrix} a_{11} & a_{12} & a_{13} & \cdots & a_{1n} \\ a_{21} & a_{22} & a_{23} & \cdots & a_{2n} \\ 0 & a_{32} & a_{33} & \cdots & a_{3n} \\ 0 & 0 & a_{43} & \cdots & a_{4n} \\ 0 & 0 & 0 & \ddots & \vdots \\ 0 & 0 & 0 & \cdots & a_{nn} \end{bmatrix}$$

The next theorem summarizes the process of transforming a real $n \times n$ matrix into into its Schur decomposed form.

Theorem 4.1 For a matrix $\mathbf{A} \in \mathbb{R}^{n \times n}$ there exits a unitary matrix $\mathbf{T} \in \mathbb{R}^{n \times n}$ such that $\mathbf{T}^T \mathbf{A} \mathbf{T} = \widetilde{\mathbf{A}}$ is upper quasi-triangular, upper triangular (all real eigenvalues), Hessenberg (all complex eigenvalues).

$$\widetilde{\mathbf{A}} = \begin{bmatrix} \mathbf{R}_{11} & \mathbf{R}_{12} & \cdots & \mathbf{R}_{1N} \\ \mathbf{0} & \mathbf{R}_{22} & \cdots & \mathbf{R}_{2N} \\ \vdots & \ddots & \ddots & \vdots \\ \mathbf{0} & \cdots & \mathbf{0} & \mathbf{R}_{NN} \end{bmatrix} \tag{4.2}$$

Matrix blocks $R_{ij}, i = j$ can be 1×1 or 2×2. 1×1 blocks correspond to real eigenvalues while 2×2 blocks correspond to complex eigenvalues.

Proof The proof of this theorem can be found in [53]. $\square$

One drawback that is associated with the QR algorithm is that it is computationally expensive. Each iteration requires $\mathcal{O}(n^3)$ operations [53]. To rectify this issue, prior to applying the QR algorithm another orthogonal similarity transformation is applied to obtain a Hessenberg matrix (at this stage the eigenvalues are not located along the diagonal). The new transformation $\mathbf{U}$ can be a Householder reflection or a product of Givens rotations (see below) [54].

The transformation of interest, $z(t) = \mathbf{T}x(t)$, obtained from the QR algorithm can be found such that the unitary matrix $\mathbf{T}$ decomposes the system into the Schur form where the eigenvalues appear arbitrarily along the diagonal of $\widetilde{\mathbf{A}}$. An additional transformation has to be employed to achieve desired reordering (ascending) of the system matrix [53], [55], [57]. A direct swapping algorithm is commonly used for adjacent eigenvalue swapping [56]. The steps of this algorithm are shown in Algorithm 3. While

---

Algorithm 3 Adjacent Eigenvalue Reordering

1: Solve the Sylvester equation

$$\mathbf{R}_{n,n}\mathbf{X} - \mathbf{X}\mathbf{R}_{n+1,n+1} = \alpha\mathbf{R}_{n,n+1}$$

where α is a constant used to avoid overflow

2: Evaluate the QR factorization

$$\begin{bmatrix} -\mathbf{X} & \alpha\mathbf{I} \end{bmatrix}^T = \mathbf{QR}$$

3: Use $\mathbf{Q}$ to obtain ordered Schur form

$$\tilde{\mathbf{A}} = \mathbf{Q}^T\mathbf{A}\mathbf{Q}$$

4: Standardize 2×2 blocks if any

---

the direct swapping method is very popular, it is usually very effective when the eigenvalues are real. Another algorithm for eigenvalue reordering which is numerically stable, quite inexpensive computationally, and deals very well when complex eigenvalues are present is based on the Givens rotation [53], [56]-[58]. For a 2×2 case let

$$\mathbf{R} = \begin{bmatrix} \lambda_1 & r_{12} \\ 0 & \lambda_2 \end{bmatrix}, \ \lambda_1 \neq \lambda_2$$

If λ_1 and λ_2 need to be swapped then, a Givens rotation $J(1, 2, \theta)$ is formed such that

$$J(1, 2, \theta) \begin{bmatrix} r_{12} \\ \lambda_2 - \lambda_1 \end{bmatrix} = \begin{bmatrix} * \\ 0 \end{bmatrix}$$

Then, the new transformation matrix $\mathbf{G} - 1 = \mathbf{T}_1 J(1, 2, \theta)^T$ is such that

$$\mathbf{G}_1^T\mathbf{A}\mathbf{G}_1 = \begin{bmatrix} \lambda_2 & r_{12} \\ 0 & \lambda_1 \end{bmatrix}$$

This method can be extended to any $n \times n$ matrix in Schur form to achieve desired ordering of the eigenvalues provided that $\lambda_i \neq \lambda_j$ (no repeated eigenvalues). The complete transformation matrix in that case would be $\mathbf{G} = \mathbf{G}_1\mathbf{G}_2 \cdots \mathbf{G}_n$ (for n swappings).

Upon applying the ordered Schur algorithm, the dynamic equation takes the following form

$$\dot{z}(t) = \widetilde{\mathbf{A}}z(t) \tag{4.3}$$

where

$$
\widetilde{\mathbf{A}} = \begin{bmatrix} \widetilde{\mathbf{A}}_{11} & \Psi_{12} & \ldots & \Psi_{1N} \\ 0 & \widetilde{\mathbf{A}}_{22} & \ldots & \Psi_{2N} \\ \vdots & \vdots & \ddots & \vdots \\ 0 & 0 & \ldots & \widetilde{\mathbf{A}}_{NN} \end{bmatrix} \tag{4.4}
$$

Diagonal block matrices $\widetilde{\mathbf{A}}_{ij}$, $i = j$ contain the system's eigenvalues in descending order. $z(t)_1, z(t)_2, \ldots, z(t)_N$ are vectors each representing each time scale and Ψ_{ij} are matrix blocks of appropriate dimensions. Note that blocks $\widetilde{\mathbf{A}}_{ij}$, $i = j$ represent individual time-scales rather than individual eigenvalues. At this point, the system is still in implicit form. In the next section, we propose a method in which the small perturbation parameters are evaluated and extracted to form a standard multi-time-scale singularly perturbed system.

4.3 Singular Perturbation Parameter Extraction

Prior to decoupling the transformed system it is essential to convert it to standard explicit singularly perturbed form by extracting the small perturbation parameters from the system matrix so that time-scale decoupling and controller design based on individual time-scales can follow. This is achieved by defining the perturbation parameters. For two time-scale systems ε is commonly evaluated as $\varepsilon = \max \operatorname{Re}\{\lambda_s\}/\min \operatorname{Re}\{\lambda_f\}$. However, since earlier we observed that fast phenomena caused by highly oscillatory modes (corresponding to large imaginary parts of the eigenvalues) have an impact in time-scale separation, we have to take into account the imaginary parts of the eigenvalues as well. Hence, we evaluate the perturbation parameter as the ratio of the magnitudes of the smallest eigenvalue of the slowest time-scale with the smallest eigenvalue of the current time-scale (for all time-scales) i.e.

$$
\varepsilon_i = \frac{\min|\lambda_{slowest}|}{\min|\lambda_{current}|}, \ i = 1, 2, \cdots, N \tag{4.5}
$$

Eq. (4.5) ensures that the singular perturbation parameters are $0 < \varepsilon_N \ll \varepsilon_{N-1} \ll \cdots \ll \varepsilon_1 = 1$. Since the system is in ordered Schur form, the perturbation parameters

can be easily evaluated using (4.5) and extracted to put the system into standard explicit singularly perturbed form. Note that after extraction, the elements of the system matrix have to be multiplied with the corresponding singular perturbation parameters accordingly to reflect the change. The standard singularly perturbed form is now as follows.

$$
\begin{bmatrix} \varepsilon_1 \dot{z}_1(t) \\ \varepsilon_2 \dot{z}_2(t) \\ \vdots \\ \varepsilon_N \dot{z}_N(t) \end{bmatrix} = \begin{bmatrix} \bar{\mathbf{A}}_{11} & \bar{\Psi}_{12} & \dots & \bar{\Psi}_{1N} \\ 0 & \bar{\mathbf{A}}_{22} & \dots & \bar{\Psi}_{2N} \\ \vdots & \vdots & \ddots & \vdots \\ 0 & 0 & \dots & \bar{\mathbf{A}}_{NN} \end{bmatrix} \begin{bmatrix} z_1(t) \\ z_2(t) \\ \vdots \\ z_N(t) \end{bmatrix} \tag{4.6}
$$

Quantities with a bar denote the modified sub-matrices after the parameters have been extracted.

The explicit system can now be successfully decoupled into multiple distinct time-scale systems using the algorithm developed in [51] by utilizing the Chang transformation (2.7) and applying it sequentially. (2.7) has been used extensively to decouple two time-scales systems but can be easily adopted to decouple multiple time-scale systems as shown in [51].

4.4   Time-Scale Decoupling

To initiate the decoupling, we start by extracting the perturbation parameter from the fastest time-scale and rewrite (4.3) as a standard two time-scale singularly perturbed problem

$$
\begin{bmatrix} \dot{Z}_1(t) \\ \varepsilon_N \dot{Z}_2(t) \end{bmatrix} = \begin{bmatrix} \bar{\mathbf{A}}_1 & \bar{\mathbf{A}}_2 \\ \bar{\mathbf{A}}_3 & \bar{\mathbf{A}}_4 \end{bmatrix} \begin{bmatrix} Z_1(t) \\ Z_2(t) \end{bmatrix} \tag{4.7}
$$

In (4.7), matrices $\bar{\mathbf{A}}_3$ and $\bar{\mathbf{A}}_4$ represent the last row of the system's matrix in (4.4) with ε_N extracted. $\bar{\mathbf{A}}_4$ represents the fastest time-scale while $\bar{\mathbf{A}}_3$ contains the rest of the matrix blocks which happen to be all zero in this case. $\bar{\mathbf{A}}_1$ and $\bar{\mathbf{A}}_2$ are matrices of appropriate dimensions covering the rest of the system matrix in (4.3).

Utilizing the transformation in (2.7), the system in (4.7) is initially decoupled into two subsystems where the fast represents the fastest time-scale available and the slow

subsystem contains the rest of the time-scales.

$$\dot{\xi}(t) = (\bar{\mathbf{A}}_1 - \bar{\mathbf{A}}_2\mathbf{L}_N)\xi(t) \tag{4.8a}$$

$$\varepsilon_N\dot{\eta}_N(t) = (\bar{\mathbf{A}}_4 + \varepsilon_N\mathbf{L}_N\bar{\mathbf{A}}_2)\eta_N(t) \tag{4.8b}$$

Matrix $\mathbf{L}_N$ (and $\mathbf{M}_N$ if input and output are present) satisfy matrix algebraic equations (2.10) and the Newton's method (2.11) can be used to obtain their solutions. The new slow subsystem (4.8a) is partitioned again as in (4.9) where ε_{N-1} is now extracted from the second fastest time-scale.

$$\begin{bmatrix} \dot{Y}_1(t) \\ \varepsilon_{N-1}\dot{Y}_2(t) \end{bmatrix} = \begin{bmatrix} \bar{\mathbf{G}}_1 & \bar{\mathbf{G}}_2 \\ \bar{\mathbf{G}}_3 & \bar{\mathbf{G}}_4 \end{bmatrix} \begin{bmatrix} Y_1(t) \\ Y_2(t) \end{bmatrix} \tag{4.9}$$

The algorithm is applied sequentially until all the perturbation parameters have been extracted and the time-scales have been decoupled. A transformation matrix is obtained that decouples the overall system into independent subsystems

$$\begin{bmatrix} \eta_1(t) \\ \eta_2(t) \\ \vdots \\ \eta_N(t) \end{bmatrix} = \mathbf{T} \begin{bmatrix} x_1(t) \\ x_2(t) \\ \vdots \\ x_N(t) \end{bmatrix} \tag{4.10}$$

where $\mathbf{T}$ is given as $\mathbf{T} = \mathbf{T}_2'\mathbf{T}_3' \cdots \mathbf{T}_{N-1}'\mathbf{T}_N$ and $\mathbf{T}_i'$ is defined as

$$\mathbf{T}_i' \triangleq \begin{bmatrix} \mathbf{T}_i & \mathbf{0} \\ \mathbf{0} & \mathbf{I} \end{bmatrix} \tag{4.11}$$

Matrix $\mathbf{T}$ and identity matrix $\mathbf{I}$ are of appropriate dimensions. Unlike in [51], the system matrix in ordered Schur form simplifies the computations. For a quasi triangular system such as (4.3), $\bar{\mathbf{A}}_3$ in (4.7) is $\mathbf{0}$. Then, (2.10) for this problem simplifies to

$$\bar{\mathbf{A}}_4\mathbf{L}_N - \varepsilon\mathbf{L}_N(\bar{\mathbf{A}}_1 - \bar{\mathbf{A}}_2\mathbf{L}_N) = \mathbf{0} \tag{4.12a}$$

$$\varepsilon(\mathbf{M}_N\mathbf{L}_N\bar{\mathbf{A}}_2 - \bar{\mathbf{A}}_1\mathbf{M}_N + \bar{\mathbf{A}}_2\mathbf{L}_N\mathbf{M}_N) - \bar{\mathbf{A}}_2 + \mathbf{M}\bar{\mathbf{A}}_4 = \mathbf{0} \tag{4.12b}$$

Upon applying the recursive algorithm (2.11), it is easy to show that matrix $\mathbf{L}_N$ in (4.12a) evaluates to $\mathbf{0}$ by solving the Sylvester equation for the first iteration

$$\mathbf{M}_N\text{vec}\,\mathbf{L}_N^{(1)} = \mathbf{0} \tag{4.13}$$

Matrix $\mathbf{M}_N$ is defined as $(\mathbf{I}_n \otimes \bar{\mathbf{A}}_4 - \varepsilon \bar{\mathbf{A}}_1^T \otimes \mathbf{I}_n)$ and is full rank. Therefore, $ker(\mathbf{M}_N) = 0$ which implies $\mathbf{L}_N^{(1)} = 0$. Since $\mathbf{L}_N^{(0)} = 0$ and $\mathbf{L}_N^{(1)} = 0$, then for all other iterations $\mathbf{L}^{(i)} = 0$. (4.12b) then becomes just a Sylvester equation

$$\mathbf{M}_N \bar{\mathbf{A}}_4 - \bar{\mathbf{A}}_2 - \varepsilon \bar{\mathbf{A}}_1 \mathbf{M}_N = \mathbf{0} \tag{4.14}$$

and (2.7) simplifies to

$$\begin{bmatrix} \xi(t) \\ \eta(t) \end{bmatrix} = \begin{bmatrix} \mathbf{I} & -\varepsilon \mathbf{M}_N \\ \mathbf{0} & \mathbf{I} \end{bmatrix} \begin{bmatrix} z_1(t) \\ z_2(t) \end{bmatrix} \tag{4.15}$$

Note that this would be true for all $\mathbf{L}$ and $\mathbf{M}$ matrices after each time-scale decoupling.

After the process is repeated for all N time-scales present in the system, the individual subsystems are then given as

$$\begin{aligned} \dot{\eta}_1(t) &= \widehat{\mathbf{A}}_1 \eta_1(t) \\ \varepsilon_2 \dot{\eta}_2(t) &= \widehat{\mathbf{A}}_2 \eta_2(t) \\ &\vdots \\ \varepsilon_N \dot{\eta}_N(t) &= \widehat{\mathbf{A}}_N \eta_N(t) \end{aligned} \tag{4.16}$$

where $\widehat{\mathbf{A}}_i, i = 1, 2, \cdots, N$ are the system matrices of the individual subsystems. System (4.16) is now completely decoupled and in standard explicit singularly perturbed form. **Comments:** While no input or output was considered here, the corresponding input and output matrices of each decoupled subsystem can easily be obtained by utilizing (2.8). As a matter of fact, an ordered Schur-decomposed system with no input or output can also be decoupled without utilizing the invariant transformation due its quasi-upper triangular form since matrix $\mathbf{M}$ is not used to obtain the system matrices of each decoupled subsystem. Namely, $\widehat{\mathbf{A}}_1 \to \bar{\mathbf{A}}_{11}, \widehat{\mathbf{A}}_2 \to \bar{\mathbf{A}}_{22}, \cdots, \widehat{\mathbf{A}}_N \to \bar{\mathbf{A}}_{NN}$. On the other hand, the shortcut would not work if input and output matrices are present. In addition, it is important to note that the transformation matrices applied to the state matrix will also be applied to the input and output matrices as well. That is, if $\mathbf{A}$, $\mathbf{B}$, and $\mathbf{C}$ are the control, input, and output matrices respectively and $\mathbf{T}$ is an invariant transformation, the system in new coordinates becomes $\bar{\mathbf{A}} = \mathbf{TAT}^{-1}$, $\bar{\mathbf{B}} = \mathbf{TB}$, $\bar{\mathbf{C}} = \mathbf{CT}^{-1}$.

Remark 4.1 Even though different transformations are used to evaluate the Schur form and reorder the eigenvalues, the proposed method is not very computationally complex. To show that this is the case, we consider the number of flops needed to perform the necessary computations for each method. A flop is a floating point operation i.e. addition, subtraction, multiplication, or division [53]. In [51] we have to solve a weakly non-linear and a linear equation to obtain matrices $\mathbf{L}$ and $\mathbf{M}$. The computational requirements for this operation include $40n^3$ flops for the weakly non-linear equation and $50n^3$ flops for the linear equation for a total of $90n^3$ flops. Here, n denotes the size of the system under consideration. In contrast, the proposed algorithms requires $27n^3$ flops for the Schur transformation and eigenvalue reordering and $30n^3$ flops for the solution of the Sylvester equations for a total of $57n^3$ flops. For additional details, the reader can refer to [53].

The overall process discussed in this section can be summarized as follows.

Algorithm 4 Time-Scale Decoupling of Implicit Singularly Perturbed Systems

---

1: **Input:** Implicit singularly perturbed system
2: Apply ordered Schur decomposition
3: **if** Eigenvalues not ordered **then**
    Apply direct swapping algorithm if eigenvalues real
    otherwise apply Givens rotation n times (n is number of swappings)

$$\mathbf{G} = \mathbf{G}_1 \mathbf{G}_2 \cdots \mathbf{G}_n$$

4: Evaluate ε_i for each time-scale and form explicit system
5: Decouple explicit system using Chang [52]
6: **Output:** Completely decoupled system

4.5 Controller Design

In this section, we study controller design of the Schur-decomposed system. Two methods have been employed: initially, controller design based on state feedback via eigenvalue placement and then a hybrid scheme where eigenvalue placement and LQR have been combined. The latter method was discussed in the previous chapter. A brief overview of controller design based on state feedback via eigenvalue placement follows.

4.5.1 Eigenvalue Placement Method

We consider an LTI single-input single-output (SISO) system

$$\dot{x}(t) = \mathbf{A}x(t) + \mathbf{B}u(t)$$
$$y(t) = \mathbf{C}x(t)$$

(4.17)

The feedthrough matrix is assumed to be $\mathbf{D} = 0$ and the pair $(\mathbf{A}, \mathbf{B})$ is assumed to be controllable. To implement state feedback, we choose the following input

$$u(t) = r(t) - \mathbf{k}x(t) = r(t) - \begin{bmatrix} k_1 & k_2 & \cdots & k_n \end{bmatrix} x(t)$$

(4.18)

where $r(t)$ represents a reference input and vector $\mathbf{k}$ is the gain that will be evaluated using the eigenvalue placement method. Substituting (4.18) in (4.17) we obtain

$$\dot{x}(t) = (\mathbf{A} - \mathbf{Bk})xt + \mathbf{B}r(t)$$
$$y(t) = \mathbf{C}x(t)$$

(4.19)

In (4.19), pair $(\mathbf{A} - \mathbf{Bk}, \mathbf{B})$ is controllable if and only if $(\mathbf{A}, \mathbf{B})$ is also controllable [86]. At this point controller design can be implemented.

One the simplest cases to obtain the gain is when the state-space system is in the controllable canonical form. The state feedback matrix becomes

$$[\mathbf{A} - \mathbf{Bk}] = \begin{bmatrix} 0 & 1 & 0 & \cdots & 0 \\ 0 & 0 & 1 & \cdots & 0 \\ \vdots & \vdots & \vdots & \ddots & \vdots \\ (-a_1 - k_1) & (-a_2 - k_2) & (-a_3 - k_3) & \cdots & (-a_n - k_n) \end{bmatrix}$$

The characteristic equation of the feedback matrix is then

$$\det[s\mathbf{I} - (\mathbf{A} - \mathbf{Bk})] = s^n + (a_n + k_n)s^{n-1} + (a_{n-1} + k_{n-1})s^{n-2} + \cdots + (a_1 + k_1)$$

The eigenvalues can now be placed arbitrarily in the left-half plane. If the desired characteristic equation is given as

$$\Delta(s) = s^n + \alpha_{n_d}s^{n-1} + \alpha_{n-1_d}s^{n-2} + \cdots + \alpha_{1_d}$$

Gain $\mathbf{k}$ is simply evaluated by matching the coefficients of the aforementioned characteristic equations. If the state-space system under investigation is not in the controllable

canonical form, then an invariant transformation is initially applied to the system [86], [124].

Note that the method described above applies only to the SISO case. For multiple-input multiple-output (MIMO) cases such as the ones considered in this dissertations techniques such as the row-reduced echelon or singular value decomposition can be used to obtain the gain [124].

4.5.2   State Feedback Control via Eigenvalue Placement

After the ordered Schur transformation has been applied and the small perturbation parameters have been extracted, the system in explicit singularly perturbed form is given by

$$\begin{bmatrix} \varepsilon_1 \dot{z}_1(t) \\ \varepsilon_2 \dot{z}_2(t) \\ \vdots \\ \varepsilon_N \dot{z}_N(t) \end{bmatrix} = \bar{\mathbf{A}} \begin{bmatrix} z_1(t) \\ z_2(t) \\ \vdots \\ z_N(t) \end{bmatrix} + \bar{\mathbf{B}} u(t) \tag{4.20}$$

where $\bar{\mathbf{B}}$ is the input matrix obtained after a corresponding transformation has been applied to the input matrix in original coordinates. Matrix $\bar{\mathbf{B}}$ is appropriately partitioned as

$$\bar{\mathbf{B}} \triangleq \begin{bmatrix} \bar{\mathbf{B}}_1 \\ \bar{\mathbf{B}}_2 \\ \vdots \\ \bar{\mathbf{B}}_N \end{bmatrix}$$

We start the controller design process by considering new matrices $\bar{\mathbf{A}}$ and $\bar{\mathbf{B}}$ obtained from the state and input matrices in (4.20) divided by the perturbation parameters.

Unlike the classical eigenvalue placement problem where the whole state vector is used for feedback, here, a sequential state feedback is proposed starting with $u(t) = -\mathbf{F}_N z_N(t) + V_{N-1}(t)$. The latter corresponds to the fastest decoupled subsystem. The state-space model takes the form

$$\dot{z}_N(t) = \mathbf{A}_N z(t) + \bar{\mathbf{B}} V_{N-1}(t) \tag{4.21}$$

where the system matrix $\mathbf{A}_N$ is

$$\mathbf{A}_N = \begin{bmatrix} \bar{\mathbf{A}}_{11} & \Psi_{12} & \dots & \Psi_{1N} - \bar{\mathbf{B}}_1\mathbf{F}_N \\ 0 & \bar{\mathbf{A}}_{22} & \dots & \Psi_{2N} - \bar{\mathbf{B}}_2\mathbf{F}_N \\ \vdots & \vdots & \ddots & \vdots \\ 0 & 0 & \dots & (\bar{\mathbf{A}}_{NN} - \bar{\mathbf{B}}_N\mathbf{F}_N) \end{bmatrix} \tag{4.22}$$

The next substitution for the new input is $V_{N-1}(t) = -\mathbf{F}_{N-1}z_{N-1}(t) + V_{N-2}(t)$. If we continue sequentially in this fashion, the overall state-space equation becomes

$$\dot{z}(t) = \mathbf{A}_{\{1,2,\cdots,N\}}z(t) + \bar{\mathbf{B}}V_0(t) \tag{4.23}$$

where the system matrix $\mathbf{A}_{1,2,\cdots,N}$ now becomes

$$\mathbf{A}_{\{1,2,\cdots,N\}} = \begin{bmatrix} \bar{\mathcal{A}}_{11} & \Psi_{12} - \bar{\mathbf{B}}_1\mathbf{F}_2 & \dots & \Psi_{1N} - \bar{\mathbf{B}}_1\mathbf{F}_N \\ 0 & \bar{\mathcal{A}}_{22} & \dots & \Psi_{2N} - \bar{\mathbf{B}}_2\mathbf{F}_N \\ \vdots & \vdots & \ddots & \vdots \\ 0 & 0 & \dots & \bar{\mathcal{A}}_{NN} \end{bmatrix} \tag{4.24}$$

and $\mathcal{A}_{ii} = \bar{\mathbf{A}}_{ii} - \bar{\mathbf{B}}_i\mathbf{F}_i$. The sequential feedback process in (4.21) and (4.24) is pictorially depicted in Fig. 4.6. Under the condition stated in Assumption 2.1, the system's

Figure 4.6: Block diagram of a system controlled via eigenvalue assignment

eigenvalues can be placed to any desired location using state feedback and the gain can be obtained by methods introduced in [86] or [124]. The advantage of using this scheme comes from the fact that control can be realized by using eigenvalue assignment for certain subsystems and different control strategies for others. Next section provides more details on creating a hybrid control architecture utilizing eigenvalue placement and LQR.

4.5.3 Combined Controller Architecture

Controller design for the decoupled subsystems can be attained also by combining the eigenvalue placement method discussed in the previous section with other control techniques such as optimal of robust control. We consider an infinite horizon optimal control problem. Unlike feedback based on eigenvalue placement, using optimal control we do not have the freedom to design a controller for all the subsystem due to unknown quantities. Hence, we only consider the last term of the ordered Schur form, namely $\bar{\mathbf{A}}_{NN}$ and its corresponding input, for optimal control and then proceed with state feedback for the rest of the system. The reason for using an optimal controller comes from the fact that even though the closed-loop eigenvalues might be located far to the left half-plane, elements of the feedback gain can be large in magnitude implying a high control cost. Using an optimal controller such as a LQR will minimize the control cost. We start with a general LQR problem where the goal is to minimize the following performance measure

$$J = \frac{1}{2} \int_0^\infty \left[z_N^T(t) \mathbf{Q} z_N(t) + u^T(t) \mathbf{R} u(t) \right] dt \tag{4.25}$$

We assume that $\mathbf{R} > 0$ and $\mathbf{Q} \geq 0$. The latter has the following structure

$$\mathbf{Q} = \begin{bmatrix} \mathbf{Q}_1 & \mathbf{Q}_2 \\ \mathbf{Q}_2^T & \mathbf{Q}_3 \end{bmatrix}$$

The solution to this optimal control problem is a control input given by [125]

$$u(t) = -\mathbf{F}_N z_N(t) \tag{4.26}$$

where the gain is given as $\mathbf{F}_N = \mathbf{R}^{-1} \bar{\mathbf{B}}_N^T \mathbf{P}$ and matrix $\mathbf{P}$ is the solution to the CARE [125]

$$\bar{\mathbf{A}}_{NN}^T \mathbf{P} + \mathbf{P} \bar{\mathbf{A}}_{NN} + \mathbf{Q} - \mathbf{P} \bar{\mathbf{B}}_N \mathbf{R}^{-1} \bar{\mathbf{B}}_N^T \mathbf{P} = 0 \tag{4.27}$$

The closed-loop matrix for the combined controller strategy is the same as in (4.24) with the only difference that gain $\mathbf{F}_N$ is evaluated using LQ control. The block diagram for the hybrid controller is shown in Fig. 4.7. In both block diagrams, the area inside the dashed rectangle denotes the state-space model under consideration.
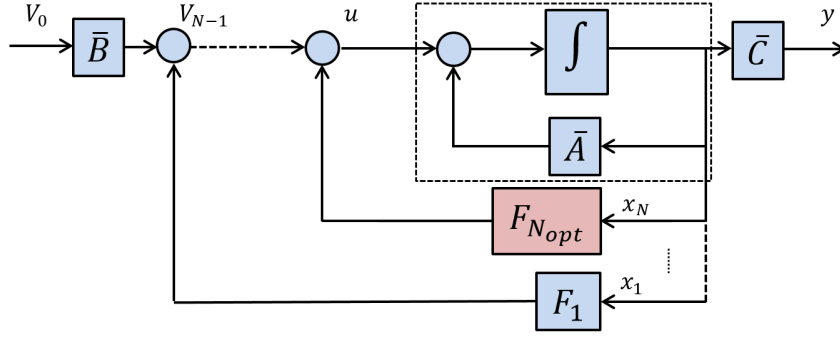
Figure 4.7: Block diagram of a system controlled using LQR and eigenvalue assignment

Comments: It is important to note that at the end, the controller has to be mapped backed to the original coordinates. This is achieved by applying the inverse of the transformations that were used in Algorithm 4.

4.6 Case Study

A multi-time-scale model of a real physical system is used in this section to demonstrate the proposed methods in this chapter.

4.6.1 Model Description

The real physical system belongs a proton exchange membrane fuel cell (PEMFC) initially modeled in [49]. The state-space matrices are as follows

$$
\mathbf{A} =
\begin{bmatrix}
-6.3091 & 0 & -10.954 & 0 & 83.7446 & 0 & 0 & 24.0587 \\
0 & -161.08 & 0 & 0 & 51.5292 & 0 & -18.026 & 0 \\
-18.786 & 0 & -46.314 & 0 & 275.659 & 0 & 0 & 158.374 \\
0 & 0 & 0 & -17.351 & 193.937 & 0 & 0 & 0 \\
1.2996 & 0 & 2.9693 & 0.3977 & -38.702 & 0.1057 & 0 & 0 \\
16.6424 & 0 & 38.0252 & 5.0666 & -479.38 & 0 & 0 & 0 \\
0 & -450.39 & 0 & 0 & 142.208 & 0 & -80.947 & 0 \\
2.0226 & 0 & 4.6212 & 0 & 0 & 0 & 0 & -51.211
\end{bmatrix}
$$

$$
\mathbf{B} = \begin{bmatrix} 0 & 0 & 0 & 3.9467 & 0 & 0 & 0 & 0 \end{bmatrix}^T
$$

$$
\mathbf{C} =
\begin{bmatrix}
0 & 0 & 0 & 5.0666 & 116.45 & 0 & 0 & 0 \\
0 & 0 & 0 & 0 & 1 & 0 & 0 & 0 \\
12.9699 & 10.3235 & 0.5693 & 0 & 0 & 0 & 0 & 0
\end{bmatrix}
$$

Table 4.1: State variables of the PEM fuel cell

Symbol	Variable
m_{O_2}	Mass flow rate of O_2 [kg/sec]
m_{H_2}	Mass flow rate of H_2 [kg/sec]
m_{N_2}	Mass flow rate of N_2 [kg/sec]
ω_{cp}	Compressor speed [rad/sec]
p_{sm}	Pressure of supply manifold [kPa]
m_{sm}	Mass flow rate in the supply manifold [kg/sec]
$m_{w,an}$	Mass flow rate of water in the anode [kg/sec]
p_{rm}	Pressure in the return manifold [kPa]

The physical meaning of each state variable is summarized in Table 4.1.

(4.28) shows the eigenvalues of the asymptotically stable model and by considering their order of magnitude, they are clustered into three distinct groups with $x_1(t) \in \mathbb{R}^3$, $x_2(t) \in \mathbb{R}^4$, and $x_3(t) \in \mathbb{R}^1$.

$$\lambda_{FC} = \{-1.403, -1.647, -2.916, -18.259, -22.403,$$
$$-46.177, -89.485, -219.624\}$$

(4.28)

where $x_3(t)$ represents the fastest cluster, $x_2(t)$ represents the second fastest, and $x_1(t)$ represents the slowest.

4.6.2 Simulation Results

From the information in (4.28) and using (4.5), the perturbation parameters are obtained

$$\varepsilon_1 = 1, \quad \varepsilon_2 = 0.160, \quad \varepsilon_3 = 0.013$$

The ordered Schur-decomposed system matrix for this example is

$$\bar{\mathbf{A}} = \begin{bmatrix} -1.4030 & -0.2086 & -2.2670 & -2.2491 & -0.1289 & 210.1544 & -241.6745 & -126.1038 \\ 0 & -1.6473 & 0.4183 & -3.9128 & -0.2 & -104.2744 & 98.8688 & 55.9802 \\ 0 & 0 & -2.9158 & -15.9344 & -0.8944 & -178.9414 & 374.8447 & 159.2652 \\ 0 & 0 & 0 & -18.2586 & 0.1643 & -25.2903 & -173.8938 & -35.7495 \\ 0 & 0 & 0 & 0 & -22.4029 & -17.6161 & 18.0423 & -455.0796 \\ 0 & 0 & 0 & 0 & 0 & -46.1771 & -13.9217 & -45.3778 \\ 0 & 0 & 0 & 0 & 0 & 0 & -89.4854 & 41.2336 \\ 0 & 0 & 0 & 0 & 0 & 0 & 0 & -219.6241 \end{bmatrix}$$

The corresponding input and output matrices after the transformation become

$$\bar{\mathbf{B}} = \begin{bmatrix} 1.2263 & -0.3820 & 2.1793 & -2.4073 & 1.4666 & 0.3248 & -0.0427 & -1.0601 \end{bmatrix}^T$$

$$\bar{\mathbf{C}} = \begin{bmatrix} -101.4725 & 8.5465 & 29.2450 & -20.3329 & 28.1893 & 30.3302 & 1.5725 & 15.1932 \\ -0.8849 & 0.0776 & 0.2271 & -0.1481 & 0.2259 & 0.2569 & 0.0140 & 0.1422 \\ -2.6876 & -5.9415 & -0.5864 & -7.5180 & -12.8880 & 1.4688 & -1.2495 & -2.4306 \end{bmatrix}$$

Using the techniques developed in this dissertation, we can easy obtain the decoupled subsystems. First by applying the Schur decomposition, then reordering the eigenvalues (for this particular example only one swap is necessary), extracting the perturbation parameters, and finally decoupling the system. The final decoupled system is as follows.

$$\begin{aligned} \varepsilon_1 \dot{\eta}_1(t) &= \begin{bmatrix} -1.40 & -0.21 & -2.27 \\ 0 & -1.65 & 0.42 \\ 0 & 0 & -2.92 \end{bmatrix} \eta_1(t) \\ \varepsilon_2 \dot{\eta}_2(t) &= \begin{bmatrix} -2.92 & 0.03 & -4.05 & -27.82 \\ 0 & -3.58 & -2.82 & 2.89 \\ 0 & 0 & -7.39 & -2.23 \\ 0 & 0 & 0 & -14.32 \end{bmatrix} \eta_2(t) \\ \varepsilon_3 \dot{\eta}_3(t) &= -2.86 \, \eta_3(t) \end{aligned} \tag{4.29}$$

Each of the reduced-order subsystems in (4.29) can be used for controller design provided that a corresponding input is introduced. Methods developed in Section 4.4 are applied next.

Without any specific requirement in mind, we arbitrarily select a set of desired eigenvalues and use the controller design techniques developed in this chapter to demonstrated the proposed methods. The desired eigenvalues are as follows.

$$\lambda_d = \{-1 \pm 2j, -4, -10, -25, -30, -35, -200\}$$

Linear simulation is used to simulate the controller response using eigenvalue placement and the combined scheme. The responses of both methods are shown in Fig. 4.8. It can be observed that we have improved the response by using the combined controller scheme. Namely, the amplitudes of the overshoot and undershoot are less compared to the response when eigenvalue placement method is used. Fig. 4.9 and Fig. 4.10 on the other hand show the state trajectories during the linear simulation. Likewise, we can see improvements in the state trajectories when the combined controller method is

used (Fig. 4.10). This is important from a physical perspective since higher overshoots or undershoots could damage the fuel cell components. Note that some of the states in Fig. 4.9 and Fig. 4.10 die out very rapidly. That occurs due to the initial conditions of the simulation.
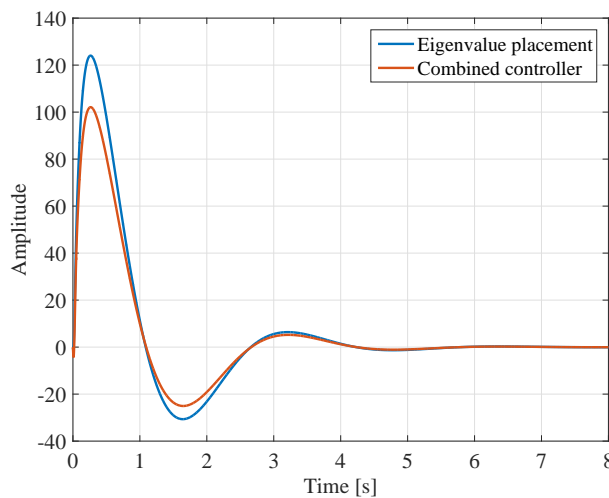

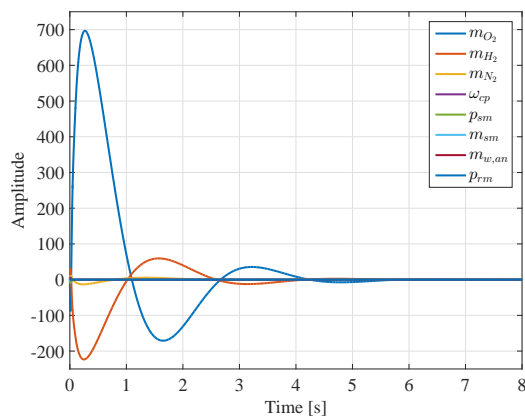Figure 4.8: Linear simulation response of two controller methods

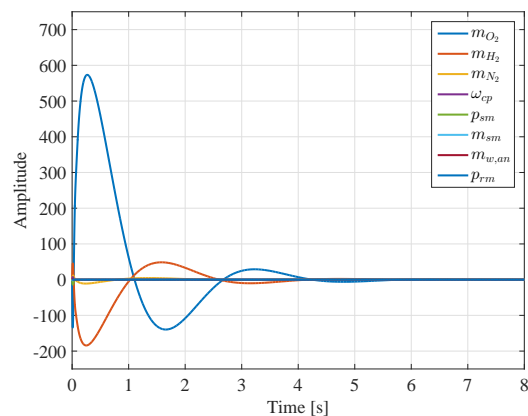Figure 4.9: State trajectory when eigenvalue placement is used

Figure 4.10: State trajectory when combined controller scheme is used

4.7   Conclusion

This chapter primarily dealt with multi-time-scale singularly perturbed systems. By utilizing an ordered Schur transformation which preserves the time-scales, we showed

that we can obtain an explicit singularly perturbed system from any implicit mulit-time-scale system. We also showed that the new system can be easily decoupled into individual subsystems. The latter were used for controller design. Initially, we considered eigenvalue assignment sequentially for each time-scale and then used an eigenvalue placement-LQR hybrid scheme that is more effective when different subsystems are more efficiently controlled by different controllers. A case study illustrated the proposed methods.

Chapter 5

Conclusions and Future Work

5.1 Conclusions

In this dissertation, we investigated a model of an IM system and found an anomaly in MOR via singular perturbations. In addition, we developed new methods for multi-time-scale linear systems with special interest in models of power systems integrated into the smart grid.

The dissertation started with a thorough time-scale investigation of an open-loop IM model and we showed that unlike typical power system models where singular perturbation methods are effectively used in model reduction, it was not the case for this model. This occurrence was shown through simulation results where common inputs such as step and impulse were used to obtain corresponding responses. Different MOR methods were tested to finalize our conclusions. First, the classical singular perturbation technique also known as the residualization method was utilized (set $\varepsilon = 0$). Following that, the exact time-scale separation technique based on the Chang transformation was tested. Very poor approximation results were observed in both cases even though the perturbation parameter was very small. Interestingly, simulations showed that the fast subsystems provided a very good approximation of the original model. An analytical investigation revealed that the model belong to *fast* and *very fast* modes, namely *slow* modes are absent and a good approximation of the original model is not expected from the slowest two states. MOR based on balancing also corroborated previous results. The HSV map revealed that a minimum of four modes is needed to approximate the original model.

Next, we studied a new class of singularly perturbed systems motivated by the model discussed in **Chapter 2** that has a specially partitioned input matrix. In this new class,

two inputs are available to control the slow and fast subsystems independently. The inputs can also be weakly coupled between each other. Three different input matrix structures which frequently occur in real physical systems were considered. These cases were as follows: the decoupled inputs case, the weakly coupled inputs case, and the weakly controlled fast subsystem case. Optimal control problems specifically LQR and LQG were then considered for each case where the problem was solved recursively in terms of reduced-order problems to avoid possible ill-conditioning that is prone to occur. In all three cases we showed that only a reduced-order CARE and an algebraic equation are needed to be solved to obtain the zero-order approximate solution ($\mathcal{O}(\varepsilon)$ approximation) of the original full-order CARE. We developed algorithms based on fixed-point iteration methods to improve on the approximation and obtain a very accurate solution of the CARE as well as the optimal cost function. The LQG was studied afterward when noise is present in the system. The Kalman filter was formulated and appropriately decoupled into its slow and fast components. The solution of the filter-type CARE was obtained iteratively as in the LQR case. Lastly, the complete iterative solution of the LQG was presented. We showed via a case study that the accurate solution is achieved in only a few iterations of the algorithm.

Finally, we investigated systems with multiple time-scale where the perturbation parameters separating the time-scales are not explicitly known. To convert the system from the implicit original configuration to its explicit singularly perturbed form where the perturbation parameters are known, we employed an ordered Schur decomposition. The latter orders the eigenvalues of the system in ascending order along the system matrix diagonal leading to an upper-triangular matrix (only real eigenvalues) or quasi-upper-triangular (Hessenberg matrix if only complex eigenvalues are present). The ratio of the magnitude of the eigenvalues is used to obtain the perturbation parameters which are then carried out of the system matrix accordingly to form the standard singularly multi-time-scale system. An important conclusion here, which also applies to the model discussed in **Chapter 1**, is that it more effective to evaluate the singular perturbation parameter by considering the magnitude of the eigenvalues. Next, we proceeded to decouple the standard singularly perturbed system into individual time scales via use

of the Chang transformation and at this point considered design of controllers. Two methods for controller design were employed. First, a method based on eigenvalue placement was employed. Unlike the conventional way where the whole state vector is used for feedback, we introduced feedback on each time-scale. This lead to the next method where LQ control was used for controller design for the fastest time-scale and eigenvalue placement was used for the rest of the time-scales. This method offer flexibility in that different controllers can be employed on different subsystems of the same system.

5.2   Future Work

Future research pertaining the work discussed in this dissertation remains to be explored. Ongoing research is aimed at investigating the behavior of the IM model discussed in **Chapter 2**. One aspect that was briefly mentioned earlier and that we are currently researching is the fact that the residualized model includes an input in the output equation. This was not the case in the original model. Future work will involve theoretical investigation as to how this would affect the overall performance of reduced models. Another area of work that remains to be studied in this chapter is the controller design based on the reduced model. One interesting example would be design of an optimal controller for the full-order orignal IM model followed by the design of sub-optimal controllers to compare performance. As concluded, the fast subsystems gave a great approximation of the original model. The question would be if corresponding sub-optimal controllers will mimic the behavior of the optimal.

Future work for **Chapter 3** will involve considering additional input matrix structures as well as different weight matrix **Q** structures not discussed here but that are common in models of real physical systems, primarily power systems. Both the LQR and the LQG problems will be investigated. In addition, an area of focus will be the process of controller design. Particularly comparison between the methods on fixed-point iterations that we employed versus other common techniques. Large or very large scale system also remains to explored in this section using the algorithms we developed. They are good candidates where ill-conditioning can occur and computational

considerations are essential.

The work of **Chapter 3** would be interesting to investigate in the context of **Chapter 4**. Since we are decoupling the system into individual time-scales, individual inputs as done in **Chapter 3** might be more effective. In addition to what was accomplished in this dissertation, other controller combinations as well as comparisons between them would a natural way to follow up.

Finally, considering all aforementioned work, future research problems in the discrete-time domain will be interesting due to the specifics of singularly perturbed systems evolving in discrete time.

Appendix A

A.1   Details for Proof of Theorem 3.1

Additional details follow for the proof of Theorem 3.1. We start by further simplifying the error equations.

$$\mathbf{D}_1^T\mathbf{E}_1 + \mathbf{E}_1\mathbf{D}_1 + \mathbf{D}_2^T\mathbf{E}_2^T + \mathbf{E}_2\mathbf{D}_2 = \varepsilon\mathbf{H}_1 \tag{A.1a}$$

$$\mathbf{E}_2\mathbf{A}_4 + \mathbf{E}_1\mathbf{A}_2 + \mathbf{D}_2^T\mathbf{E}_3 + \mathbf{Q}_2 = \mathbf{H}_2 + \varepsilon\mathbf{H}_3 \tag{A.1b}$$

$$\mathbf{E}_3\mathbf{A}_4 + \mathbf{A}_4^T\mathbf{E}_3 + \mathbf{Q}_3 + \mathbf{P}_2^{(0)T}\mathbf{A}_2 + \mathbf{A}_2^T\mathbf{P}_2^{(0)} = -\varepsilon(\mathbf{A}_2^T\mathbf{E}_2 + \mathbf{E}_2^T\mathbf{A}_2) + \varepsilon\mathbf{H}_4 \tag{A.1c}$$

E_2 is isolated from (A.1b) and plugged in (A.1a). After the substitution is carried out, (A.1a) becomes

$$\mathbf{E}_1\mathbf{D}_1 + \mathbf{D}_1^T\mathbf{E}_1 - \mathbf{D}_2^T\mathbf{A}_4^{-T}(\mathbf{D}_2^T\mathbf{E}_3 + \mathbf{E}_1\mathbf{A}_2)^T$$
$$- (\mathbf{D}_2^T\mathbf{E}_3 + \mathbf{E}_1\mathbf{A}_2)\mathbf{A}_4^{-1}\mathbf{D}_2 + \mathcal{O}(I) + \mathcal{O}(\varepsilon) = \mathbf{0} \tag{A.2}$$

$\mathcal{O}(I)$ represents known functions of $\mathbf{P}_1^{(0)}$ and $\mathbf{P}_2^{(0)}$ and $\mathcal{O}(\varepsilon)$ represents quantities multiplied by ε. (A.2) is rewritten as

$$\mathbf{E}_1\mathbf{D}_1 + \mathbf{D}_1^T\mathbf{E}_1 - \mathbf{D}_2^T\mathbf{A}_4^{-T}\mathbf{E}_3\mathbf{D}_2 - \mathbf{D}_2^T\mathbf{A}_4^{-T}\mathbf{A}_2^T\mathbf{E}_1$$
$$- \mathbf{D}_2^T\mathbf{E}_3\mathbf{A}_4^{-1}\mathbf{D}_2 - \mathbf{E}_1\mathbf{A}_2\mathbf{A}_4^{-1}\mathbf{D}_2 + \mathcal{O}(I) + \mathcal{O}(\varepsilon) = \mathbf{0} \tag{A.3}$$

To eliminate dependency on E_3 from (A.3), (A.1c) is further manipulated. Multiplying (A.1c) by $\mathbf{A}_4^{-T}$ on the left and $\mathbf{A}_4^{-1}$ on the right-hand side we obtain

$$\mathbf{A}_4^{-T}\mathbf{E}_3 + \mathbf{E}_3\mathbf{A}_4^{-1} + \mathcal{O}(I) + \mathcal{O}(\varepsilon) = \mathbf{0} \tag{A.4}$$

(A.4) is multiplied by $-\mathbf{D}_2^T$ on the left and D_2 on the right-hand side to obtain

$$- \mathbf{D}_2^T\mathbf{A}_4^{-T}\mathbf{E}_3\mathbf{D}_2 - \mathbf{D}_2^T\mathbf{E}_3\mathbf{A}_4^{-1}\mathbf{D}_2 + \mathcal{O}(I) + \mathcal{O}(\varepsilon) = \mathbf{0} \tag{A.5}$$

Substituting (A.5) in (A.3), the final form of (3.20) becomes

$$\mathbf{A}_s^T \mathbf{E}_1 + \mathbf{E}_1 A_s = \mathcal{O}(\varepsilon) + \mathcal{O}(I) \qquad \text{(A.6)}$$

where $\mathbf{A}_s = \mathbf{D}_1 - \mathbf{A}_2 \mathbf{A}_4^{-1} \mathbf{D}_2$ with $\mathcal{O}(I)$ being constant.

References

[1] E. Santacana, G. Rackliffe, L. Tang and X. Feng "Getting Smart," *IEEE Power and Energy Mag.*, vol. 8, no. 2, pp. 41-48, March-April 2010.

[2] I. K. Vlachos, "A hybrid W-BPL Smart Grid project in Greece - Lessons learnt and next steps," in *Proc. IEEE PES Conference on Innovative Smart Grid Technologies - Middle East*, Jeddah, 2011, pp. 1-8.

[3] H. G. S. Filho, J. P. Filho and A. J. G. Pinto, "New methodology for smart grids in Brazil," in *Proc. Chilean Conference on Electrical, Electronics Engineering, Information and Communication Technologies*, Santiago, 2015, pp. 573-578.

[4] F. Girbau-Llistuella et al., "Demonstration and experience of the smart rural grid project," in *Proc. IEEE PES Innovative Smart Grid Technologies Conference Europe*, Ljubljana, Slovenia, 2016, pp. 1-6.

[5] A. Bari, J. Jiang, W. Saad and A. Jaekel, "Challenges in the Smart Grid applications: An overview," *Int. J. Distrib. Sens. N.*, 2014.

[6] M. El-Hawary, "The Smart Grid – State-of-the-art and future trends," *Electr. Pow. Compo. Sys. Journal*, vol. 42, no. 3-4, pp. 239-250, 2014.

[7] M. S. Mahmoud, S. A. Hussain and M. A. Abido "Modeling and control of microgrid: An overview," *J. Franklin Inst.*, vol. 351, pp. 2822-2859, 2014.

[8] D. V. Dollen, "Report to NIST on the Smart Grid interoperability standards roadmap," Electric Power Research Institute (EPRI), Palo Alto, CA, Aug. 2009.

[9] Q. D. Ho, Y. Gao and T. Le-Ngoc, "Challenges and research opportunities in wireless communication networks for smart grid," *IEEE Wireless Commun.*, vol. 20, no. 3, pp. 89-95, Jun. 2013.

[10] T. Liu et al., "A dynamic secret-based encryption scheme for smart grid wireless communication," *IEEE Trans. Smart Grid*, vol. 5, no. 3, pp. 1175-1182, May 2014.

[11] D. He et al., "An enhanced public key infrastructure to secure smart grid wireless communication networks," *IEEE Network*, vol. 28, no. 1, pp. 10-16, Jan.-Feb. 2014.

[12] Z. Han et al., *Game Theory in Wireless and Communication Networks: Theory, Models and Applications*, Cambridge, UK: Cambridge University Press, 2011.

[13] E. Hossain, Z. Han and H. V. Poor, *Smart Grid Communications and Networking*, Cambridge, UK,: Cambridge University Press, 2012.

[14] D. Li and S. K. Jayaweera, "Machine-learning aided optimal customer decisions for an interactive smart grid," *IEEE Syst. J.*, vol. 9, no. 4, pp. 1529-1540, Dec. 2015.

[15] D. Zhang, S. Li, M. Sun and Z. ONeill,, "An optimal and learning-based demand response and home energy management system," *IEEE Trans. Smart Grid*, vol. 7, no. 4, pp. 1790-1801, Jul. 2016.

[16] S. Massoud Amin and B. F. Wollenberg, "Toward a smart grid: power delivery for the 21st century," *IEEE Power and Energy Mag.*, vol. 3, no. 5, pp. 34-41, Sept.-Oct. 2005.

[17] P. McDaniel and S. McLaughlin, "Security and privacy challenges in the smart grid," *IEEE Security Privacy*, vol. 7, no. 3, pp. 75-77, May-Jun. 2009.

[18] F. Pasqualetti, F. Dorfler and F. Bullo, "Attack detection and identification in cyber-physical systems," *IEEE Trans. Autom. Contr.*, vol. 58, no. 11, pp. 27152729, Nov. 2013.

[19] F. Pasqualetti, F. Dorfler and F. Bullo, "Control-theoretic methods for cyber-physical security: Geometric principles for optimal cross-layer resilient control systems," *IEEE Control Syst.*, vol. 35, no. 1, pp. 110-127, Feb. 2015.

[20] P. Basak, S. Chowdhury, S. Halder and S. P. Chowdhury "A literature review on integration of distributed energy resources in the perspective of control, protection and stability of the microgrid," *Renew. Sustainable Energy Rev.*, vol. 16, no. 8, pp. 5545-5556, Oct. 2012.

[21] A. S. Dobakhshari, S. Azizi and A. M. Ranjbar, "Control of microgrids: Aspects and prospects," in *Proc. of International Conference on Networking, Sensing and Control*, Delft, Apr. 2011, pp. 38-43.

[22] D.E. Olivares et al., "Trends in microgrid control," *IEEE Trans. on Smart Grid*, vol. 5, no. 4, pp.1905-1919, Jul. 2014.

[23] A. Parisio, E. Rikos, and L. Glielmo, "A model predictive control approach to microgrid operation optimization," *IEEE Trans. Control Sys. Tech.*, vol. 22, no.5, pp.1813-1827, Sept. 2014.

[24] K. M. Abo-al-ez, A.Elaiw and X. Xia, "A dual-loop model predictive voltage control/sliding-mode current control for voltage source inverter operation in smart microgrids," *Electr. Pow. Compo. Sys. Journal*, vol. 21, no. 3-4, pp. 348-360, Feb. 2014.

[25] J. Annoni and P. Seiler, "A low-order model for wind farm control," in *Proc. American Control Conference*, Chicago, IL, 2015, pp. 1721-1727.

[26] L. Luo and S. V. Dhople "Spatiotemporal model reduction of inverter-based islanded microgrids," *IEEE Trans. on Energy Convers.*, vol. 29, no. 4, pp. 823-832, Dec. 2014.

[27] J. H. Chow, J. R. Winkelman, M.A. Pai and P. V. Kokotovic, "Application of singular perturbation theory to power system modeling and stability analysis," in *Proc. American Control Conference*, Boston, MA, Jun. 1985, pp. 1401-1407.

[28] G. Peponides, P. Kokotovic and J. Chow, "Singular perturbations and time scales in nonlinear models of power systems," *IEEE Trans. Circuits Syst.*, vol. 29, no. 11, pp. 758-767, Nov. 1982.

[29] X. Xu, R. M. Mathur, J. Jiang, G. J. Rogers and P. Kundur, "Modeling of generators and their controls in power system simulations using singular perturbations," *IEEE Trans. on Power Syst.*, vol. 13, no. 1, pp. 109-114, Feb. 1998.

[30] D. Kumar and S. K. Nagar, "Order reduction of power system models using square-root balanced approach," in *Proc. National Power Systems Conference*, Guwahati, 2014, pp. 1-6.

[31] B. Moore, "Principal component analysis in linear systems: controllability, observability, and model reduction," *IEEE Trans. on Autom. Control*, vol. 26, no. 1, pp. 17-32, Feb. 1981.

[32] K. Zhou and J. C. Doyle, *Essentials of Robust Control*, Upper Saddle River, NJ: Prentice Hall, 1998.

[33] Y. Liu and B. D. O. Anderson, "Singular perturbation approximation of balanced systems," *Int. J. Control*, vol. 50, no. 4, pp. 1379-1405, Mar. 1989.

[34] S. Gugercin and A. Antoulas, "A survey of model reduction by balanced truncation and some new results," *Int. J. Control*, vol. 77, no. 8, 748-766, Apr. 2004.

[35] L. Pernebo and L. Silverman, "Model reduction via state space representations," *IEEE Trans. on Autom. Control*, vol. 27, no. 2, pp. 382-387, Apr. 1982.

[36] Ramirez et al., "Application of balanced realizations for model-order reduction of dynamic power system equivalents," *IEEE Trans. Power Del.*, vol. 31, no. 5, pp. 2304-2312, Oct. 2016.

[37] D. Chaniotis and M. A. Pai "Model reduction in power systems using Krylov subspace methods," *IEEE Trans. on Power Sys.*, vol. 20, no. 2, pp. 888-894, May 2005.

[38] F. D. Freitas, J. Rommes and N. Martins "Gramian-based reduction method applied to large sparse power system descriptor models," *IEEE Trans. on Power Sys.*, vol. 23, no. 3, pp.1258-1270, Aug. 2008.

[39] F. Dorfler and F. Bullo, "Kron reduction of graphs with applications to electrical networks," *IEEE Trans. Circuits Syst. I, Reg. Papers*, vol. 60, no. 1, pp. 150-163, Jan. 2013.

[40] P. W. Sauer, D. F. LaGesse, S. Ahmed-Zaid and M. A. Pai, "Reduced order modeling of interconnected multimachine power systems using time-scale decomposition," *IEEE Trans. on Power Syst.*, vol. PWRS-2, no. 2, pp. 310-320, May 1987.

[41] J. H. Chow, J. J. Allemong and P. V. Kokotovic, "Singular perturbation analysis of systems with sustained high frequency oscillations," *Automatica*, vol. 14, pp. 271-279, May 1978.

[42] P. V. Kokotovic, R. E. OḾalley and P. Sannuti, "Singular perturbations and order reduction in control theory An overview," *Automatica*, vol. 12, no. 2, pp. 123-132, 1976.

[43] D. S. Naidu and A. J. Calise, "Singular perturbations and time scales in guidance and control of aerospace systems: A survey," *J. Guid. Control Dynam.*, vol. 24, no. 6, pp. 1057-1078, 2001.

[44] K. Kodra, M. Skataric and Z. Gajic, "Controllability and observability grammians for balancing linear singularly perturbed systems," in *Proc. Annual Conference on Information Sciences and Systems*, Princeton, NJ, 2014, pp. 1-6.

[45] K. Kodra, M. Skataric, and Z. Gajic, "Finding Hankel singular values for singularly perturbed linear continuous-time systems," *IET Control Theory*, 2017, doi:10.1049/iet-cta.2016.1240.

[46] P. Kokotovic, H. Khalil and J. O'Reilly, *Singular Perturbation Methods in Control: Analysis and Design*, Orlando, FL: Academic Press, 1986.

[47] P. Li et al., "Research on order reduction of power system modeling for dynamic voltage stability analysis," in *Proc. Transmission and Distribution Conference and Exposition*, New Orleans, USA, 2010.

[48] H. Karimi, E. J. Davidson and R. Iravani, "Multivariable servomechanism controller for autonomous operation of a distributed generation unit: design and performance evaluation," *IEEE Trans. on Power Sys.*, vol. 25, pp. 853-865, May 2010.

[49] J.T. Pukrushpan, A.G. Stefanopoulou and H. Peng, *Control of Fuel Cell Power Systems: Principles, Modeling, Analysis and Feedback Design*, New York, NY: Springer, 2004.

[50] K. Kodra and Z. Gajic, "Order reduction via balancing and suboptimal control of a fuel cell - reformer system," *Int. J. Hydrog. Energy*, vol. 39, no. 5, pp. 2215-2223, Feb. 2014.

[51] N. Prljaca and Z. Gajic, "General transformation for block diagonalization of multitime-scale singularly perturbed linear systems", *IEEE Trans. on Autom. Control*, vol. 53, no. 5, pp. 1303-1305, June 2008.

[52] K. W. Chang, "Singular perturbations of a general boundary value problem," *SIAM J. Math. Anal.*, vol. 3, no. 3, pp. 520-526, 1972.

[53] G. Golub and C. F. Van Loan, *Matrix Computations*, Baltimore, MD: Johns Hopkins University Press, 2012.

[54] S. H. Friedberg and A. J. Insel, *Linear Algebra*, New York, NY: Pearson, 2002.

[55] L. K. Balyan, "An Algorithm of ordered Schur factorization for real nonsymmetric matrix," in *Proc. World Academy of Science, Engineering and Technology*, vol. 4, 2010.

[56] Z. Bai and J. W. Demmel, "On swapping diagonal blocks in real Schur form," *Linear Algebra and its Applications*, vol. 186, pp. 75-95, Jun. 1993.

[57] G. W. Stewart, "HQR3 and EXCHNG: Fortran Subroutines for Calculating and Ordering the Eigenvalues of a Real Upper Hessenberg Matrix," *ACM Trans. Math. Softw.*, vol 2, No. 3, Sep. 1976.

[58] B. Kågström, "A direct method for reordering eigenvalues in the generalized real Schur form of a regular matrix pair (A,B)," in *Linear Algebra for Large Scale and Real-Time Applications,* M. S. Moonen et al., Eds. Dordrecht: Springer Netherlands, 1993, pp. 195-218.

[59] Z. Gajic, D. Petkovski and X. Shen, *Singularly Perturbed and Weakly Coupled Linear Control Systems*, New York, NY: Springer Publishing, 1990.

[60] D. Skataric and Z. Gajic, "Linear control on nearly singularly perturbed hydropower plants," *Automatica*, vol. 28, no. 1, pp. 159-163, 1992.

[61] H. Mukaidani and K. Mizukami, "The guaranteed cost control problem of uncertain singularly perturbed systems," *J. Math. Anal. Appl.*, vol. 251, no. 2, pp.716-735, 2000.

[62] Z. Aganovic and Z. Gajic, *Linear optimal control of bilinear systems*, London: Springer-Verlag, 1995.

[63] Z. Gajic and M. Lim, *Optimal control of singularly perturbed linear systems with applications: High accuracy techniques*, New York, NY: Marcel Dekker, 2001.

[64] Z. Gajic and X. Shen, *Parallel algorithms for optimal control of large scale linear systems*, New York, NY: Springer-Verlag, 1993.

[65] P. Kokotovic and R. A. Yackel, "Singular perturbation of linear regulators: basic theorems," *IEEE Trans. Autom. Control*, vol. 17, no. 1, 29-37, Feb. 1972.

[66] R. A. Yackel and P. Kokotovic, "A boundary layer method for the matrix Riccati equation," *IEEE Trans. Autom. Control*, vol. 18, no. 1, 17-24, Feb. 1973.

[67] Z. Gajic, "Numerical fixed-point solution for near-optimum regulators of linear quadratic gaussian control problems for singularly perturbed systems," *Int. J. Control*, vol. 43, no. 2, pp. 373-387, 1986.

[68] X. Shen, "Near-optimum reduced-order stochastic control of linear discrete and continuous systems with small parameters," *Ph.D. dissertation*, Rutgers University, New Brunswick, NJ, 1989.

[69] N. Harkara, D.J. Petkovski, and Z. Gajic, "The recursive algorithm for optimal output feedback control problem of linear weakly coupled systems," *Int. J. Control*, vol. 50, no. 1, pp. 1-11, 1989.

[70] Z. Gajic and X. Shen, "Parallel reduced-order controllers for stochastic linear singularly perturbed discrete systems," *IEEE Trans. Autom. Control*, vol. 36, no. 1, pp. 87-90, Jan. 1991.

[71] K. Kodra, N. Zhong, and Z. Gajic, "Model order reduction of an islanded microgrid using singular perturbations," in *Proc. American Control Conference*, Boston, MA, 2016, pp. 3650-3655.

[72] K. Kodra and Z. Gajic, "Anomaly in time-scale decomposition using singular perturbations," to be Submitted in 2017.

[73] K. Kodra and Z. Gajic, "Optimal control for a new class of singularly perturbed linear systems," *Automatica*, 2017, doi:10.1016/j.automatica.2017.03.017.

[74] K. Kodra and Z. Gajic, "Linear-quadratic-Gaussian problem for a new class of singularly perturbed stochastic systems," in *Proc. Conference on Decision and Control*, Las Vegas, NV, 2016, pp. 7365-7370.

[75] K. Kodra and Z. Gajic, "Reduced-order optimal control for a new class of singularly perturbed linear stochastic systems," *Int. J. Syst. Sci.*, Submitted, 2017.

[76] K. Kodra, N. Zhong and Z. Gajic, "Multi-time-scale systems control via use of combined controllers," in *Proc. European Control Conference*, Aalborg, Denmark, 2016, pp. 2638-2643.

[77] A. N. Tikhonov, "Systems of differential equations containing small parameters multiplying some of the derivatives," *Mathematic Sbovenic*, vol. 31, no. 73, pp. 575-586, 1952.

[78] H. Khalil, "Feedback control of nonstandard singularly perturbed systems," *IEEE Trans. Autom. Control*, vol. 34, no.10, pp. 1052-1060, 1989.

[79] C. Kuehn, *Multiple Time Scale Dynamics*, New York: Springer, Feb. 2015.

[80] L. Cao and H. Schwartz, "Complementary results on the stability bounds of singularly perturbed systems," *IEEE Trans. Autom. Control*, vol. 49, no. 11, pp. 2017-2021, Nov. 2004.

[81] C. Yang, J. Sun and X. Ma, "Stabilization bound of singularly perturbed systems subject to actuator saturation," *Automatica*, vol. 49, no. 2, pp. 457-462, Feb. 2013.

[82] Z. Gajic and T. Grodt, "The recursive reduced-order numerical solution of the singularly perturbed matrix differential equation," *IEEE Trans. on Autom. Control*, vol. 33, no. 8, pp. 751-754, Aug. 1988.

[83] V. Kecman, S. Bingulac and Z. Gajic, "Eigenvector approach for order-reduction of singularly perturbed linear-quadratic optimal control problems," *Automatica*, no. 1, vol. 35, pp. 151-158, Jan. 1999.

[84] Z. Gajic and M. Qureshi, *Lyapunov Matrix Equation in Stability and Control*, San Diego, CA: Academic Press, 1995.

[85] Z. Gajic and M. Lelic, "Improvement of systems order reduction via balancing using the method of singular perturbations," *Automatica*, vol. 37, no. 11, pp. 1859-1865, Nov. 2001.

[86] C-T. Chen, *Linear System Theory and Design*, New York, NY: Oxford University Press, 1998.

[87] M. A. Pai and P. G. Murthy, "On Lyapunov functions for power systems with transfer conductances," *IEEE Trans. Autom. Control*, vol. 18, no. 2, pp. 181-183, Apr. 1973.

[88] M. R. Opmeer and T. Reis, "A lower bound for the balanced truncation error for MIMO systems," *IEEE Trans. Autom. Control*, vol. 60, no. 8, pp. 2207-2212, Aug. 2015.

[89] F. Gao and M. R. Iravani, "A control strategy for a distributed generation unit in grid-connected and autonomous modes of operation," *IEEE Trans. Power Del.*, vol. 28, no. 2, pp. 850-859, Apr. 2008.

[90] B. Bahrani, M. Saeedifard, A. Karimi and A. Rufer, "A multivariable design methodology for voltage control of a single-DG-unit microgrid," *IEEE Trans. Ind. Informat.*, vol. 9, no. 2, pp. 589-599, May 2013.

[91] A. E. Pearson and Y. K. Chin, "Identification of MIMO systems with partially decoupled parameters," *IEEE Trans. Autom. Control*, vol. 24, no. 4, pp. 599-604, Aug. 1979.

[92] H. Khalil and P. Kokotovic, "Control strategies for decision makers using different models of the same systems," *IEEE Trans. Autom. Control*, vol. 23, no. 2, pp. 289-298, Apr. 1978.

[93] Z. Gajic and H. Khalil, "Multimodel strategies under random disturbances and imperfect partial observations," *Automatica*, vol. 22, no.1, pp. 121-125, Jan. 1986.

[94] C. Coumarbatch and Z. Gajic, "Exact decomposition of the algebraic Ricatti equation of deterministic multimodeling optimal control problems," *IEEE Trans. Autom. Control*, vol. 45, no. 4, pp. 790-794, Apr. 2000.

[95] C. Coumarbatch and Z. Gajic, "Parallel optimal Kalman filtering for stochastic systems in multimodeling form," *J. Dyn. Syst. Meas. Control*, vol. 122, no. 12, pp. 542-550, Jan. 2000.

[96] H. Mukaidani, "A new approach to robust guaranteed cost for uncertain multi-modeling systems," *Automatica*, vol. 41, no. 6, pp. 1055-1062, Jun. 2005.

[97] H. Mukaidani and T. Yamamoto, "Nash strategy for multiparameter singularly perturbed Markov jump stochastic systems," *IET Control Theory*, vol. 6, no. 14, pp. 2337-2345, Sept. 2012.

[98] A. J. Laub, "A Schur method for solving algebraic Riccati equations," *IEEE Trans. Autom. Control*, AC-21, no. 3, pp. 378-382, Jun. 1976.

[99] A. G. J. MacFarlane, "An eigenvector solution of the optimal linear regulator," *J. Elect. Cont.*, vol. 14, no. 6, pp. 643-654, Jun. 1963.

[100] Z. Gajic and X. Shen, *Parallel algorithms for optimal control of large scale linear systems*, New York, NY: Springer-Verlag, 1993.

[101] P. Kokotovic and J. B. Cruz, "An approximation theorem for linear optimal regulators," *J. Math. Anal. Appl.*, vol. 27, no. 2, pp. 249-252, Aug. 1969.

[102] P. V. Kokotovic, W.R. Perkins, J.B. Cruz and G. D'Ans, "ε-coupling method for near-optimum design of large-scale linear systems," *P. I. Elect. Eng.*, vol.116, no.5, pp.889-892, May 1969.

[103] A. B. Birchfield et al., "Statistical considerations in the creation of realistic synthetic power grids for geomagnetic disturbance studies," *IEEE Trans. Power Syst.*, vol. 32, no. 2, Mar. 2017.

[104] A. Ukil and R. Zivanovic, "Application of abrupt change detection in power systems disturbance analysis and relay performance monitoring," *IEEE Trans. Power Del.*, vol. 22, no. 1, Jan. 2007.

[105] S. Li et al., "Artificial neural networks for control of a grid-connected rectifier/inverter under disturbance, dynamic and power converter switching conditions," *IEEE Trans. Neural Netw. Learn Syst.*, vol. 25, no. 4, Apr. 2014.

[106] P. Kokotovic, J. J. Allemong, J. R. Winkelman and J. H. Chow, "Singular perturbation and iterative separation of time scales," *Automatica*, vol. 16, no. 1, pp. 23-33, Jan. 1980.

[107] M. Athans and P. L. Falb, *Optimal Control: An Introduction to the Theory and Its Applications*, New York, NY: Dover Publications, 2007.

[108] H. Kwakernaak and R. Sivan, *Linear Optimal Control Systems*, New York, NY: Wiley-Interscience, 1972.

[109] F. Zenith and S. Skogestad, "Control of the mass and energy dynamics of polybenzimidazole-membrane fuel cells," *J. Process Contr.*, vol. 19, no. 3, 415-432, Mar. 2009.

[110] R. K. Munje, B. M. Patre and A. P. Tiwari, "Periodic output feedback for spatial control of AHWR: A three-time-scale approach," *IEEE Trans. Nucl. Sci.*, vol. 39, no. 5, pp. 2215-2223, Aug. 2014.

[111] S. R. Shimjith, A. P. Tiwari and B. Bandyopadhyay, "A three-time-scale approach for design of linear state regulator for spatial control of advanced heavy water reactor," *IEEE Trans. Nucl. Sci.*, vol. 58, no. 3, pp. 1264-1276, Jun. 2011.

[112] S. R. Shimjith, A. P. Tiwari, B. Bandyopadhyay and R. K. Patil, "Spatial stabilization of advanced heavy water reactor," *Ann. Nucl. Energy*, vol. 38, pp. 1545-1558, Jul. 2011.

[113] A. Kummrow, M. Emde, A. Baltsuka, M. Pshebichnikov and D. Wiersma, "Hydrated electron dynamics at a five femtosecond time scale," *Zeitschrift fur Physikalissche Chemie*, vol. 212, no. 2, 153-159, 1999.

[114] C. Lee and G. Othmer, "A Multi-time-scale analysis of chemical reaction networks: I. deterministic systems," *J. Math. Biol.*, vol. 60, no. 3, pp. 387-450, Mar. 2010.

[115] S. Esteban, F. Gordillo, and J. Aracil, "Three-time scale singular perturbation control and stability analysis for an autonomous helicopter on a platform," *Int. J. Robust Nonlin.*, vol. 23, no. 12, pp. 1360-1392, Aug. 2013.

[116] J. Jalics, M. Krupa and H. Rotstein, "Mixed-mode oscillations in a three time-scale system of ODEs motivated by a neuronal model," *Dynam. Syst.*, vol. 25, no. 4, pp. 445-482, Feb. 2010.

[117] F. Umbria, J. Aracil, and F. Gordillo, "Three-time-scale singular perturbation stability analysis of three-phase power converters," *Asian J. Control*, vol. 16, no. 5, pp. 1361-1372, 2014.

[118] W. Wedig, "Multi-time scale dynamics of road vehicle systems," *Probabilist. Eng. Mech.*, vol. 37, pp. 180-184, Jul. 2014.

[119] N. Prljaca and Z. Gajic, "A method for optimal control and filtering of multitime-scale linear singularly-perturbed stochastic systems," *Automatica*, vol. 44, no. 8, pp. 2149-2156, Aug. 2008.

[120] H. Khalil and P. Kokotovic, "Control of linear systems with multiparameter singular perturbations," *Automatica*, vol. 15, no. 2, pp. 197-207, 1979.

[121] H. Mukaidani, "A new design approach for solving linear quadratic Nash games of multiparameter singularly perturbed systems," *IEEE Trans. Circuits Syst. I, Fundam. Theory.*, vol. 52, no. 5, pp. 960-974, Jul. 2005.

[122] H. Mukaidani, "Local uniqueness for Nash solutions of multiparameter singularly perturbed systems," *IEEE Trans. Circuits Syst. II, Exp. Briefs*, vol. 53, no. 10, pp. 1103-1107, Oct. 2006.

[123] G. Ladde and S. Rajalakshmi, "Singular perturbations with multiparameters and multiple time scales," *J. Math. Anal. Appl.*, vol. 129, pp. 457-481, Mar. 1988.

[124] T. Kaliath, *Linear Systems*, Englewood Cliffs, NJ: Prentice Hall, 1980.

[125] D. Kirk, *Optimal Control Theory: An Introduction*, Englewood Cliffs, NJ: Prentice Hall, 1998.